UNIVERSITÀ
DEGLI STUDI
DI PADOVA

Sede Amministrativa: Università degli Studi di Padova

Dipartimento di BIOLOGIA

SCUOLA DI DOTTORATO DI RICERCA IN : BIOSCIENZE E BIOTECNOLOGIE
INDIRIZZO: BIOTECNOLOGIE
CICLO: XXVIII

STUDYING OXYGENASES OF BIOCATALYTIC INTEREST

Direttore della Scuola : Ch.mo Prof. Paolo Bernardi
Coordinatore d'indirizzo: Ch.ma Prof. Fiorella Lo Schiavo
Supervisore :Ch.ma Prof. Elisabetta Bergantino

Dottorando : Mattia Niero

“The darker the night, the brighter the stars.”

February, 1st 2016

Index

Summary

The thesis is composed by three chapter. The first chapter deals with the biochemical and biocathalytic characterization of a novel Baeyer-Villiger monooxygenase from the halophilic archibacterium *Haloterrigena turkmenica.* The second chapter deals with the studying of the functional role of novel Baeyer-Villiger monooxygenases from two photosynthetic organisms: the moss *Physcomitrella patens* and the red alga *Cynidioschyzon merolae*. The third chapter deals with the studying of the recombinant expression and the enzymatic activity of the carotenoid cleavage dioxygenase involved in the biosynthesis of saffron in *Crocus sativus.*

1.1 Chapter I

Baeyer–Villiger monooxygenases (BVMOs) are attractive "green" catalysts able to produce chiral esters or lactones starting from ketones. They can act as natural equivalents of peroxyacids that are the catalysts classically used in the organic synthesis reactions, consisting in the cleavage of C-C bonds with the concomitant insertion of an oxygen atom. In this study the gene encoding a Baeyer-Villiger monooxygenase from *Haloterrigena turkmenica* (*Ht*)*,* a halophilic archibacterium from the sulfate saline soil of Turkmenistan, was cloned and expressed in *Escherichia coli*. The recombinant protein, *Ht*-BVMO, was purified and biochemically characterized. This novel BVMO is the first enzyme of this class that originates from the Archaea domain. The particular amino acid composition of this BVMO is consistent with other halophilic enzymes, which are characterized by a large number of negatively charged aminoacids on their surface to prevent the precipitation in high salt environments. Some ketone compounds described as standard substrates of BVMOs have been tested in enzymatic assays and the effect of salt concentration on the enzyme was studied using different kinds of inorganic salts at different concentration. A clear salt-dependent activity was observed, with no detectable activity in the absence of salt and maximum activity in molar salt concentrations.
Despite the particular conditions required for the enzyme to be functional, we investigated the biocatalityc potential of *Haloterrigena turkmenica* Baeyer Villiger monooxygenase (Ht-BVMO) in converting the ketone substrates into ester products.
The main issue that we had to face was finding the proper reaction conditions useful for both a halophilic enzyme and a mesophilic NADPH regeneration enzyme. We tested the residual activity of both enzymes in a range of NaCl concentrations and chose to carry out the bioconversions in 1 M NaCl. In this condition the enzymes resulted stable and all the tested substrates were completely converted.
As salt tends to greatly reduce water activity of the medium, halophilic enzymes are though to have interesting applications in biocatalytic processes performed in low water

activity environments, like aqueous/organic media. In order to probe the potentialities of *Ht*-BVMO in these kind of media, the effect of various organic solvents was evaluated on the catalytic activity. Results shows that salt at high concentration, essential to maintain the enzymatic activity of the halophilic enzyme under standard conditions, may be partially replaced by organic solvents.
The new enzyme, beside widening the panel of available Baeyer-Villiger monooxygenases, displays peculiar biochemical properties and tolerance to organic solvent that render it interesting for biotechnological applications.

1.2 Chapter II

All identified Baeyer-Villiger monooxygenases originate from bacteria or fungi and most of them work in catabolic pathway, in which they are involved in the degradation of organic molecules.
Two novel BVMOs from an acidophilic red alga, *Cyanidioschyzon merolae*, and the moss *Physcomitrella patens* have been recently cloned and expressed in recombinant form. These two proteins are the first Baeyer-Villiger monooxygenases found in photosynthetic organisms. To characterize these new enzymes several known BVMO substrates were tested. The enzymes showed a slight preference for long chain aliphatic ketones; however, the catalytic activity resulted rather low.
Their activity on long chain aliphatic ketones, already verified *in vitro*, raises the hypothesis of a possible involvement of these BVMOs in the degradative or synthetic pathways of photosynthetic pigments. To study the physiological function of these novel enzymes, so far unexplored in photosynthetic organisms, but also to probe their effective biocathalytic potentialities, we are interested in discovering their natural substrate. To this aim, we have chosen a reverse genetic approach. It is known that both *Physcomitrella patens* and *Cyanidioschyzon merolae* are organisms prone to homologous recombination. *Physcomitrella patens*, in particular, is a well-known model organism. Gene targeting techniques have been widely applied to *P. patens,* providing useful information for understanding plant evolution mechanisms.
We obtained BVMO knock-out mutants, for this organism, but unluckily we were not able to identify a clear phenotype associated with the null mutants. The chromatographic profiles of the photosynthetic pigments extracted from the wild type moss and the BVMOs knock-out mutants were compared, but no significant variations emerged.
On the other hand, *Cyanidioschyzon merolae* is an acidophilic unicellular red alga whose nuclear and plastidial genomes have been sequenced. Although gene targeting has been already reported [95], routine tools and methods are still missing. We planned to produce a BVMO knock-out of this alga, reverting the prototrophy in a *Cyanidioschyzon merolae* mutant (called M4) that shows auxotrophy for uracil.
Using the M4 mutant as recipient, we planned to disrupt the BVMO gene using a DNA construct composed by the wild type URA 5.3 (the gene encoding the orotidine 5'-monophosphate decarboxylase in *C. merolae*) as marker gene and the 5' and 3' sequence

of the BVMO as flanking regions for the homologous recombination. The techniques for laboratory cultivation and genetic manipulation for this organism still require optimizations and although we were able to growth the alga in both liquid and solid medium, the attempts to obtain transformants resulted unsuccessful.

1.3 Chapter III

Carotenoid cleavage dioxygenases are enzymes that catalyse the cleavage of carbon double bond in organic molecules. The possibility to use these enzymes for biocatalytic applications caught the interest of many chemical companies. Unlike other biocatalysts that catalyse the double bond cleavage (e.g peroxygenases), carotenoid dioxygenases are characterized by an exquisite regiosectivity and are not affected by promiscuous activities that can produce side-products. Most of CCDs are able to accept a broad range of carotenoids, but their cleavage activity shows a strict selectivity towards the position of the double bond in the substrate. The initial aim of the project was to evaluate the *in vitro* activity of CsZCD, the enzyme identified as responsible of the zeaxanthin cleavage at the position 7-8 (7', 8') in *Crocus sativus*. Controversial data are reported in literature about the reproducibility of the enzymatic activity of this protein [124, 125] and, in 2014, a novel carotenoid cleavage dioxygenase, the Cs-CCD2, was identified as the enzyme that cleaves the zeaxanthin at the 7-8 (7'-8') position in *Crocus sativus* [120]. We decided to include also this enzyme of more recent identification into our study. Therefore, we aimed to characterize the ZCD and the novel CCD2, exploring their potential as enzymes useful for biocatalytic processes. Carotenoid cleavage dioxygenases are enzymes characterized by a low solubility and often they are studied as fusion protein, with glutathione s-transferase or thioredoxin as fusion-partners. In order to enhance the solubility of ZCD and CCD2 from *Crocus sativus* and facilitate their purification, the recombinant form of these enzymes were tagged with the glutathione s-transferase and the thioredoxin. Although both the enzymes showed a high expression level in *E.coli*, they were purified with a very low yield. The activity of the purified proteins and the cell lysate of *E.coli*, expressing these enzymes, were tested *in vitro.* The enzymatic assay was carried out on the natural substrate of these enzyme, zeaxanthin, and the results were analysed by HPLC chromatography. The chromatographic profiles of the reactions did not show the formation of the cleavage products, the 3-OH-β-apo-8'-carotenal and crocetin dialdheyde, therefore the enzymatic cleavage activity was not detected. Our results led to the conclusion that the produced enzymes were inactive, probably due to an incorrect protein folding that led to a tertiary structure not functional for the enzymatic activity.

Sommario

La tesi si divide in tre capitoli. Il primo capitolo tratta della caratterizzazione biochimica e biocatalitica di una nuova Baeyer-Villiger monoossigenasi dall' Archea alofilico *Haloterrigena turkmenica.* Il secondo capitolo tratta lo studio del ruolo funzionale di due Baeyer-Villiger monossigenasi da organismi fotosintetici: il muschio *Physcomitrella patens* e l'alga rossa *Cyanidioschyzon merolae.* Il terzo capitolo tratta lo studio dell'espressione ricombinante e dell'attività di ossigenasi di CCDs (carotenoid cleavage oxygenases) coinvolte nella biosintesi dello zafferano in *Crocus sativus.*

1.1 Capitolo I

Le Baeyer-Viliger monoossigenasi (BVMOs) sono biocatalizzatori che sono in grado di produrre esteri chirali o lattoni a partire da chetoni. Come catalizzatori possono svolgere un ruolo equivalente a quello dei peracidi che sono convenzionalmente utilizzati in chimica organica sintetica, ossia quello di rompere il legame C-C di molecole organiche inserendo un atomo di ossigeno. In questo studio il gene codificante la putativa Baeyer-Villiger monoossigenasi da *Haloterrigena turkmenica* (Ht), un Archaea alofilo originario del terreno solforico delle saline del Turkmenistan, è stato clonato ed espresso in *E. coli.* La proteina ricombinante, Ht-BVMO, è stata purificata e caratterizzata biochimicamente. Questa nuova BVMO è il primo enzima di questa classe identificato in un Archaea. La particolare composizione amminoacidica di questa BVMO è coerente con quella di altri enzimi alofili, ed è caratterizzata da un'alta percentuale di amminoacidi carichi negativamente sulla superficie che hanno la funzione di prevenire l'aggregazione proteica in presenza di alte concentrazioni di sale. Alcuni substrati chetonici, considerati substrati standard delle BVMOs, sono stati testati in saggi enzimatici e l'effetto della concentrazione del sale sull'enzima è stata valutata usando diversi tipi di sali inorganici a concentrazioni diverse. L'enzima ha mostrato un'attività dipendente dalla concentrazione di sale, in particolare è risultato totalmente inattivo in assenza di sale, raggiungendo, invece, l'attività ottimale a concentrazioni molari di sale. Nonostante le particolari condizioni richieste dall'enzima per essere attivo, abbiamo indagato sulla possibilità di utilizzarlo come biocatalizzatore per convertire substrati chetonici in esteri. L'ostacolo principale che abbiamo dovuto affrontare è stata proprio l'aloficità di questo enzima e la necessità di dover accoppiare la sua attività a un enzima di rigenerazione del cofattore proveniente da un organismo mesofilo. Abbiamo testato l'attività residua di entrambi gli enzimi a diverse concentrazioni di NaCl e abbiamo scelto di condurre le bioconversioni in 1M NaCl. In queste condizioni entrambi gli enzimi sono risultati stabili e tutti i substrati testati sono stati completamente convertiti.
Poiché il sale ad alte concentrazioni riduce l'attività dell'acqua, gli enzimi alofili sono considerati avere potenziali applicazioni in processi biocatalitici in ambienti con una bassa attività dell'acqua, come le miscele di acqua e solvente organico. Le potenzialità di

Ht-BVMO, come biocatalizzatore in miscele organiche, sono state esplorate saggiandone l'attività residua in presenza di diversi solventi organici. I risultati hanno mostrato che le alte concentrazioni di sale, necessarie a mantenere l'attività enzimatica, possono essere parzialmente sostituite dai solventi organici. Questo nuovo enzima, oltre ad ampliare il pannello delle Baeyer-Villiger monoossigenasi disponibili, mostra delle peculiari proprietà biochimiche e una tolleranza ai solventi organici che lo rendono particolarmente interessante per applicazioni biotecnologiche.

1.2 Capitolo II

Le Baeyer-Villiger monoossigenasi sono enzimi che sono stati identificati in batteri e funghi e la maggior parte di essi è coinvolta in vie cataboliche per la degradazione di molecole organiche. Recentemente sono state identificate ed espresse in forma ricombinante due nuove BVMOs da un'alga rossa acidofila, *Cyanidioschyzon merolae*, e da il muschio *Physcomitrella patens.* Queste due proteine sono le prime Baeyer-Villiger monoossigenasi che sono state identificate in organismi fotosintetici. L'attività catalitica di questi enzimi è stata testata su una vasta gamma di substrati. Gli enzimi hanno mostrato preferenza per substrati chetonici con lunga catena alifatica, tuttavia l'attività catalitica è risultata piuttosto bassa. Per studiare la funzione fisiologica di questi nuovi enzimi, finora inesplorati in organismi fotosintetici, e per indagare ulteriormente sulle loro potenzialità biocatalitiche, siamo interessati a scoprire il loro substrato naturale. La loro attività su substrati chetonici a lunga catena alifatica, già verificata *in vitro*, ci ha fatto ipotizzare un loro coinvolgimento nelle vie degradative o di sintesi dei pigmenti fotosintetici. Con questo scopo, abbiamo deciso di adottare un approccio di "reverse genetic". *Physcomitrella patens* e *Cyanidioschyzon merolae* sono organismi soggetti a ricombinazione omologa. In particolare, *Physcomitrella patens* è un organismo modello per il quale le tecniche di "gene targeting" sono state ampiamente sviluppate e applicate per studi evolutivi sulle piante. Siamo stati in grado di ottenere mutanti knock-out per il gene codificante la Baeyer-Villiger monoossigenasi in *Physcomitrella,* ma non sono stati identificati fenotipi associati a questi mutanti. Per verificare il possibile coinvolgimento di questo enzima nella sintesi o degradazione dei pigmenti fotosintetici, abbiamo confrontato il profillo cromatografico dei pigmenti estratti da un organismo "wild-type" e dai mutanti Knock-out, ma non è stata osservata alcuna variazione significativa nella composizione dell'estratto. *Cyanidioschyzon merolae*, invece, è un'alga rossa acidofila unicellulare il cui genoma nucleare e plastidiale è stato recentemente sequenziato. Abbiamo progettato di produrre un'alga knock-out per la BVMO revertendo la prototroficità in un mutante di *Cyanidioschyzon merolae* (chiamato M4) che mostra auxotrofia per l'uracile. Usando Il mutante M4 come ricevente, abbiamo tentato di interrompere la sequenza codificante la BVMO usando un costrutto composto da il gene wild type URA 5.3 (codificante l'orotidina 5'-monofosfato decarbossilasi in C.merolae) fiancheggiato dalle sequenze al 5' e 3' della regione codificante la BVMO. Sebbene tecniche di "gene targeting" siano state applicate [95], metodi e strumenti per la

modificazione genetica e la coltivazione in condizioni di laboratorio devono ancora essere ottimizzati per questo organismo. Sebbene siamo stati in grado di crescere l'organismo sia in terreno liquido che solido, tutti i tentativi di ottenere transformanti sono risultati vani.

1.3 Capitolo III

Le CCDs (carotenoid cleavage dioxygenases) sono enzimi che catalizzano il taglio di un doppio legame carbonio-carbonio in molecole organiche. La possibilità di utilizzare questi enzimi per applicazioni biocatalitiche ha suscitato l'interesse di numerose aziende chimiche. Diversamente da altri enzimi che tagliano il doppio legame C-C (come le perossidasi), le CCDs sono caratterizzate da un'alta regioselettività e la loro attività catalitica non porta a prodotti secondari.
La maggior parte delle CCDs accetta come substrati un'ampia gamma di carotenoidi, ma la loro attività catalitica è selettiva nei confronti della posizione del doppio legame nel carotenoide. Lo scopo iniziale del progetto era quello di valutare l'attività *in vitro* di CsZCD, l'enzima identificato come responsabile dell'attività di taglio della zeaxantina alla posizione 7, 8 (7', 8') in *Crocus sativus* [119]. La riproducibilità dei dati ottenuti dalla caratterizzazione biochimica di CsZCD è oggetto di discussione [124,125], e più recentemente, nel 2014, una nuova carotenoid cleavage dioxygenase, CsCCD2, è stata identificata come responsabile del del taglio ossidativo del doppio legame della zeaxantina alla posizione 7-8 (7'-8') in *Crocus sativus* [120].
In questo progetto abbiamo cercato di caratterizzare gli enzimi ZCD e CCD2 con lo scopo di indagare sul loro potenziale di enzimi utili a processi biocatalitici. Le forme ricombinanti di queste proteine sono state fuse a glutatione s-transferasi o a tioredossina per aumentarne la solubilità e facilitarne la purificazione. Sebbene entrambi gli enzimi siano stati altamente espressi in *E.coli*, la loro purificazione ha portato a rese molto basse. L'attività delle proteine purificate e del lisato cellulare di *E. coli* contenente gli enzimi di interesse è stata testata *in vitro*. Il saggio enzimatico è stato condotto sul substrato naturale di questo enzima, la zeaxantina, e i risultati sono stati analizzati con cromatografia HPLC. I profili cromatografici delle reazioni non hanno rilevato la formazione dei prodotti di taglio, il 3-OH-β-apo-8'-carotenale e la crocetina dialdeide, perciò non è stata osservata alcuna attività catalitica per gli enzimi purificati. I risultati portano a concludere che gli enzimi prodotti siano inattivi, probabilmente a causa di uno scorretto ripiegamento durante l'espressione, che ha portato a una struttura terziaria non funzionale all'attività enzimatica.

General Introduction

2.1 Biocatalysis

Biocatalysis is defined as the use of natural catalysts such as protein enzymes to perform chemical transformations on organic compounds. Enzymes, in the form of fermentation, have been used for thousands of years by mankind to produce foodstuffs as chees, beer, vinegar and wine. Nevertheless, the use of enzyme in organic chemistry has a more recent origin. In 1858 Louis Pasteur treated an aqueous solution of racemic tartaric acid ammonium salt with a culture of the mold *Penicillium glaucum*, leading to the consumption of (+)-tartaric and concomitant enrichment of the (−)-enantiomer [1]. This was the first example of an enzyme-catalyzed kinetic resolution and placed a milestone in that, years later, it will be called biocatalysis. Another cornerstone of biocatalysis was the fermentation of sugar by cell-free yeast extract, reported by Eduard Buchner in 1897 [2]. This constituted the proof that biological transformations do not necessarily require living cells. In the first half of the 20th century scientists in academia and industry began to learn how to use whole cells, cell extracts. or partially purified enzymes in various biocatalytic process. One of the main problem that hampered the diffusion of biocatalysis in industrial processes was how to obtain proteins in sufficient quantities for practical applications. So far, enzymes were isolated from their respective source, such as microorganisms, fungi, plants or mammalian species. The procedures to isolate them resulted often tedious, and in many case reasonable amount of enzymes were not accessible. The turning point came with the development of DNA recombinant technology, by means of which a given enzyme occurring in one organism can be overexpressed in another host organism [3]. Expressing enzymes in organisms such as *E. coli, B. subtilis, S. cerevisae,* which can be easily cultivated and manipulated in artificial conditions, gave access a large quantities of proteins. Industrial companies such as Henkel (Germany) or Novozyme (Denmark) were able to produce ton amounts of enzymes, like protein-based detergents. Today, both the academic and the industrial community see biocatalysis as a highly promising area of research, especially for the development of sustainable technologies for the production of chemicals (green chemistry) and more selective and complex active ingredients in pharmaceuticals and agro chemicals.

2.2 Enzyme limitations

Although the use of enzymes as biocatalysts in the industrial manufacture of fine chemicals and pharmaceuticals has enormous potential, application is frequently limited. Often interesting enzymes that catalyze reactions that are difficult to perform in conventional chemical way, show a limited applicability, due to their evolution-led catalyst traits.
These limitations are the same that occur for traditional chemical catalysts

- Insufficient stereoselectivity
- Poor regioselectivity
- Narrow substrate scope
- Low conversion rate
- Insufficient stability under operating conditions
- Product inhibition

In order to expand the applications of biocatalysts, several recent scientific advances help to overcome these limitations. The exploration of Earth's biodiversity and the development of bioinformatics tools, facilitate the discovery of enzymes with catalytic proprieties that withstand industrial reaction conditions. Moreover, technologies such as directed evolution [4], gene and genome shuffling [5] offers the possibilities to customize and optimize enzymes to fit required process conditions.

2.3 Key biocatalyst properties

The proprieties of an enzyme that influence a biocatalytic process will be discussed below.

2.3.1 Turnover

The primary objective of an industrial biotransformation process is a high degree of substrate conversion to product in the minimum possible time. The k_{cat} turnover number is the maximum number of substrate molecules converted to product per unit time per active site and represents a key factor for the ideal biocatalyst concept. It depends on the mechanism of the catalyzed reaction but also on *in vivo* reaction equilibria and its position in the metabolic flux of the native organism. Enzymes involved in secondary metabolism process are often characterized by turnover number too low for practical applications. In these cases, technologies as directed evolution or rational design may be required. In the contest of a bioconversion process the turnover number may be influenced not only by the genetically determined functional capacity of the protein but also by the operating

conditions and the microenvironment of the biocatalyst. For example, chemical modifications for enzyme immobilization may influence the k_{cat} by decreasing the accessibility of the substrate to the active site or by affecting the flexibility and conformational changes required for the catalysis.
The temperature is another key factor that influence the turnover number. According to the Arrhenius kinetics, higher the temperature higher the reaction rate. The temperature for a bioprocess is often selected for the exigency to stabilize a reagent, or enhance the substrate/product solubility, or decrease sideproducts. However, such a selection is limited by the protein stability.

2.3.2 Substrate specificity

The specificity for a determinate substrate (Kcat/Km) is a property evolved specifically in relation to the metabolic role of the enzyme. The substrates scope of a highly specialized mammalian enzyme may be relatively narrow if compared to that of hydrolytic enzymes secreted by some species of fungi. The preference for a broad substrate range or a selective substrate scope depends on the type of biocatalytic process. For instance, hydrolytic enzymes for laundry detergents are required with a broad substrate specificity, whereas enzymes for the production of fine chemicals and pharmaceutical compounds are required with a stricter substrate specificity. The enzymatic pocket for substrate acceptance can often be altered, using molecular engineering methods. In some cases, through these methods, compounds of very different steric structure and chemical nature from the natural substrates can be efficiently converted by the biocatalyst.

2.3.3 Stability

The stability of an enzyme may heavily affect the economic balance of a biocatalytic process. Reaction catalyzed by poor stable biocatalyst result in a reduced efficiency process. This is due to the longer time required for the conversion and the increased frequency of catalyst replacement. Extreme conditions of temperature, ionic strength and pH required by the bioprocess are often outside of the range of stability-window tolerated by the enzyme. Moreover, the presence of detergents or organic solvents, often increase the solubility of the reagents involved in the reaction but act as denaturants for the proteins.
The intrinsic molecular stability of a protein depends on its aminoacidic sequence properties and thus by the organism from which the protein originates. Protein of extremely high thermal stability (80-115 °C) have been isolated from hyperthermophilic organisms. These kind of organisms represents a source of stable biocatalysts and work optimally at near the organism's growth temperature. Beside the strain selection, technique to change protein stability include: chemical modification (immobilization, chemical crosslinking), classical mutagenesis, or random mutagenesis. Among them chemical modification is still the most widely used technology in industry, probably for its cost-effectiveness and simplicity of the process respect with the mutagenesis

techniques.

Table 1. Definitions of the key biocatalyst parameters [128]

T_m	Protein melting (denaturation) temperature, typically determined by physical methods such as fluorescence, circular dichroism (CD) or calorimetry.
T_{opt}	Apparent temperature optimum for enzyme activity, for a defined set of reaction conditions
k_{cat}	Turnover number = maximum number of substrate molecules converted to product per unit time per active site; a function of the rate constants for the conversion of enzyme–substrate complex to enzyme + product.
K_M	Michaelis constant, representative of the dissociation of the enzyme–substrate complex, taken as an indication of substrate binding to the active site.
k_{cat}/K_M	Specificity constant; indicates the rate of association of enzyme and substrate and also indicates specificity for competing substrates.

2.4 Biodiversity as a toolkit for bioprocesses

The range of enzymes potentially available to the bioprocesses firstly depend on genetic diversity. The total amount of distinct functional sequences may be as great as 10^{13}. This genetic diversity can be depicted as the native sequence space, that virtually contains all the functional and unfuctional protein sequences available from nature. This native sequence space is only a very small part of the the total sequence space, that consider all the permutations of 20 amino acids (20^{100} for a polypeptide of 100 amino acids).
Nowadays, only a relatively small proportion of native sequence space is available to the scientific and bioindustrial community, for the simple reason that many of them have not been investigated. Moreover, the largest portion of the biodiversity results "unculturable" [6] and this restricts the access to genomes and genome products.
Despite the fact that to date more than 3000 different enzymes have been identified and many of these have been applied in industrial biotechnological processes, the present enzyme toolbox is still not sufficient to meet all demands. A major cause for this is the fact that many available enzymes do not withstand industrial reaction conditions and present one or more of the limitations indicated above. The recent literature continuously reports examples on how the molecular engineering techniques and the *in vitro* evolution offer the possibilities to overcome these limitations. However, despite the recent development of molecular engineering and screening technologies, our ability to move around sequence space through these techniques is still limited. For example, despite the

focus and the energies spent in defining the molecular basis for thermostability, a design rule for increasing the thermostability by site directed mutagenesis, has not yet been established [7,8].
Methods and strategies for predicting multiple additive mutations on solvent stability, specificity, pH behavior, are not available. For this reasons a methagenomic screening would give a widen and more reasonable access to the sequence space. Genomes and genomic products of organisms that are able to live in extreme environment are of particular interest for the development of novel bioprocess. Such extremophiles are a valuable source of novel enzymes with great applicability potential [9]

2.5 Extremophiles

Extreme environmental condition can refer to a wide range of different conditions, to physical condition such as pressure, temperature or radiation or to geochemical conditions, such as salinity and pH. Most of the organisms that have been identified to thrive in extreme environment belong to the domain of Archaea, but some species have also been identified in the eubacterial and eukaryotic kingdoms. Considering that extremophiles are able to survive non conventional environments, also their enzyme are believed to have adapted to such conditions. This assumption makes these organisms of great interest for industrial applications, indeed the properties of their enzymes may be suited for the harsh condition often required in industrial bioprocess.

2.5.1 Thermophiles

The reasons that makes thermostable enzyme preferable are quite obvious. At elevated temperatures the solubility of many substrates and products are increased, the risk of contaminations is reduced and the rate of the reactions increased, in accordance to the Arrhenius kinetics. Different studies have been led on the molecular basis of the thermostabilizations [10, 11].
In these studies, thermophilic and mesophilic proteins were compared and structural algnement and homology modeling was applied in order to identify some general molecular properties involved in thermostability. The thermostability resulted the combinations of several factors, including increased surface charge, increased protein core hydrophobicity, increased frequency of salt bridges and sidechain-sidechain hydrogen bonds. In addition thermophiles have a larger fraction of their residues in α-helical conformation and avoid proline in their α-helices.

2.5.2 Psychrophile

In a historical period of time characterized by the development of novel low energy consumption technology, enzymes from psychrophiles have become interesting for industrial application. With psychophilic lipases, amylase and proteases became feasible to develop laundry applications that can be performed at low temperature. The higher activity of these enzyme at low temperature is probably due to an increased flexibility of

the protein structure that correlate with a decreased protein stability [12].

2.5.3 Alkaliphiles/acidophiles

Alkalophiles and acidophiles are interesting organisms for bioprocess that requires extreme pH condition. However, these microorganisms spend a big effort in maintaining a neutral pH internally, and so their intracellular enzymes do not need to be adapted to extreme growth conditions. The situation is different for extracellular proteins, which have to function in low or high pH environments in the case of acidophiles and alkaliphiles, respectively. An example of a potential application of acidophilic enzymes is the employment of amylases, glucoamylases and glucosidases in the hydrolysis of starch at low pH.

2.5.4 Piezophiles

The pressure can not be considered one of the main forces that act on the denaturation of the protein, therefore it has minor influence on the evolution of the proprieties of the proteins. It has been observed that a pressure of 400MPa has to be applied for the denaturation of a single polypeptic chain of a mesophilic protein [13]. Piezophiles are organisms that live exposed to pressures that does not exceed 120MPa. Under this conditions their proteins does not require particular environment adaptation to be functional. However, in literature are reported some cases of pressure adaptations of proteins [14].

2.5.5 Halophiles

Before 1940 hypersaline environment as naturally occurring salt and soda lakes, where the NaCl concentration can approach 6 M, were considered completely sterile. Studies on the microflora of the Dead Sea revealed the existence of numerous species that inhabitant such environments, mainly prokaryotes from the archaea kingdom but also eubacteria and unicellular eukaryotes. In order to overcome the osmotic pressure, halophilic bacteria and arhaea adopt different strategies. Halophilic bacteria, but also eukaryotes exposed to osmotic stress, accumulate neutral organic compatible solutes and exclude most of the inorganic salts. In contrast halophilic archaea balance the external high salt concentration by intracellular accumulation of inorganic ions to concentrations that can exceed that of the external environment [9]. Therefore, the soluble proteins and the intracellular components of the halophilic archaea must be adapted to operate and be functional at the high intracellular salt concentration. For this reason, halophilic enzymes, while performing identical enzymatic function as their mesophilic counterpart, are characterized by a strictly salt dependence activity. These enzymes show their activity optimum in a range of 1-4M salt concentration and a total inactivity or a very low activity in absence of salts.

Of particular interest for the porpoise of this thesis is the biochemical and functional characterization of these enzymes. A more detailed description of the effect of the salts on proteins and some potential applications of these enzyme will be discus in the next chapter.

2.6 Structural basis of protein halophilicity

Proteins are composed of aminoacidic residues characterized by different chemical properties in terms of hydrophobicity, polarity and charge. The tridimensional structure of a protein is not determined by only the interactions between the residues that compose the polypeptide chain. The main force that guides and determines the folding of a protein is the interaction of these residues with the solvent [15]. Interaction of hydrophobic residues with water cause the formation of organized structure, clathrates, in the solvent, that cause a large decrease in the entropy of the overall system. To minimise this unfavorable entropy change, hyrophobic aminoacids are driven deep inside the protein structure where they contribute in reducing the free energy with van der Waals bonds. Whereas polar and charged aminoacids are driven toward the surface of the protein and form an hydration layer with the solvent molecules. This layer can be considered an interface between protein and solvent. At this interface is applied the surface tension, or surface energy of the cohesive hydrogen-hydrogen bonds of the aqueous solvent. As a consequence of the cohesive forces the proteins tends to acquire a globular shape, since this structure minimizes the surface energy with the lowest surface area to volume ratio (figure 1)

Inorganic salts have the effect to increase the surface tension of the water and, therefore, they promote the formation of the compact native protein. The surface tension increase proportionally to the salt concentration and over a certain extent, it promotes the formation of protein aggregates that further reduce the solvent accessible surface, resulting in protein precipitation.

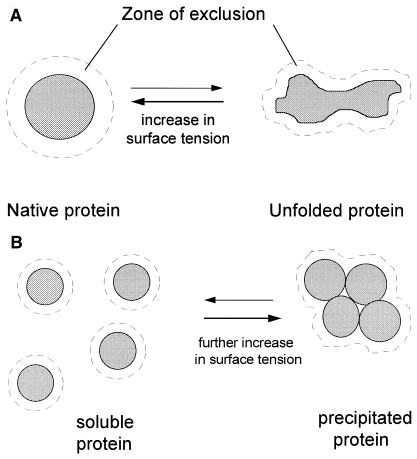

Figure 1. Schematic representation of the effects of salt on protein folding and precipitation. (A) Salt-induced increase in surface tension at the protein-water interface. (B) Aggregation effect caused by the high salt concentration [126].

A substance that increase the surface tension of the solvent has the tendency to be excluded from the surface layer that surround the protein [16]. However, the protein surface is not inert and the polar and charged residues act as attractive or repulsive forces on the ions, counterbalancing the preferential exclusion of the additive. In conclusion the net effect of salt on the protein results as the balance between the surface energy and the entity of the interaction of the ions. The entity of the forces involved in this equilibrium largely depends by the nature of the salt as described by the Hofmeisters series. For example, SO_4^- ions are characterized by a strong exclusion capacity, favouring an high surface tension, whereas Cl^- has a stronger capacity to bind with the protein surface. For this reason, SO_4^- enhance the salting out effect more then the chloride ion.
Since NaCl and KCl are both salting-out agents, at high salt concentration, halophilic proteins need to attract water molecules back to their surface to ensure the proper water layer around the single protein unit. At the same time, they have to reduce their surface hydrophobicity in order to prevent the precipitation effect and maintain their solubility. From statistical analysis it results clear that the amminoacidic composition of halophilic enzymes presents a higher proportion of acidic residues and show a decrease in aliphatic residues respect with their mesophilic counterpart [17].
The malate dehydrogenase of *Haloarcula marismourti* (*Hm* MalDH) is probably the most characterized halophilic enzyme and the extensive data on its biochemical properties and crystallographic structure have provided the first solvation stabilization model for halophilic enzymes [18]. In the model the protein forms a particle stabilized by complex hydrated ion network organized by the carboxyl groups properly oriented in the tertiary structure of the protein. The key factor of this model is the cooperative nature of the binding between hydrated ions and protein. Indeed, carboxyl groups are known to be strongly hydrated whether in the folded or unfolded form of a polypeptide [19], however they contribute to the increasing of the solvation and stabilization of the protein only when they are arranged in a precise conformation in the folded state. Therefore, the halophilic adaptation would be the result of a specific arrangement of carboxyl groups in the folded structure and not only the consequence of the excess of negative charges in the protein composition. In conclusion halophilic enzyme cannot be considered as a simply set of folded polypeptide chains that interact with each other. Conceptually, the structure of a halophilic protein is better described by a complex of protein and solvation shell. This complex is the results of specific interactions between solvated ions, water molecules and polypeptide chains.

2.7 Potential applications of halophilic enzymes

Halophilic enzyme are proteins adapted to an environment that has a low water activity. Water activity (a_w) is expressed as the ratio between the measured water pressure and the vapor pressure of pure water, and it can be considered as a measure of the available amount of free water molecules. It is expressed as value between 0 and 1, with pure water having a_w of 1. A saturated solution of sodium chloride (≈ 6M) has, at room temperature a water activity of 0,75. This value of water activity is similar to that of a 60% (v/v) solution of dimethyl formamide [20]. Due to the low water activity of molar salt solutions, halophilic proteins are believed to have a great potential in biocatalysis applications with water/organic solvent mixture, which also have a low water activity. Various co-solute such as sucrose or glycerol have shown are commonly used to stabilize proteins. This stabilizing effect is attributed to the effect of the co-solvents in increasing the surface tension and contributing to the formation of a ordered shell of water molecules around the protein. If such co-solvent stabilizes a protein in general, organic solvent are supposed to stabilize the halophilic proteins at low salt concentrations, compensating the effect of salt on the folding of the protein. The halophilic catalase from *H. salinarum* have been observed to have an activity dependent on the molar concentration of DMSO, showing that halophilic proteins do not necessarily require salt for their activity and that salt can be replaced by addition of organic solvent [21].

2.8 Potentiality of halophilic enzymes employment in reverse micelles.

In the field of biocatalysis in organic solvents halophilic enzymes have shown to have interesting potential applications in the area of reverse micelles. Reverse micelles consist of tree components: amphiphilic surfactant molecules, water and a non polar organic solvent. In this system the polar heads of the surfactant molecules are oriented toward an interior water core, whereas the hydrophobic tales are exposed to the solvent. Boielli and co-workers in 1982 suggested that the water structure inside the water core of the reverse micelle mimics the microenvironment that enzyme encounter in proximity of the cellular membrane [22]. The enzyme behavior in reverse micelles is mainly determined by the water/surfactant molar ratio (w_0 = [H_2O]/[surfactant]), that regulate the size of the micelles in a direct relationship [23]. The w_0 and therefore the micellar size determines the structure of water molecules within the micelle. If the size of the micelle increase, also the amount of free water (the water not bounded with the surfactant polar heads) inside the reverse micelle, increase [24]. By consequence, the available molecules of water inside the reverse micelle environment may affect the catalytic behavior. In this

sense reverse micelle can be considered as micro-reactors whose physical properties can be readily manipulated.

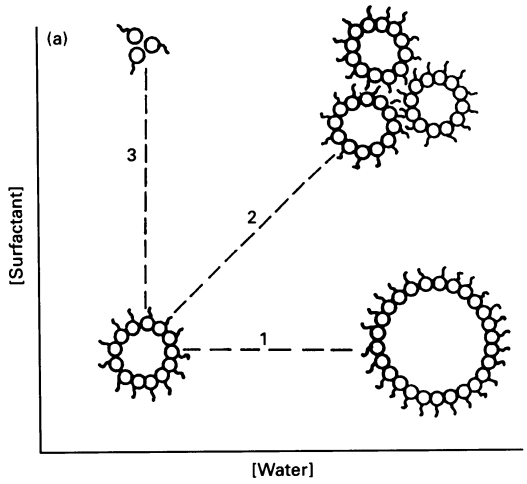

Figure 2. Structural changes in reverse micelles upon variation of water and surfactant [26]

The kinetic parameters of a halophilic enzyme in a reverse micellar system was studied on Alkaline *p*-nitrophenylphosphate phosphatase (*p*NPPase) from the halophilic archaeobacterium *Halobacterium salinarum* [25]. The enzyme was able to maintain its catalytic properties at low salt concentration (0,1 M NaCl) when encapsulated in reverse micelle constituted of 0,2 M CTAB and 1M 1-butanol in cyclohexane. The profile of the activity as function of w_0 exhibited a bell shaped curve (figure 3). Indeed, in reverse micelle, cationic surfactants such as CTAB (Cetyl trimethylammonium bromide) may have a similar effect of high salt concentrations on water hydrogen bonds. The bell shaped activity on w_0 can be explained considering the two regions with different water structures that may exist inside the reverse micelle. One region consists of water structured around the polar heads of the surfactant, whereas the other region consists of free water in the center of the water pool within the micelle [26]. At low w_0 values, all water is arranged around the polar heads of surfactant molecules and this structured water matrix may limit the activity of the enzyme. When w_0 is increased, also the water content inside the reverse micelle increase and the inner core of the reverse micelle presents a more flexible structure of the water.

p-Nitrophenylphosphate phosphatase, as a typical halophilic enzyme, requires high salt concentrations for maximal activity and its solvent exposed surface can be considered negatively charged. At low w_0 values, due to the the small size of the reverse micelles, the cationic polar heads of CTAB molecules could play the same role as cations in the cytoplasm of halophilic archaea. When the size of the micelle interior is increased, the

enzyme encapsulated within the micelle is less likely to come into contact with the cationic heads of the surfactant molecules (27). At high w_0 values, the local environment of the enzyme is characterized by a condition that would be similar to an aqueous medium at low salt concentration, and this cause a decrease in the activity of the halophilic enzyme.

The feasibility of performing reactions in reverse micelle systems is an example of the synthetic potential of halophilic enzymes for biocatalysis in low water environments. Despite these enzymes are inactive at low salt concentrations in normal aqueous solutions, their particular biochemical properties can be exploited for novel biotechnological applications in aqueous-organic media.

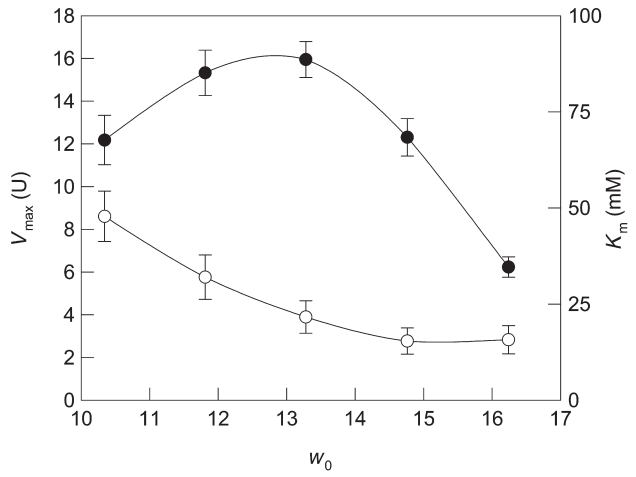

Figure 3. Effect of micellar water content (w_0 = [H_2O]/[surfactant]) on the kinetic parameters of pNPPase from *H.salinarum* in reverse micelles (0,2M CTAB and 1M 1-butanol in cyclohexane) [25].

Chapter I

Cloning, expression and characterization of a novel Baeyer-Villiger monooxygenase from the extreme halophile *Haloterrigena turkmenica*

3.1 Introduction

3.1.2 Monooxygenases

Monooxygenases are enzymes that catalyze the insertion of an oxygen atom from the molecular oxygen into an organic substrate. Despite the reaction between molecular oxygen and the carbon of an organic compound is thermodynamically favored, the high barrier energy required for activating the process is what prevent the spontaneous combustion of organic matter.
This reaction is indeed spin forbidden, nevertheless many enzymes such as monooxygenases have found a way to overcome this issue and activate molecular oxygen. This activation occurs upon donation of electrons to molecular oxygen. The electron for the activation can come from the substrate itself (internal monoxygenases) or from an external donor (external monooxygenases), for example NADH or NADPH. In most cases, to transfer this electron to the oxygen, monooxygenases adopt an organic or metallic cofactor including heme prostetic group (e.g. cytochrome P450), copper (e.g. dopamine β monooxygenases), pterin (e.g. phenylalanine 4- monooxygenase), iron (e.g methane monooxygenase). For few monooxygenases the cofactor is not required for the catalysis, like the ActVA-orf6 from *Streptomyces coelicolor*.
An efficient and specific insertion of one oxygen atom into an organic substrate is a reaction difficult to perform in a chemical way. Monooxygenases are of extreme interest for synthetic purpose, the specific oxygenations catalyzed by this class of enzyme is unequalled by any chemical catalyst. Moreover, in monooxygenase catalyzed reactions, one atom of molecular oxygen is introduced into a substrate and the other oxygen undergoes reduction to water. In a historical period of time in which the environmental sustainability is becoming more and more a priority, having water as byproduct can not be more suitable to increment cleaner process in the chemical industries.

3.2.3 Baeyer-Villiger reaction

The transformation of ketones into esters or ketone into lactones by peracids is known as Baeyer-Villiger oxidation, in synthetic organic chemistry. The reaction has a wide range of application, from the synthesis of steroids, antibiotics, and pheromones to the synthesis of monomers for polymerization. The mechanism of the reaction consists in the nucleophilic attack of the peroxy acid to the carbonyl to form a tetrahedral intermediate, known as the Criegee intermediate (Figure 4). The reaction proceeds with a concerted

migration of one of the adjacent carbons to the electron deficient oxygen atom, with simultaneous dissociation of the O-O bond and release of the ester or lactone. In general the tendency of the adjacent carbons to migrate to the oxygen depend on its nucleophilicity, for example a tertiary alkyl group migrate more readily then a methyl group.

. Two prerequisite must be satisfied for successful alkyl migration (Figure5) [28]:

1. The migrating C-C bond has to be in a antiperiplanar position with respect to the peroxy bond.
2. A lone pair of the hydroxy oxygen atom must be in the *anti* position to permit the electron release to the migrating group.

Despite the classical Baeyer-Villiger oxidation is still widen used for the synthesis of chemical and pharmaceutical compounds, it lacks of the chemo-, regio-, and enantioselectivity that are needed and expected for organic synthesis. Moreover, many of the chemical oxidant which are used to perform the reaction (*m*-chloroperoxybenzoic acid, trifluoroperoxyacetic acid, peroxyacetic acid, and hydrogen peroxide) are often unstable, costly, shock sensitive, or explosive in condensed form. The use of these organic peracids produce an equivalent amount of carboxylic acids which need to be treated or recycled. These limitations to applications of the chemical Bayer-Villiger reaction addressed the research field towards its biological counterpart. The biocatalytic equivalent to the peracids is rep- resented by Baeyer-Villiger monooxygenases.

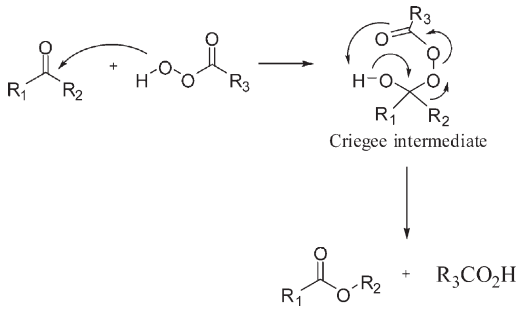

Figure 4. Baeyer-Villiger oxidation by paracids [37]

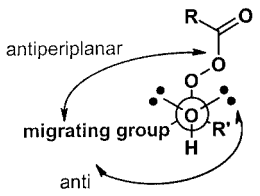

Figure 5. Stereoelectronic requirements for migration [127]

3.2.4 Baeyer-Villiger monoxygenases

Baeyer-Villiger monooxygenases are flavoenzymes that catalyse regio- and enatioselective Baeyer-Villiger oxidations and sulfoxidations. For their selectivity and catalytic efficiency, BVMOs are considered highly valuable catalysts for the synthesis of fine chemicals. These enzymes are NAD(P)H dependent flavoproteins and can be classified into two group: Type I BVMOs are composed by a unique polypeptide and contain a tightly bound flavin adenine dinucleotide (FAD) as cofactor and use NADPH as electrons source. As indicated by the presence of two Rossmann sequence motif (GxGxxG), this class of enzymes binds the flavin and the nicotinamide cofactor in two distinct domains. Members of this enzyme class can be identified by the presence of a strictly conserved sequence motif "FxGxxxHxxxWD/P" [29].
Type II BVMOs use FMN as flavin cofactor and NADH as electron donor and are composed of $\alpha_2\beta$ trimers. Recentely novel types of enzymes that catalyze Baeyer-Villiger reaction have been described. the bacterial flavoprotein monooxygenase MtmOIV and plant heme containing BVMO are enzymes that catalyze the baeyer-villiger reaction but not belong to class I nether class II BVMO. MtmOIV is involved in the synthesis of mithramycin, an antibiotic produced by the soil bacterium Streptomyces argillaceus. Heme dependent BVMOs have been found involved in the synthesis of brassinosteroids, steroidal hormones essential for the growth and development of plants.
Most biochemical and biocatalytic studies have been performed with Type I BVMOs. These monooxygenases are typically soluble and composed of only one polypeptide, representing a relatively uncomplicated oxygenase system with great potential in industrial applications.

3.2.5 BVMOs Biodiversity

Nowadays the genomic sequences of a wide variety of organisms are publicly available. With the development of novel sequencing techniques and bioinformatic tools it is possible to apply a genome mining approach also on organisms that are difficult or impossible to grow in artificial conditions. This silica pool of genomes offers an efficient way of retrieving novel putative BVMO genes. Although the molecular function and the basis for the conservation of the residues in the sequence motif (FxGxxxHxxxWD/P) remained obscure until recently, this *consensus* has represented a reliable tool to survey the (meta)genomes for Type I BVMOs. Bioinformatic analysis revealed a wide distribution of these enzymes among organisms. BVMO genes are particularly frequent among bacteria (about 1 BVMO per bacteria genome), whereas no Type I BVMO have been found in human and animal genomes. Among bacteria, these enzymes are prevalent in actinomycetes species, rendering these bacteria an interesting source for novel BVMOs. Also fungal genomes are relatively rich in BVMOs but only recently a BVMO from *Cylindrocarpon radicicola* have been cloned and produced in the recombinant form (30). Among plants only two Type I BVMO have been identified in *Physcomitrella patens* and *Cyanidioschyzon merolae* [31].

Studies on the biotransformation of natural products demonstrated that BVMOs play a vital role in microbial metabolic pathways. These enzymes, are largely found in catabolic pathways where catalyze key steps in the degradation of, for example, acetone [32]. Bulky cyclic aliphatic ketones [33], and linear ketones [34, 35, 36]. Microorganisms capable of growth on cycloalkanol or cycloalkanone metabolize the respective substrate to carboxylic acids that are further oxidized to acetyl-coenzyme A, through the fatty acid β-oxidation pathway. In this degradation pathway (Figure 6) the initial alcohol is converted in cycloalcanone by a dehydrogenase, then a BVMO catalyze the oxidation of the cycloalcanone into the coresponding lactone. Lactonization of a cycloalkanone prepares the ring-expanded molecule for hydrolysis by ring- opening enzymes such as ε-caprolactone hydrolase in the degradative pathways. [37]

Besides the important role in microbial degradation pathway, some BVMOs have also been identified in biosynthetic pathway. PtlE for example is responsible to the synthesis of neopentalenolactone D, a precursor of a sesquiterpenoid antibiotic, pentalenolactone, found in the Gram-positive soil bacterium *Streptomyces avermitilis* [38]. It has also been demonstrated that BVMOs play a role in another important biosynthetic pathway, the polyketide-derived secondary metabolites (aflatoxins) produced by *Aspergillus parasiticus* [39].

The main interest for BVMOs derive from their great potential as biocatalyst in industrial application but some BVMOs can also be of medical relevance. The etaA gene of Mycobacterium tuberculosis encode for a BVMO that has been shown to be responsible for activating thiocarbamide prodrugs [40]. Mutations in this gene make M. tuberculosis drug-resistant. These findings open the route for the design of novel drugs that have BVMO as (pro)drug target. These novel drugs may have the great advantages to be high specific for the pathogenic metabolism, as BVMOs are prevalent in proteomes of microbes while no BVMO gene is present in the human genome.

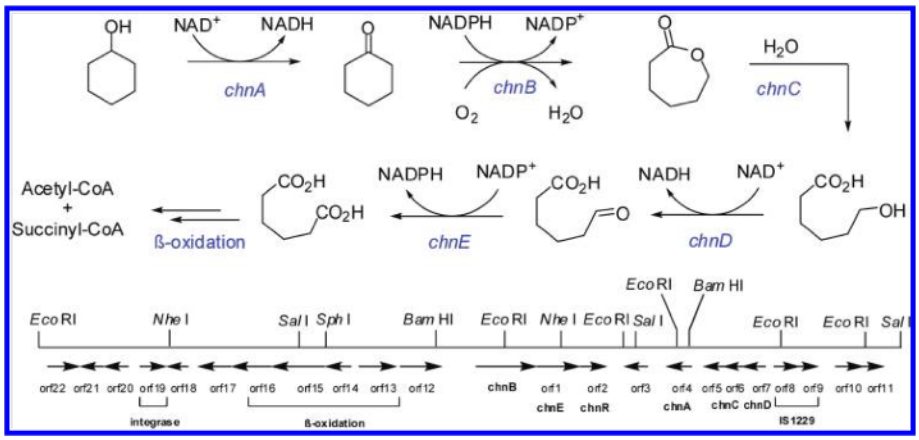

Figure 6. Biochemical steps of cyclohexanol degradation and the responsible genes in Acinetobacter sp NCIMB 9871 [37]

3.2.6 Mechanism of Type I BVMO

Spectoscopic and kinetic data on Cyclohexanone monooxygenase (CHMO) from *Acinetobacter calcoaceticus* outlined the first accepted mechanism for the enzymatic Baeyer-Villiger reaction. The mechanism have been demonstrated to be conceptually identical to that of the equivalent non-enzymatic processes [41].
The biocatalytic process is initiated by reduction of the tightly bound FAD (A, Figure 7) by NADPH. The reduced FAD (B, Figure 7) is rapidly oxidized by molecular oxygen to produce the flavin 4a-peroxyde anion (C, Figure 7), which is in equilibrium with the corresponding peroxide, the 4a-hydroperoxide (D, Figure 7). This intermediate constitutes the oxygenating species in the subsequent reaction and plays a role equivalent to peroxyacids in the chemical Baeyer-villiger oxidation. Oxidized $NADP^+$ remains tightly bound throughout the catalytic process and does not dissociate before the final hydrolysis and regeneration of the oxidized flavin.
The peroxide, attacks the carbonyl group of the substrate to give the ‘‘classical’’ tetrahedral Criegee intermediate. Rearrangement of this species results in formation of the product lactone and 4a-hydroxyflavin (E, Figure 7). The catalytic cycle is closed by elimination of water to form FAD and release of product and cofactor.

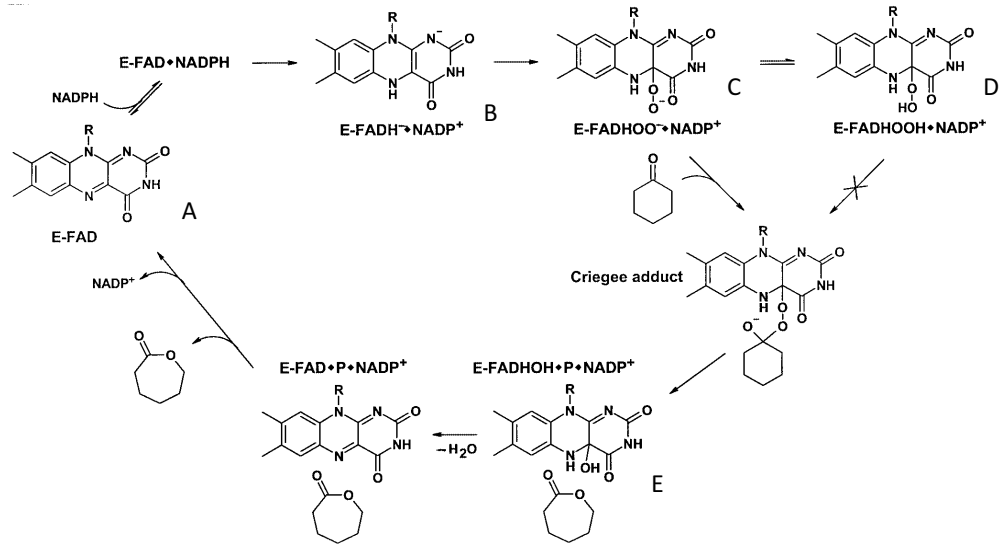

Figure 7. Scheme of the general mechanism of flavin-dependent Baeyer-Villiger monooxygenases

3.2.7 Structural features of BVMOs

The first crystallographic structure of a Baeyer-Villiger monooxygenase was obtained by Enrico Malito and coworkers in 2004 [42]. The thermostable Phenylacetone

monooxygenase from *Thermobifida fusca*, was crystalized and the general structure of Type I BVMOs was described for the first time.
PAMO consists of two domains (Figure 8) : the FAD-binding domain and the NADP-binding domain, Both domains exhibit the typical dinucleotide-binding fold.
The FAD cofactor exhibits the same binding mode found in flavoenzyme structures. The Ade ring is partly solvent-accessible, whereas the remaining part of the cofactor interact with the protein through van der Waals and H-bonds. On the *re* side of the flavin is located an arginine residues (Arg 337 in PAMO), that is strictly conserved among Baeyer-Villiger monooxygenases. Site directed mutagenesis on 4-hydroxyacetophenone showed the the mutation of the corresponding arginine into alanine completely knocks out the ability to catalyse the insertion of the oxygen atom into the substrate [43]. The crystal structure shows that it is part of the active site, located in front of flavin C4a atom, the locus where the peroxide adduct is formed. The positive charge of this Arg residue is supposed to stabilize the negatively charged flavin-peroxide intermediate, possibly forming direct H-bonds.

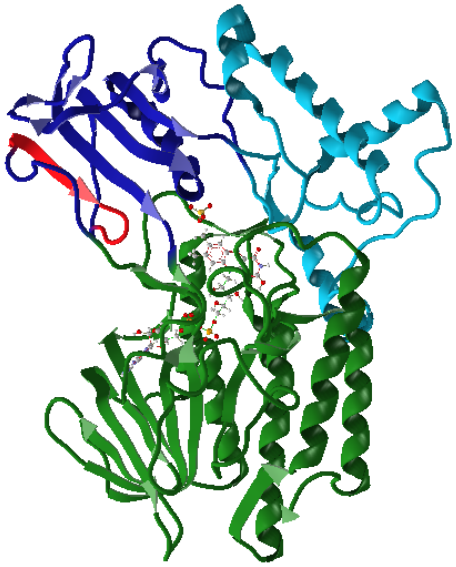

Figure 8. Ribbon diagram of the PAMO monomer. FAD binding domain is represented in green, NADP-binding domain in blue and the fingerprint motif in red. In cyano is represented a sub-domain of the classical NADP binding domain.

3.2.8 Catalytic cycle and conformational changes

The crystallographic structure of PAMO outlined the general structure of Baeyer-Villiger monooxygenases and gave some clues about the residues involved in the catalytic process. However, a more detailed models of the catalytic mechanism have been described in the following years, with the crystallographic structure of different conformation of CHMO bounded to the nicotinamide cofactors and the substrate [44].

the fingerprint motif aminoacids (FxGxxxHxxxWD/P), that identify type I BVMO, belong to the linker segment that connects the FAD-binding domain to the NADP-binding domain and are not directly part of the active site. Despite the motif is localized far from the active site, it plays an essential role in cofactor binding and catalysis. the strictly conserved aromatic ends are buried deep within the NADP binding domain and serve as "sticky ends" that fix the signature motif as a pin. The position of the central histidine is more flexible and depend on the presence or the absence of the nicotinamide cofactor. in the absence of NADP+/H this residue is completely solvent exposed, in presence of NADP+ however, this residue is rotated inward the structure and play an important role in the interaction between the FAD and NADP(H) binding domains and is also important in positioning the $NADP^+$ during the catalysis.

A complete model of the catalytic mechanism of a BVMO, which consider the conformational changes and different positions of the $NADP^+$ during the catalysis, was proposed in 2012 with the crystallographic structure of CHMO bounded to the substrate [45]. The fig. illustrates the catalytic mechanism, that begins with the enzyme in the NADP(H) and substrate-free form (state A, Figure 9). After binding of NADPH (state B, Figure 9) FAD cofactor is reduced while the enzyme assumes an Open-like conformation. Following the reduction the $NADP^+$ and the arginine (329 in CHMO or 335 in PAMO) will occupy positions that stabilize the reduced flavin. At this point the reduced flavin will react with molecular oxygen, forming the peroxyanion intermediate (state C, Figure 9), which is also stabilized by the same residues. The peroxyanion formation and the weak binding of the substrate in the binding pocket (state D, Figure 9), trigger a conformational change that permit the enzyme to adopt a tight-binding, CLOSED-like structure (state E, Figure 9). This particular conformation determines whether a substrate will be accepted by the enzyme, as well as what the regio- and enantiospecificity will be. From there, the enzyme will switch into a further conformational change that involves the rotation of $NADP^+$, the migration of the substrate into the catalytic position, and the shifting of R329 (state F, Figure 9). The R329 plays the role of a chaperone guiding the substrate into the catalytic position without allowing it to reorient, allowing at the same time the preservation of the stereochemical requirements imposed in the Closed conformation. The position of the $NADP^+$ at this point obstruct the exit pathway, preventing the substrate from diffusing away from the reaction site. Formation of the Criegee intermediate will occur (state G, Figure 9), followed by the formation of the lactone product. Once the product is formed, the enzyme will reverse its steps adopting once again the open-like conformation (state H and state I, Figure 9). the Open conformation causes the release of of the product to the solvent (state J, Figure 9), followed by the release of the oxidized nicotinamide cofactor (state A, Figure 9).

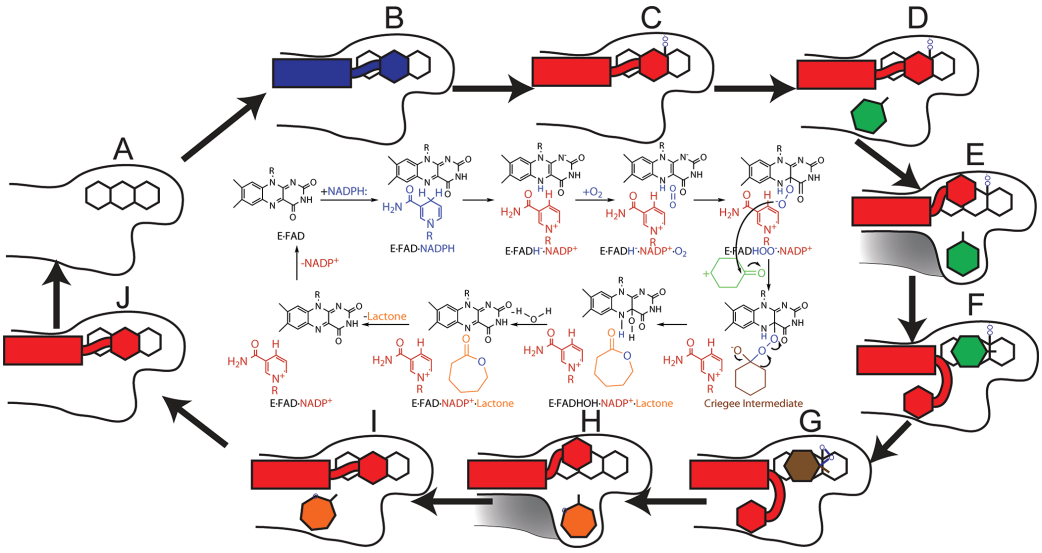

Figure 9. Scheme of the proposed mechanism for CHMO. The reduced NADPH is shown in blue, the oxidized $NADP^+$ in red, the substrate in green, the product in orange and the intermediate in brown.

3.2.9 Synthetic Application of Baeyer-Villiger monooxygenases

The enantio-,regio- and chemoselectivity of BVMOs have been exploited in several kinetic resolutions, regiodivergent oxidations and deracemizations to obtain enantiomerically pure intermediates.

3.2.9.1 Kinetic resolution

In a kinetic resolution the enantiomerically preferred substrate of an enzyme is rapidly converted, whereas the enantiomer that show a lower affinity with the enzyme is accumulated in an enantiomeric excess. Starting from an initial racemic substrate, this technique allows the recover of a maximum 50% yeld of the desired product or substrate enantiomer. Baeyer-Villiger monooxygenase have been applied in several kinetic resolutions of functionalized cycloketones to obtain bioactive chiral compounds (Figure 10) [37].

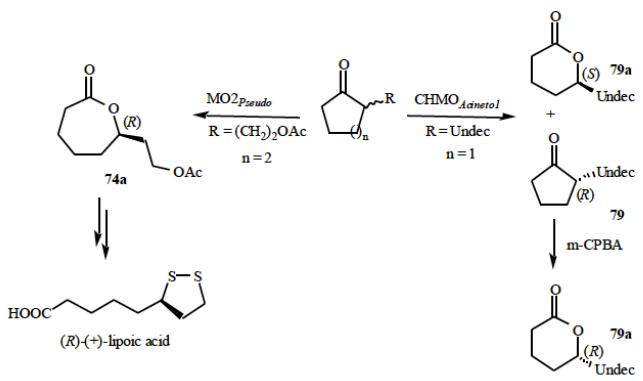

Figure 10. Chiral compounds obtained upon kinetic resolution of alpha-substitued cycloketones [37]

3.2.9.2 Dynamic kinetic resolution

Kinetic resolution process allows a maximum yeld of 50%, since only one isomer is converted, moreover the kinetic of the reaction must be controlled and interrupted before the enantiomerically non-preferred substrate start to be converted. To avoid this drawback a BVMO-mediated dynamic kinetic resolution has been developed for the enantioselective oxidation of 2-benzyloxymethyl cyclopentanone. In a dynamic kinetic resolution process the unconverted isomer of the substrate is racemized by mean a racemization reaction. In order to obtain a good enantiomeric excess the racemization must be faster or at least as fast as the conversion reaction. The racemization of (S) 2-benzyloxymethyl cyclopentanone was obtained by keto-enol tautamerization at pH 9 (Figure 11). Indeed, at basic pH the equilibrium between the ketone and the enol form spontaneously racemized the substrate, providing the preferred enantiomer to the enzyme. The process allowed the recover of (*R*)-6-Benzyloxymethyltetrahydropyran-2-one with a 85% yield and 96% enantiomeric excess [46].

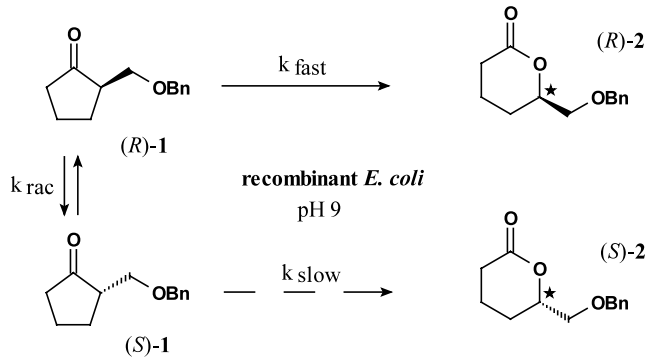

Figure 11. Dynamic kinetic resolution of 2-benzyloxymethyl cyclopentanone by *E.coli* whole cells expressing recombinant CHMO from *Acinetobacter* NCIMB 9871. [37]

3.2.9.3 Desymmetrizations

Unsubstitued cyclic ketones are prochiral compounds, and this mean that the addition of one atom disrupt the symmetry of these molecules, that become chiral compounds. Since BVMOs catalyze the insertion of one oxygen atom, these enzymes are the ideal biocatalytic tools for the desymmetrization of prochiral ketones. Moreover, the catalytic pocket of these enzymes often show an affinity higher toward only one of the possible product enantiomers. For example, we report here the desymmetrization of 3,5 dimethylcyclohexanone catalyzed by a purified form of CHMO from *Acinetobacter,* that allowed the recover of the product with a good enantiomeric purity. This process represented one fundamental step for the synthesis of the C_{11}-C_{16} subunit of ionomycin (Figure 12), a natural occurring polyeter antibiotic [47].

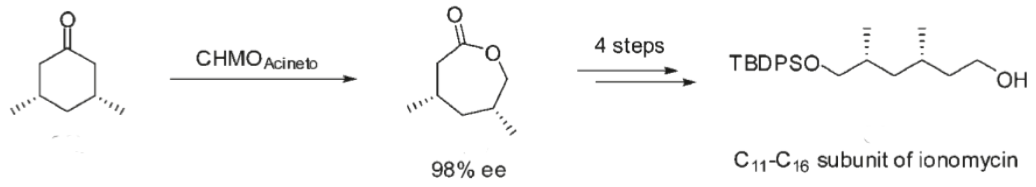

Figure 12. CHMO-mediated biosynthesis of C_{11}-C_{16} subunit of ionomycin. [37]

3.2.9.4 Regiodivergent oxidations

One of the most remarkable advantages of a BVMO-mediated oxidation of ketone is the possibility to yield two regioisomeric products. In contrast to the chemical Baeyer-Villiger reaction catalysed by peroxyacids, some biotransformation catalysed by BVMO are characterized by regiodivergency. In conventional Baeyer-Villiger oxidation, the expected "normal" lactone results by the migration of the more nucleophilic centre adjacent to the carbonyl group and "normally" this nucleophilic centre is the most substituted carbon atom. However, it has been observed that in BVMO-mediated oxidations a second product, the "abnormal" lactone is formed by the migration of the less nucleophilic centre and in many cases the two regioisomers are yielded in a ratio of 1:1 in high enantioselectivity. This difference respect to the chemical reaction can be explained considering that the substrate can be allocated in two different positions inside the active site. If in both the positions assumed by the substrate the different groups are arranged antiperiplanar to the peroxide functionality of the Criegee intermediate, the reaction is catalysed by the enzyme regardless of the nucleophilicity of migrating group. For instance the bioconversion of bicyclo-[3.2.0]hept-2-en-6-one yelded the "normal" and the "abnormal" corresponding lactone in a ratio of 1:1 using whole cells of *Acinetobacter* as biocatalysts. Both products, in good enantiomeric excess, are useful intermediate of building block: one for the syntesis of prostaglandine and the other for the synthesis of various brown algae pheromones. (48, 49)

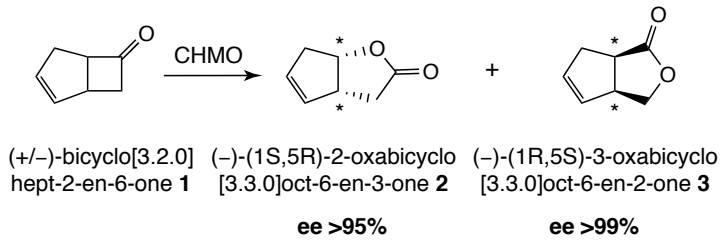

Figure 13. Oxidation scheme of bicyclo-[3.2.0]hept-2-en-6-one [37]

3.3 Aim of the project

The Baeyer-Villiger oxidation is an oxygenation reaction of ketones to esters and represents a powerful methodology in organic synthesis to insert an oxygen atom into a carbon-carbon bond. Biocatalysts like Baeyer-Villiger monooxygenases (BVMOs) are interesting instruments to perform this reaction, getting rapid access to valuable enantiomerically pure esters or lactones in moderate pH and temperature reaction conditions. Importantly, in a "green" perspective of industrial chemistry, BVMO enzymes represent a valuable alternative to catalysis by peroxyacids.

Over the last years, the identification of numerous Baeyer-Villiger monooxygenases have boosted the research on these enzymes, leading to a better understanding of the biocatalytic mechanisms and to a structure-inspired redesign for industrial application purposes.

In this line of research, we aimed to discover a novel BVMO to enlarge the toolbox of recombinant biocatalysts able to perform oxidation reactions of molecules with a potential pharmaceutical interest. Driven by the increasing industrial interest for biocatalysts that can cope with harsh reaction conditions, we focused our research on extremophile organisms, as potential source of robust and stable enzymes. Our bioinformatic analysis highlighted a putative BVMO in an uncommon organism for this class of enzymes, the halophilic archaebacterium *Haloterrigena turkmenica.* This organism was isolated from a sulphate saline soil in Turkmenistan, it requires at least 2M NaCl in the growth medium and shows an optimum growth temperature of 51 °C. Considering the particular features of this organism we planned to clone, express in recombinant form and characterize the putative Baeyer-Villiger monooxygenase of *Haloterrigena turkmenica*.

3.4 Results

3.4.1 Bioinformatic Identification

Over last years the number of available BVMOs has grown significantly, nevertheless the demand for other BVMOs keep growing to expand the biocatalytic diversity. All identified Baeyer-Villiger monooxygenases originate from bacteria or fungi and most of them work in catabolic pathway, in which they are involved in the degradation of organic molecules. Only recently two novel BVMOs were identified and characterized from two photosynthetic organisms: the red algae *Cyanidioschyzon meroale* and the moss *Physcomitrella patens* [31]. Genes for this class of enzyme were not found in Archeabacteria or Animal Kingdoms [50].

To cover a broader range of substrate types and enantio- and/or regioselectivities, new BVMOs have to be discovered. In the past, the common method adopted for discovering new enzymes has been the culture of microorganisms showing a specific activity, and then the rescue of the gene of interest through cloning. This time-consuming method was used for many years and has been successful to obtain most of the best-known BVMOs. However, up to 99% of bacteria in the environment are not readily cultured in the lab [51], especially extremophile microorganisms. In this way, most of the novel potential enzyme activities result unavailable.

Nowadays the genomes of a wide variety of organisms have been sequenced, offering a new and efficient way of retrieving BVMO genes. The development of genome databases and bioinformatics tools allow to look directly into this pool of genes *in silico* without growing and isolating any microorganism.

The BLAST research is one of the most powerful bioinformatics tool to perform the so called in silico genome mining. PAMO is one of the best characterized BVMO, its crystallographic structure is available and its thermostability features make it one of the most promising BVMO for industrial application. For all these reasons PAMO seemed a good candidate to be used as template to retrieve new putative BVMOs with promising biocatalitic features, and we chose its sequence for a tBLAST search. However, the simply searching for homologous sequences might have found many genes coding for flavoprotein monooxygenase that do not catalyze Baeyer-Villiger reactions. Therefore, the search for BVMO encoding genes was refined by looking for the presence, in the translated proteins, of the motif FxGxxxHxxxWD/P, that had been previously identified as specific of Type I BVMO by comparing sequences of characterized BVMOs [29].

Among the retrieved sequences, we looked for putative BVMO from organisms which are considered unusual for these class of enzymes, looking in particular at extremophiles. Using these screening criteria we identified a putative BMVO from the extreme halophilic archaea *Haloterrigena turkmenica* (Ht).

An accurate analysis of this sequence revealed several conserved regions containing sequence motifs that are known to be involved in dinucleotide cofactor binding; for

example, the two GXGXX(G/A) motifs highlighted the presence of two Rossmann fold. Furthermore, before the second Rossmann fold motif, the FXGXXXHXXXW(D/P) motif identifyed this sequence as a putative BVMO [29].

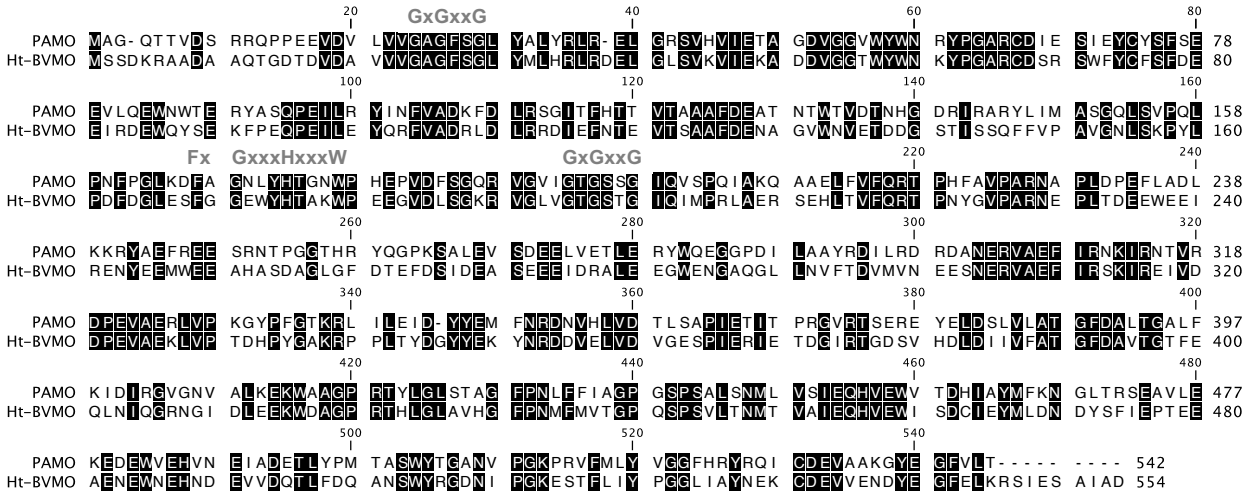

Figure 14. Alignment of Ht-BMO and PAMO aminoacidic sequences.

Haloterrigena turkmenica DSM 5511 is an extreme halophilic archaeobacterium isolated from a sulphate saline soil in Turkmenistan. It occurs mostly as single cells, rarely in pairs or tetrads, described as Gram-negative, ovoid to coccoid, 1.5-2 μm in diameter but can also be rod-shaped [52] (Figure 15). Neither spores, nor flagella, nor lipid granules were reported. Colonies are pigmented red or light pink due of the presence of C_{50}-carotenoids [52]. The strain $4k^T$ is chemoorganotrophic and aerobic, and requires at least 2M NaCl.

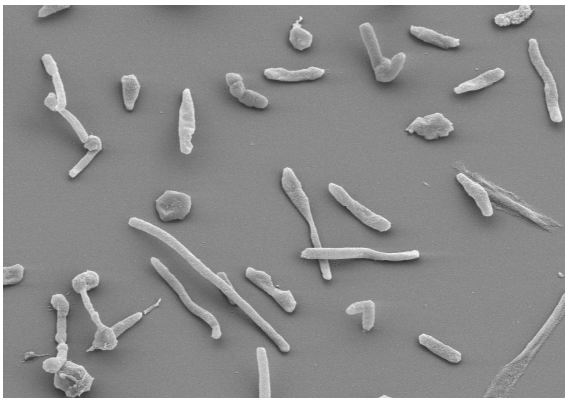

Figure 15. Scanning electron micrograph of H. turkmenica strain 4k [52]

The genome was fully sequenced in 2010 [53] and comprises one main circular chromosome of 3,889,038 bp length and six circular plasmids of 15.8 to 698.5 kbp length. The putative gene Ht-BVMO has been identified on one of these plasmid, pHTUR01.

3.4.2 Cloning of Ht-BVMO gene for the expression in *E. coli*

Protein expression in the bacterium *E. coli* is the most popular means of producing recombinant proteins. *E. coli* is a well-established host that offers short culturing time, easy genetic manipulation and low cost media. Within the realm of *E. coli* expression, the T7 system is the most popular approach for producing proteins. Plasmid pET28a (+), which carries the T7 promoter, the kanamycin resistance gene, and permits to add a hexahistidine coding sequence tail at the cloned ORF was used as expression vector. A common host for this expression system is the *E. coli* strain BL21 (DE3), which carries a chromosomal copy of the phage T7 RNA polymerase gene controlled by the inducible promoter lac. When the inducer Isopropyl β-D-1-thiogalactopyranoside (IPTG) is added, T7 RNA polymerase is expressed and becomes dedicated to transcription of the gene of interest.

The genomic DNA of *Haloterrigena turkmenica* does not represent a good choice as a starting material for the amplification and cloning of the gene of interest. Although the organism is available at the German Collection of Microorganisms and Cell Cultures (DSMZ), the presence of the plasmid pHTUR01 is not assured. Furthermore, differences in codon usage preference may lead to a variety of problems concerning heterologous gene expression. The analysis of the sequence for rare codons in *E.coli* reveals that the 16 % of the sense triplets in Ht-BVMO sequence have less than the 10% of codon frequency in *E. coli* (red bars in figure 16.). The presence of regions with underrepresented codons closed one to the other can lead to a significant reduction of the expression of the heterologous protein.

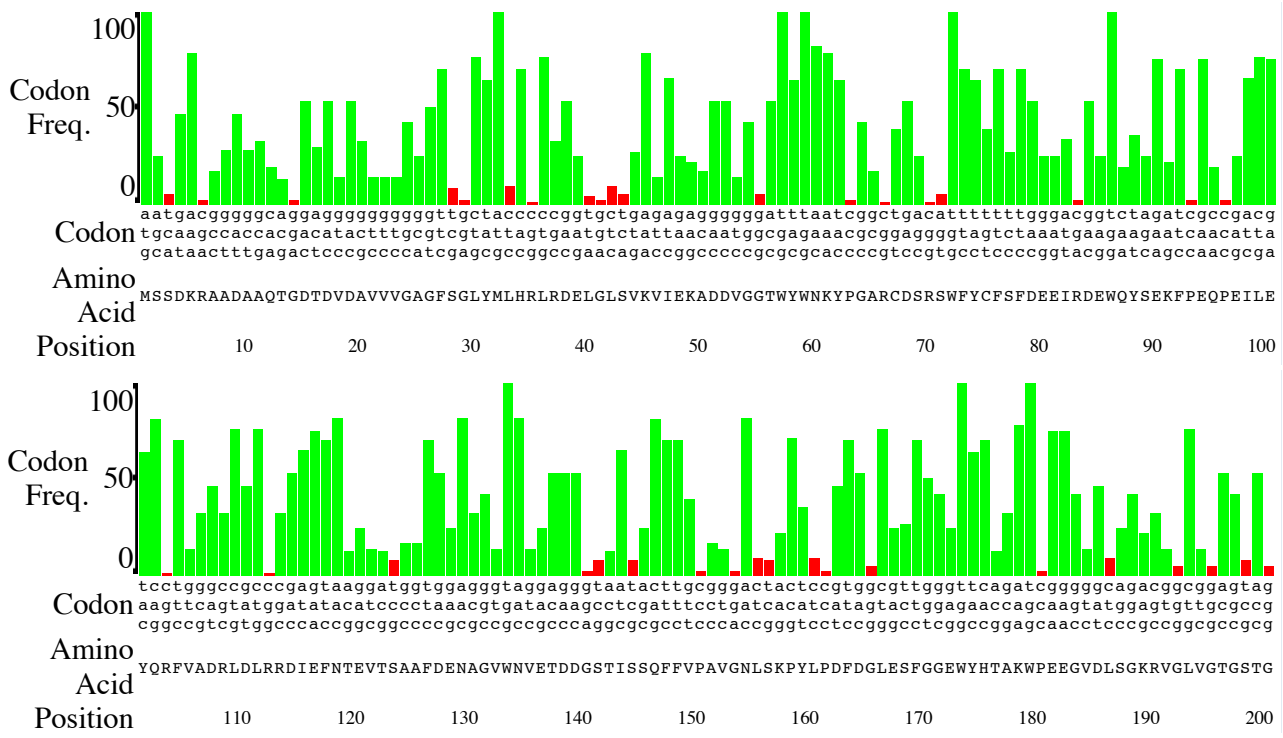

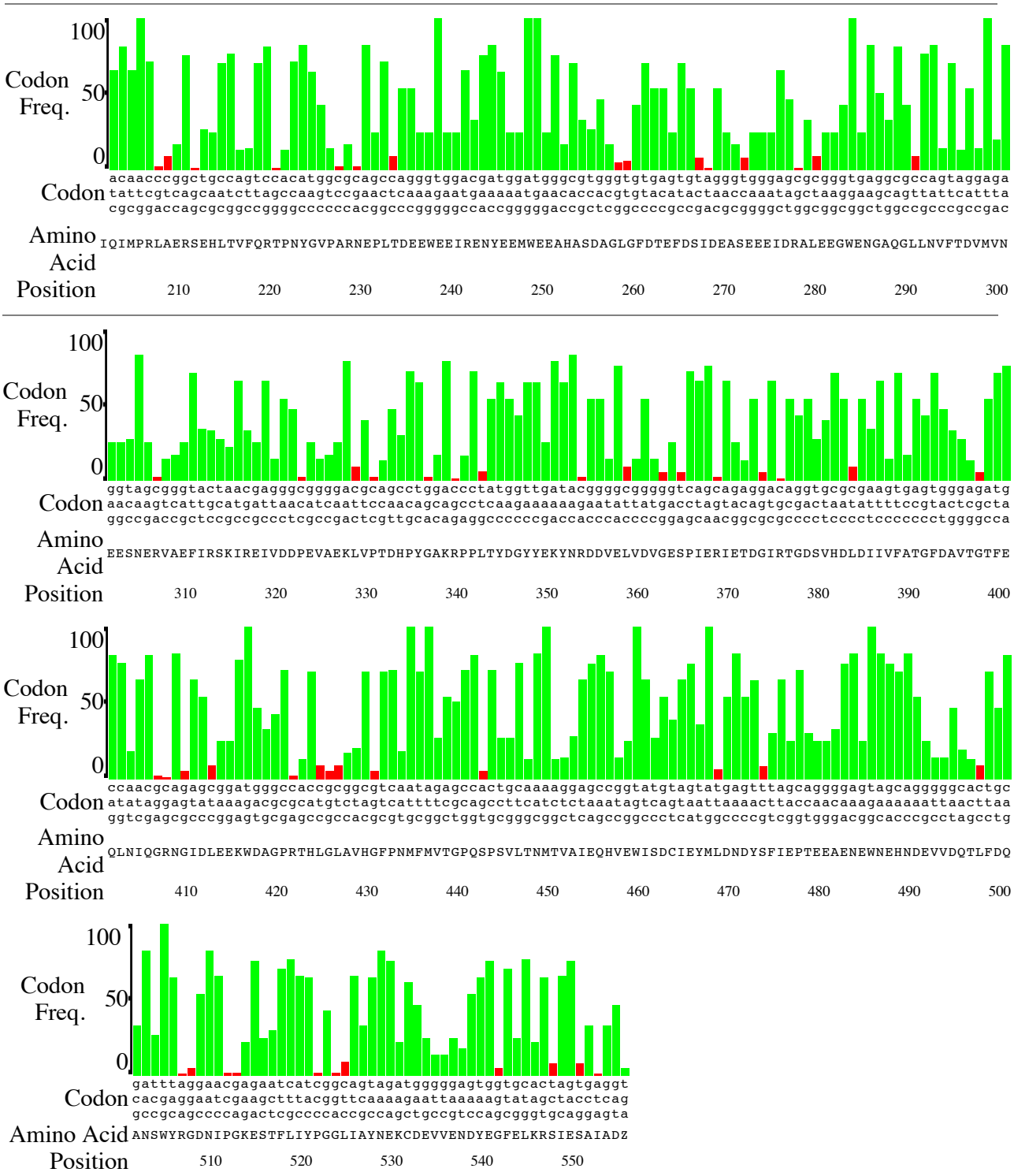

Figure 16 . Graphic report showing the sequence of Ht-BVMO and frequency with which each codon is used in *E. coli.* Red bars indicate a frequency below 10%, green bar indicate indicate a frequency of at least 10%

For these reasons, a synthetic gene (pHtur-CHMO) adapted to the *E. coli* codon usage and encoding the putative BVMO was assembled by GeneArt® and cloned into the plasmid pMK-RQ (conferring Kanamicin resistance). Recognition sites for the restriction enzymes *NcoI/NotI* were introduced to facilitate the cloning in the pET28a vector.

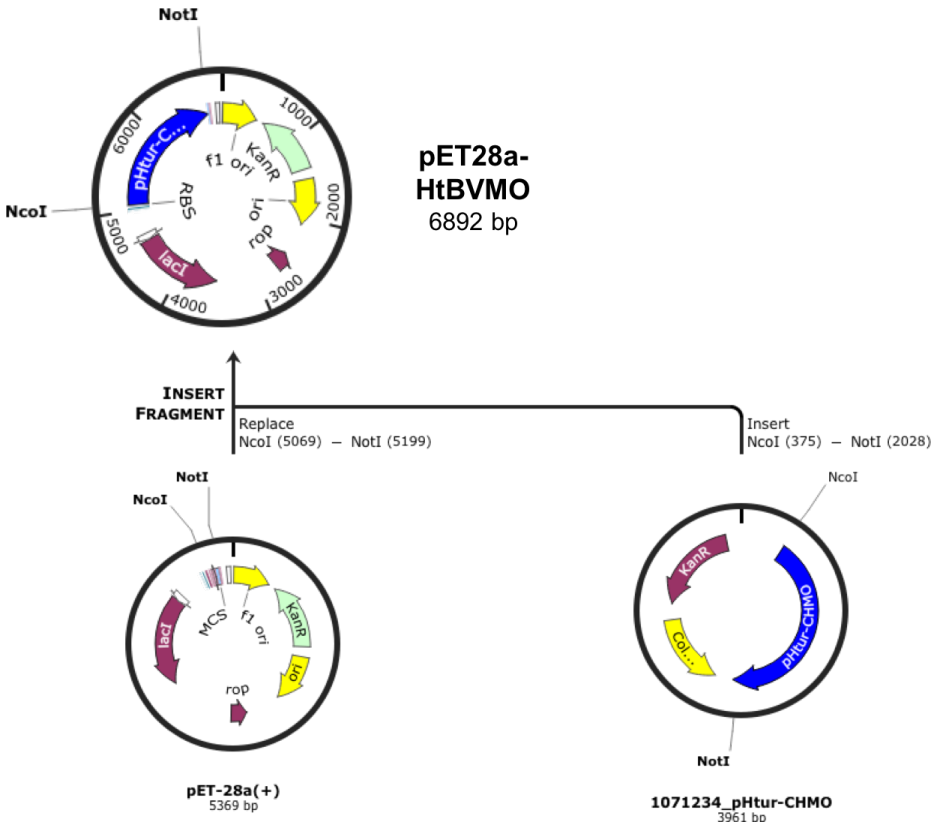

Figure 17. Scheme showing the cloning strategy adopted for the heterologous expression of Ht-BVMO in *E. coli*

The digestion of the purchased plasmid with NcoI and NotI restriction enzymes resulted in three DNA fragments due to the presence of a second NcoI site in the host pMK-RQ plasmid. All the produced DNA fragments were mixed in the same reaction with the pre-digested pT28a vector, in a so called "shot-gun" ligation. This technique has the advantage to skip the gel-extraction step of the DNA insert of interest. Nevertheless, a particular attention to the screening of the colonies is required, since different combinations of constructs could result.

The ligation mix was used to transform chemically competent XL1-BLUE cells and the resulting, kanamycin resistant, recombinant colonies were picked up for the screening. The plasmid present in each colony was purified and screened by digestion with NcoI and NotI. As expected, the screening showed the restriction pattern of different constructs; two colonies, named Ht-5 and Ht-35, showed the pET28a plasmid band at 5369 pb and the correct size of Ht-BVMO insert at 1653 pb (Figure 18). The ligation product of Ht-5 colony was further confirmed by sequencing the insert, which corresponded to the correct pHtur-CHMO sequence.

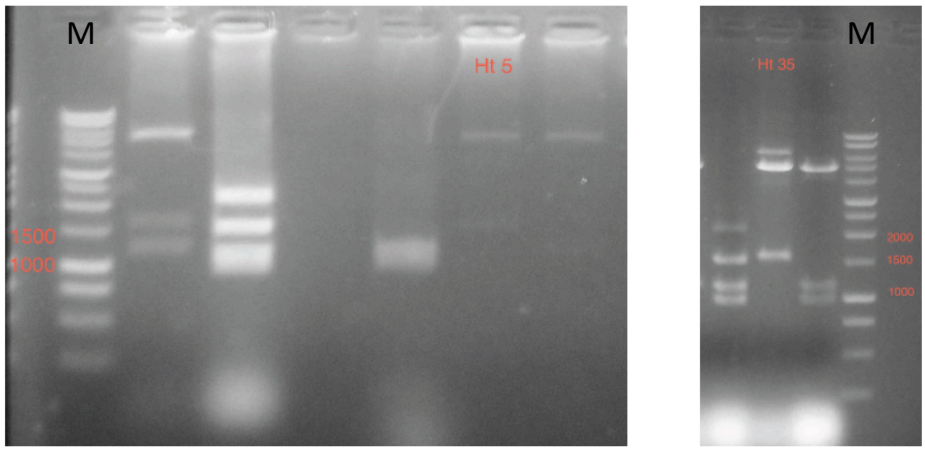

Figure 18. 1% agarose gel analysis of the digestion of the obtained clones using *NcoI/NotI*. M: standard marker.

3.4.3 Preliminary expression experiments

The pET28a construct was transformed in the BL21 (DE3) strain for preliminary expression analysis. In order to set up the proper conditions to obtain the recombinant soluble protein, different growth temperature were tested. Indeed, expression temperature has long been known as a key factor determining solubility of recombinant proteins in the cytoplasm of *E. coli* [54]. The SDS-PAGE in Figure 19 shows the proteins profile of cells at different induction times and at three different temperature (18, 30, 37° C), and compares the soluble and insoluble fractions obtained by centrifugation after cell disruption.

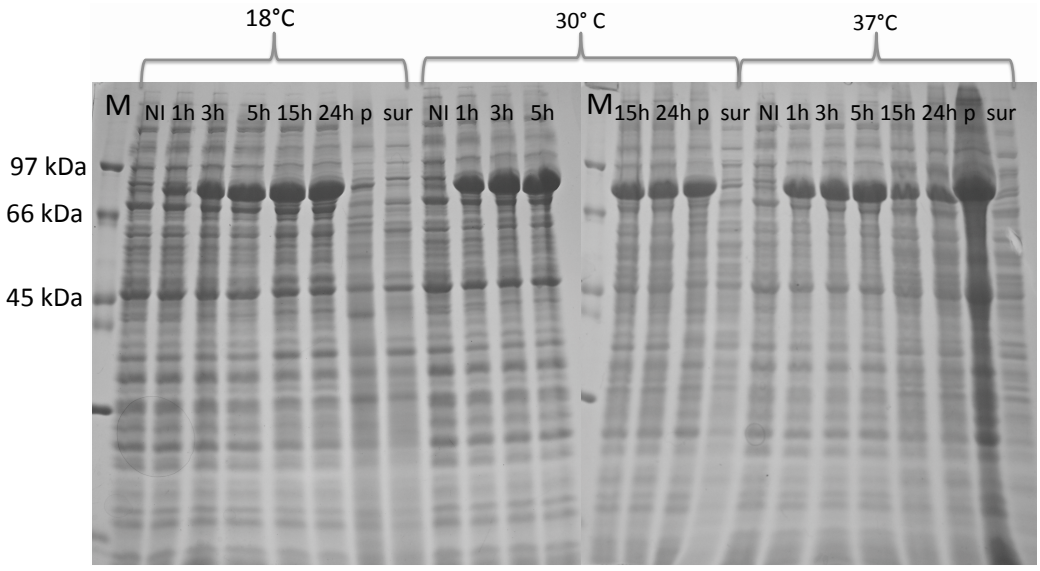

Figure 19. 12% SDS-PAGE analysis Ht-BVMO grown at 18, 30 and 37 °C induced with IPTG 0.2 mM. M: protein standard marker; NI: noninduced sample; 1h: 1 hour induced sample; 3h: 3 hours induced sample; 5h: 5 hours induced sample; 15h: 15 hours induced sample; 24h: 24 hours induced sample; p: pellet fraction of induced sample; sur: soluble fraction of induced sample.

It can be noted that, only three hours after the induction, a large amount of protein is accumulated. The high level of expression is verified at all the tested temperature, but after cell disruption the recombinant protein is detectable only in the insoluble cell fraction, collected as pellet. The immunoblot assay performed by using an anti-His-tag antibody, confirmed the identity of the recombinant protein and its expression as an insoluble product (likely accumulated in the cell as inclusion bodies).

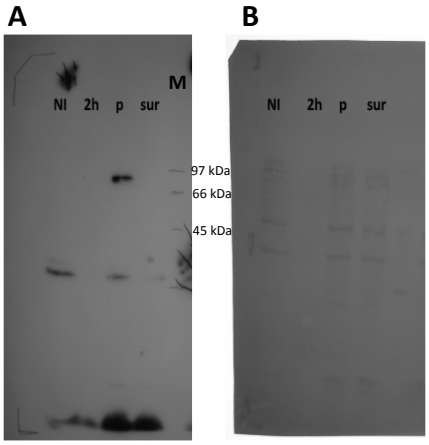

Figure 20. Western Blot (A) and PVDF membrane (B) of Ht-BVMO. M: protein standard marker; NI: noninduced sample; 1h: 1 hour induced sample; p: pellet fraction of induced sample; sur: soluble fraction of induced sample.

Beside the insolubility of the recombinant protein in the tested conditions, the SDS-PAGE also shows an aberrant electrophoretic mobility of the recombinant protein. Despite the calculated theoretical molecular weight of 63 kDa, the protein migrates at a height corresponding to about 80 KDa., The denaturing conditions adopted in the SDS-PAGE and the boiling of the samples before loading make unlikely the presence peptides attached to protein as a reason for the observed aberrant migration. To further confirm the identity of the recombinant protein we digested by trypsin the corresponding band of the acrylamide gel for a peptide mass fingerprinting analysis.

MSSDKRAADAAQTGDTDVDAVVVGAGFSGLYMLHRLRDELGLSVKVIEKADDVGGTWYWNKYPGARCDSRSWFYCFSFDE
EIRDEWQYSEKFPEQPEILEYQRFVADRLDLRRDIEFNTEVTSAAFDENAGVWNVETDDGSTISSQFFVPAVGNLSKPYL
PDFDGLESFGGEWYHTAKWPEEGVDLSGKRVGLVGTGSTGIQIMPRLAERSEHLTVFQRTPNYGVPARNEPLTDEEWEEI
RENYEEMWEEAHASDAGLGFDTEFDSIDEASEEEIDRALEEGWENGAQGLLNVFTDVMVNEESNERVAEFIRSKIREIVD
DPEVAEKLVPTDHPYGAKRPPLTYDGYYEKYNRDDVELVDVGESPIERIETDGIRTGDSVHDLDIIVFATGFDAVTGTFE
QLNIQGRNGIDLEEKWDAGPRTHLGLAVHGFPNMFMVTGPQSPSVLTNMTVAIEQHVEWISDCIEYMLDNDYSFIEPTEE
AENEWNEHNDEVVDQTLFDQANSWYRGDNIPGKESTFLIYPGGLIAYNEKCDEVVENDYEGFELKRSIESAIAD

Figure 21. Recostruction of Amminoacid sequence of Ht-BVMO. The eleven peptides (highlighted in red) from the triptic digestion of the overexpressed protein have been aligned with the amminoacid sequence of Ht-BVMO.

Eleven fragments, out of a total 22 obtained by the tryptic digestion, resulted significant peptides and matched with the sequence of the putative *Haloterrigena turkmenica* BVMO (prot_score 827), for a total coverage of 35,9% (Figure21).
The immunoblot assay and the mass fingerprinting analysis confirmed that the overexpressed protein corresponded to the recombinant BVMO of *Haloterrigena turkmenica.*
It is worth noting that this aberrant migration is characteristic of proteins from halophilic organisms and probably occurs due to the unusually high proportion of negatively charged residues (Asp and Glu) present in these proteins. The amino acidic sequence of the putative BVMO presents 120 aspartic and glutamic acid resuides (in a total 554 amino acids), which confers to the protein a pI of 4.1. This particular feature likely reduces the binding of SDS molecules to the unfolded protein, that exposes short hydrophobic regions interrupted by charged aminoacids, making the SDS-protein complex much less mobile. This modified electrophoretic run has already been described for other proteins purified from halophilic organisms [55].
In order to increase the fraction of correctly folded, soluble recombinant protein, we tried the expression of Ht-BVMO in the *E.coli* ArcticExpress (DE3) strain, grown at 12°C. This strain produces the heterologous chaperonin Cpn60 and co-chaperonin Cpn10, from the psychrophilic bacterium *Oleispira antarctica*, which both show high protein refolding activities at 4°C to 12°C and allow *E. coli* to grow at high rates (0.28 to 0.45 h-1) in this temperature range [56].

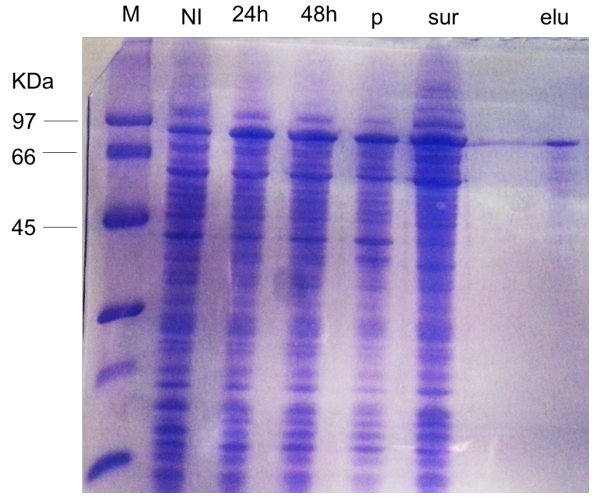

Figure 22. The ARCTICexpress strain was used as host for expression, induced by 0,2 mM IPTG and grown at 12°C. M: protein standard marker; NI: noninduced sample; 24h: 24 hour induced sample; 48h: 48 hour induced sample; p: pellet fraction of induced sample; sur: soluble fraction of induced sample, elu: elution by 250mM imidazole of the protein after loading onto a Nikel affinity matrix.

The capability of ARCTIC strain to grow and express the recombinant protein at low temperature was evaluated by collecting culture samples and checking the optical density at 24 and 48 hours. The culture reached the stationary phase at an optical density of 5,2

in 24h. After 48h, we did not observe a significant increase of total cell biomass nor in the level of expressed protein.
As shown in Figure 22, by expressing in ArcticExpress strain at 12°C, the recombinant protein was recovered in the supernatant fraction of the cell lysate. We proceeded to protein purification by applying a conventional protocol for IMAC chromatography through nickel affinity gel. By eluting in a standard buffer, such as 50 mM TRIS-HCl, we recovered about 8 mg of protein from one liter of culture. However, the purified form of the protein resulted colorless, even if highly concentrated at 20 mg/ml, contrary to what was expected. In fact, BVMOs are flavoproteins binding the flavin adenine dinucleotide, a molecule characterized by an absorption pick at 450 nm, and therefore appear yellow. The activity of the recovered recombinant protein was tested on several ketonic compounds, such as 2-butanone, 3-nonanone or cicloesanone, which are considered standard substrates for Baeyer-Villiger monooxygenases. Since these enzymes are oxidoreductases that catalyze Baeyer-Villiger reaction oxidizing NADPH, the activity assay was carried out at the spectrophotometer monitoring the NADPH consumption at 340 nm. In all these preliminary tests, the purified protein resulted completely inactive.

3.4.4 Customized protocol for the expression and purification of active Ht-BVMO

The lack of activity and the colorless aspect of the recombinant protein suggested the possibility of protein misfolding, that can be tentatively explained by considering the characteristic of the source organism of this enzyme. *Haloterrigena turkmenica* is described as an halophilic archaeobacterium which requires at least 2M NaCl for growth. Halophilic microorganisms have developed two different adaptive strategies to cope with osmotic pressure induced by the high NaCl concentration of the medium [57]. The strategy most frequently encountered in halophilic and halotolerant bacteria involves the synthesis and accumulation of organic compatible compounds in their cytoplasms. Reported studies on enzymes from halotolerant bacteria have shown that their molecular properties are not very different from those of non-halophilic proteins, in particular their enzymatic activity is inhibited by high salt concentration. In contrast, extreme halophilic archaea accumulate high concentrations of ions, such as potassium and chloride. Their soluble enzymes are, therefore, themeselves adapted to a high salt environment. Malate dehydrogenase from the halophilic archaeobacterium *Haloarcula marismortui* has been purified by pioneering methods 20 years ago and is now one one of the most studied and chacterized among halophilic proteins [17]. This protein requires NaCl or KCl concentrations higher than 2M to maintain its native state. The particular biochemical properties of halophilic proteins suggested therefore the possibility that the purified Ht-BVMO was inactive because of improper solvent environment and that this BVMO required a high ionic strength to be active and properly folded.
We modified the purification protocol by adding a concentration of NaCl up to 2M and the flavine adenine dinucleotide to a final concentration of 100 μM to the cell lysate. Through this step we aimed to assure the ionic strength required for folding of the protein

and facilitate the uptake of the cofactor during this process. Since the protein folding is a process that requires time, we incubated the cell lysate at 4°C for at least 12h. After the incubation we recovered the soluble proteins and proceeded with the nickel affinity chromatography, always keeping NaCl at a concentration of 2M in the equilibration and elution buffer. By using this protocol we were able to recover an active form of Ht-BVMO, which appeared bright yellow if concentrated.

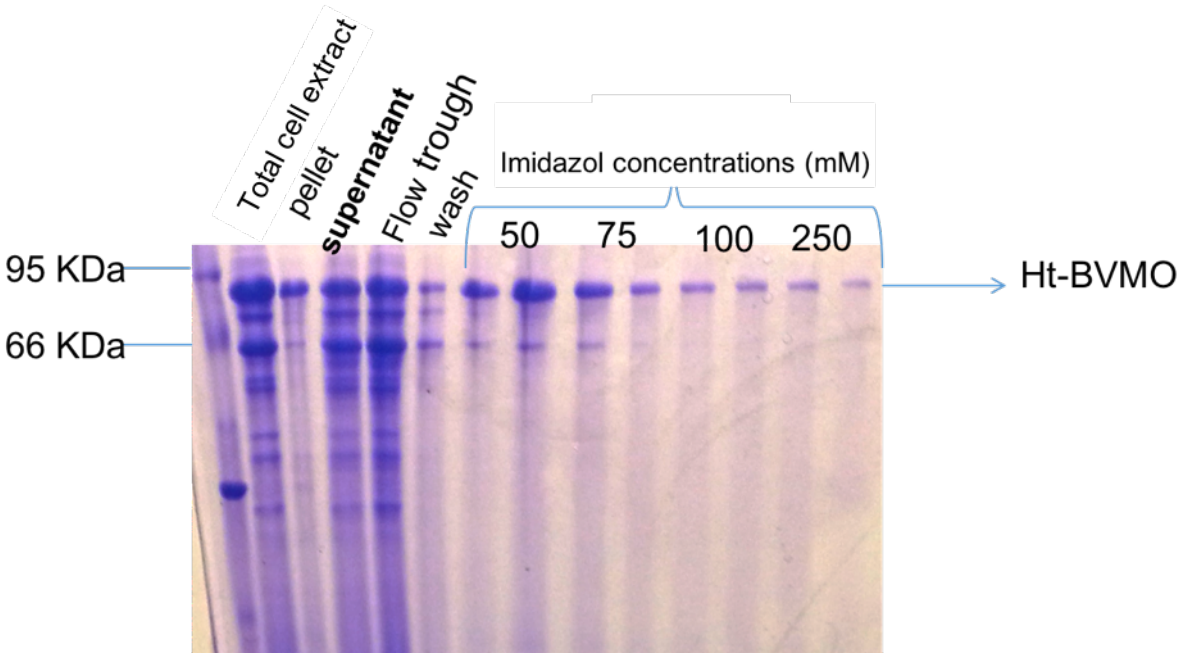

Figure 23. SDS-PAGE of Ht-BVMO purification by IMAC chromatography.

3.4.5 Optimization of the purification procedure

The SDS-PAGE in Figure 23 shows that a significant amount of recombinant protein was not retained by the resin during the purification and was lost in the flow through fraction. This is probably due to the high concentration of NaCl. In nickel affinity chromatography a concentration of 0,2 M NaCl is conventionally used to optimize the purification and get rid off the proteins that aspecifically bind to the resin. A concentration ten fold higher of positively charged sodium ions may compete also in the binding between the His-tagged protein and the nickel. Such hypothesis of a feeble binding is renforced by the relative low concentration (50 mM) of imidazole required for the elution of most part the recombinant protein. From the Figure 23 we can also observe that Ht-BVMO co-purify with a protein having a molecular mass of about 60 KDa. The contamination probably corresponds to the hetherologous chaperonin Cpn60 of the Arctic strain, that is observable as overexpressed protein in the non-induced sample in Figure 24.
Different approaches to remove this undesired contaminant were tested.

Presuming that the chaperone Cpn60 co-purify because bound to Ht-BVMO, we tried to remove it in column by adding a washing step with MgATP buffer before the elution. Indeed, substrate binding and release from chaperones are coupled to their ATPase activity. The ATP induces a turnover in the sites for substrate binding and produce an alternation of the chaperonine conformations. The two conformations are: the ATP-bound state, with low affinity and fast exchange rate for substrate, and the ADP-bound state with high affinity and slow exchange rates for substrate [58].

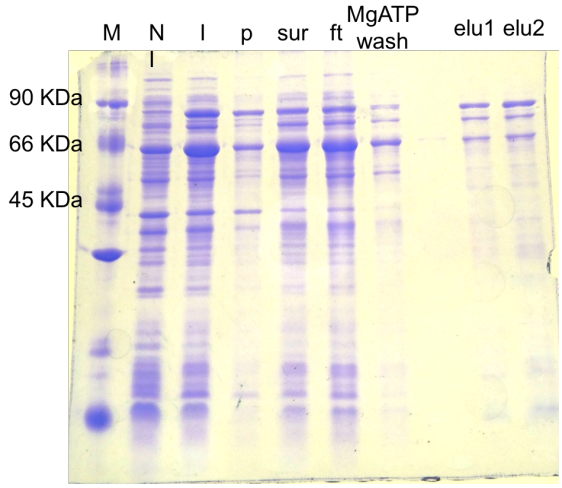

Figure 24. SDS-PAGE of fractions obtained from Ht-BVMO expression and from steps of the chromatographic purifications (in particular, wash in Mg-ATP for elution of the chaperonine Cpn60). M: protein standard for molecular weights; NI: non induced sample; I: 24 hour induced sample; p: pellet fraction from induced sample; sur: soluble fraction from induced sample, FT: flow through from IMAC chromatography. MgATP wash: wash of column with 5 mM MgATP. Elu: proteins eluted in 250mM imidazole .

The 5 mM MgATP buffer eluted the 60 KDa protein, but the removal was only partial and the final imidazole elution resulted still contaminated.

Since the MgATP wash resulted ineffective, in order to get a better purification, we tried a different approach by adding an additional step of ammonium sulphate precipitation after IMAC chromatography. The principle of ammonium sulphate precipitation lies in "salting out" proteins from the solution. The proteins are prevented to form hydrogen bonds with water and the salt facilitates their interaction with each other forming aggregates that are no more soluble and precipitate out of solution. By using this method we wanted to test the capability of Ht-BVMO to maintain the solubility in high concentration of ammonium sulphate, exploiting its properties as halophilic protein against the undesireded contaminants. For this purpose we dialyzed aliquots of purified protein (200 μl each) in ammonium sulphate buffer, testing different concentrations (0,5M, 1M, 1.5M and 2M). The dialyzed samples were collected after a 4°C overnight incubation and the soluble proteins were separated from the aggregates by centrifugation. The effect of the increasing concentration of ammonium sulphate on the quality of the purification can be evaluated in the SDS-PAGE in Figure 25, in which the precipitated

aggregates and the soluble fraction of the samples were compared.

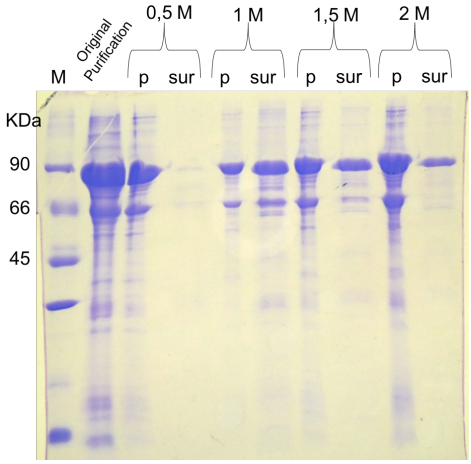

Figure 25. SDS-PAGE analysis of soluble and precipitated fractions obtained by dialysis at different ammonium sulphate concentrations. The concentration of the salt used for the dialysis is indicated. M: protein marker. Original purification: Ht-BVMO purified by IMAC chromatography. P: aggregated proteins collected as pellets after dialysis. Sur: soluble fractions collected after dialysis.

The increasing concentration of ammonium sulphate cause the aggregation of the undesired proteins in the samples and partially maintains the recombinant Ht-BVMO in a soluble state. The effect of the ammonium sulphate in cleaning the purification is particularly evident in the sample dialyzed against a concentration of 2M salt. Despite the ammonium sulphate precipitation helps in increasing the quality of the purified protein, the dialysis process sensibly lower the yield of soluble Ht-BVMO product (less then 1mg per liter of culture).

The Cpn60 of *Oleispira antarctica* expressed by the ARCTIC strain is a chaperonin that, unlike *E.coli* chaperonin GroEL/ES, is fully active at temperature below 15 °C. This strain of *E. coli* offers the advantages to express heterologous protein at low temperature maintaining the activity of the chaperonins. Moreover, it grows much faster than the parental strain at different temperatures: 3-fold faster at 15°C, 36-fold faster at 10°C and 141-fold faster at 8°C. [56].

Despite the advantages offered by the ARCTIC strain we tested the capability of BL21 to express Ht-BVMO at 12°C, so evaluating if the Cpn60 plays an actual role in folding the recombinant protein apart from increasing the growth rate of *E.coli* at low temperatures.

The SDS-PAGE presented in in Figure 26 shows that in both strains, BL21 and ARCTIC, the recombinant Ht-BVMO is expressed and that at least the 50% of the total yield results soluble. 1 liter of BL21 culture reaches an OD_{600} of about 5 in three days at 12°C, while the ARCTIC strain need only 1 day to reach the same optical density. In conclusion, apart from the low growth rate, the BL21 strain permits a better purification of the recombinant Ht-BVMO.

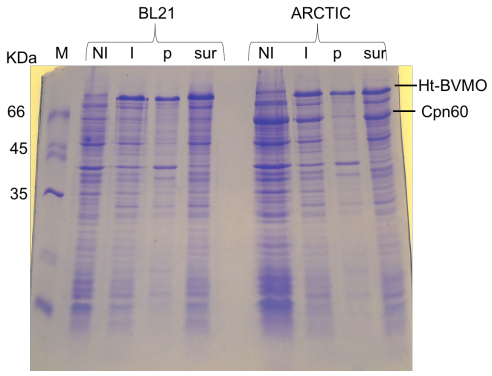

Figure 26. Comparison of total cell extracts from *E. coli* strains BL21 and ARCTIC expressing Ht.BVMO at 12°C. M: protein standard; NI: non induced samples; I: 24 hour induced samples; p: pellet fractions from induced samples; sur: soluble fraction from induced samples.

The cell lysate of BL21 was incubated in 2M NaCl and 100 μM FAD at 4°C overnight, and after IMAC chromatography in 2M NaCl buffer, the active form of Ht-BVMO was obtained. From the SDS-PAGE analysis of the eluted protein, the quality of the purification resulted still low. Although the contaminating Cpn60 was eliminated, the purification in a 2M NaCl buffer probably favors the formation of aggregates that can interact with the column matrix. Therefore we choose to introduce a further step of purification by using a butyl sepharose matrix. The graph in Figure 27A represents the chromatographic profile of the hydrophobic chromatography (HIC). 50 mM TRIS and 2M NaCl at pH 8 was used for elution; under this conditions the majority of the protein present in the injected sample was eluted with the solvent front, which appeared bright yellow while collecting the fraction. After collecting the protein of interest, the NaCl concentration of the elution buffer was decreased and the fractions 2, 3 and 4 were collected during the process. As shown in Figure 27 B, by exploiting the solubility of Ht-BVMO in high salt concentration, we were able to elute it in 2M NaCl buffer, while the contaminants were retained on the hydrophobic matrix of the column and eluted only at a lower concentration of salt (fractions 2, 3, 4 Figure 27 A and B).

A

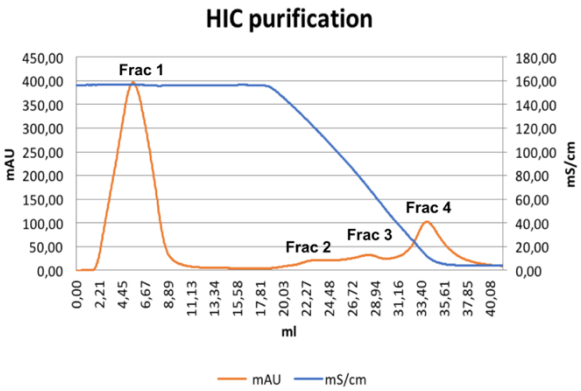

B

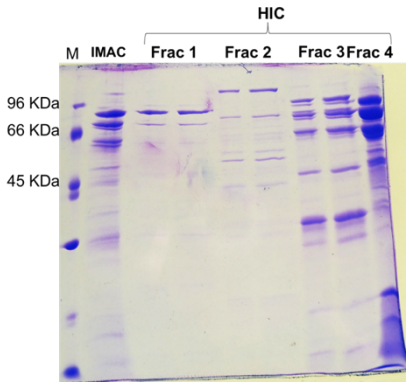

Figure 27. Hydrophobic chromatography purification profile (A) and SDS-PAGE analysis of the collected fractions (B)

From the SDS-PAGE analysis in Figure 27 B, HIC purification results effective in eliminating the contaminants retained in the affinity chromatography. In order to explore the possibility to further purify the protein we carried out a gel-filtration chromatography. The stationary phase of this chromatographic technique adsorb small molecules in pores. In contrast, molecules too large to enter the pores flow through the column more quickly and, therefore, are characterized by a lower retention time.
Besides the possibility of separating proteins on a dimensional criterion, gel-filtration chromatography gives also information about the molar mass and the quaternary state of the analyzed proteins.
The protein Ht-BVMO eluted from the previous HIC chromatography was then loaded on a Super OS 12 column and further eluted by a 2M NaCl buffer. The chromatographic profile of BSA, which is characterized by a molecular weight (68 KDa) similar to that of Ht-BVMO, was used as reference. As shown in Figure 28 B, the purification in 2M NaCl buffer of pure BSA protein produced 2 peaks in the chromatographic profile. Indeed, the high concentration of salt of this Buffer may favor the formation of aggregates, which in an exclusion size chromatography are characterized by a retention time lower than the monomeric form of the protein.
In contrast, in the chromatographic profile relative to the recombinant Ht-BVMO, the halophilic protein appears largely monodisperse. Moreover, the comparison of the profiles of the two proteins confirms that molecular weight of Ht-BVMO is about 63 KDa, similar to that of the BSA. As shown in the SDS-PAGE in Figure 28 B, the gel filtration technique seems do not significantly increase the quality of the purification respect to the hydrophobic chromatography. Considering this result, we decided to purify the protein by using only a preliminary IMAC chromatography and a final HIC chromatography.

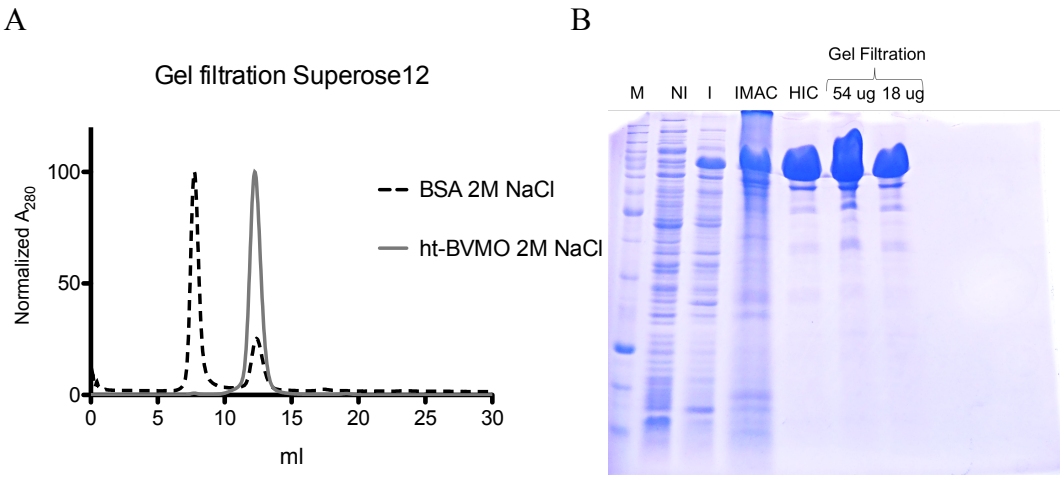

Figure 28. Gel filtration chromatographic profile of Ht-BVMO and pure BSA (A), and SDS-PAGE analysis of the collected fraction (B).

3.4.6 Spectroscopic properties of the flavin cofactor and determination of enzyme concentration.

Ht-BVMO and, more generally, Baeyer-Villiger oxygenases are enzymes that bound the flavine adenine dinucleotide as prosthetic group. The FAD cofactor originates from the riboflavine precursor, also known as riboflavin. Riboflavine (RF) consists of a ribityl side chain linked to an aromatic isoalloxazine ring structure. Riboflavin is phosphorylated to give FMN by flavokinase, and FMN is subsequently converted to FAD by FAD synthetase. Whereas free riboflavin does not have biological activity, the flavin cofactors FMN and FAD are the active groups of a large number of flavoproteins, in most cases non-covalently bound. The RF derivatives FMN and FAD are characterized by the ability of participate in both one- and two-electron transfer processes. This means that flavin molecules can exist in three different redox states: oxidized, singularly reduced (semiquinone) and doubly reduced. Therefore, they can participate in redox reactions as either one- and two-electron mediators, making the flavoenzymes very versatile in terms of substrate and type of catalysed reactions [59]. This is a major reason for the ubiquity of flavin-dependent enzymes in biological systems. In addition, the oxidized flavin molecule is susceptible to nucleophilic attack, especially at N-5 and C-4a.

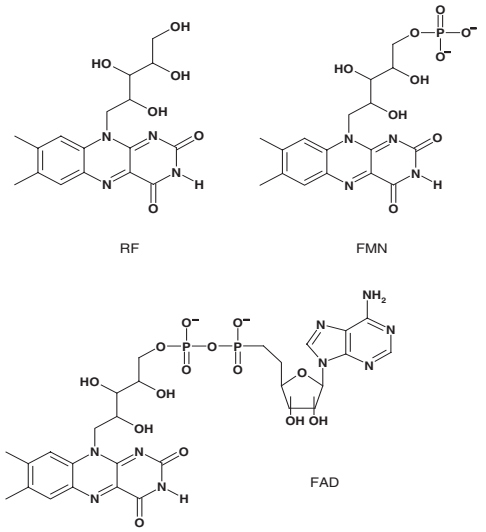

Figure 29. Chemical structure of riboflavin (FD), flavine mononucleotide (FMN) and flavine adenine dinucleotide (FAD)

In free solution (when not bound to an enzyme), the equilibrium of the different flavin species is dependent on pH, as shown in Figure 29. The scheme presents the different redox states and the different protonation states for each of them: oxidized, semiquinone (one-electron reduced) and fully reduced (two-electron reduced). Upon binding to a specific protein, this equilibrium can change dramatically and the redox potential can greatly vary, due to the crucial role of the protein environment. The redox potential for a free fully reduced flavin is about -200 mV, but in a protein complex it can range from -

400 mV to + 60mV. In general, the proximity of a positive charge is believed to increase the redox potential; a negative charge or a hydrophobic environment are expected to lower it [60]. Only 5-10 % of all flavoproteins are known to covalently link a FAD molecule, and site-directed mutagenesis studies suggest that the covalent interaction could increase the oxidative power of the flavin [61].

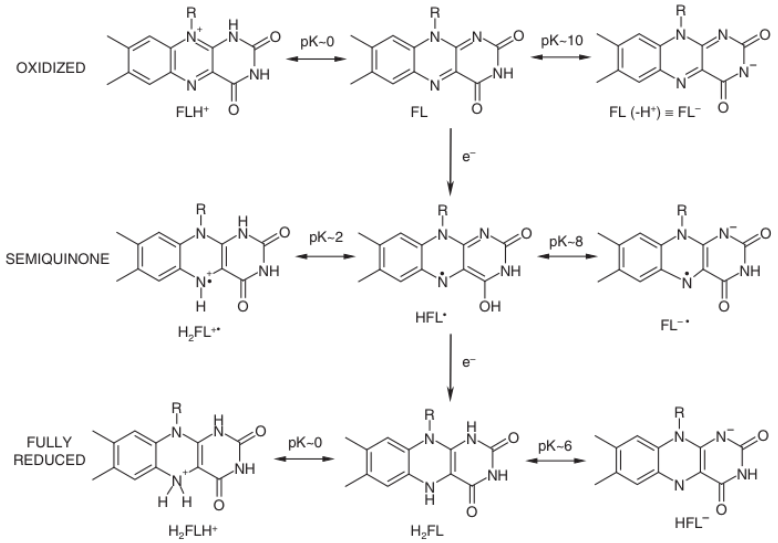

Figure 30. Redox and acid-base equilibria of flavins

The electronic absorption spectrum of flavin in aqueous solution exhibits two distinct peaks at 445 and 375 nm, indicative of π-π* transitions of the isoalloxazine moiety. The precise positions of the absorption maxima and the intensity of the absorption depend on the environment of the flavin chromophore. Therefore, the molar adsorption coefficient for the flavin cofactor bounded to the protein, differently and distinctly characterize each flavoenzyme.

The flavoenzyme binds the FAD cofactor in a stoichiometric way: therefore, by knowing the extinction coefficient for free FAD ($\varepsilon_{FAD,\ 450\ nm} = 11{,}300\ M^{-1}\ cm^{-1}$) it is possible to quantify the exact amount of the flavoprotein by measuring the concentration of free FAD after denaturation of the enzyme. The denaturing process is conventionally carried out by addition of 1% SDS in sample buffer: in the case of Ht-BVMO, since the protein was prepared and conserved in 2M NaCl buffer, we denatured the flavoprotein by heating the sample at 90°C for 10 minutes, so to avoid aggregation of SDS molecules. The concentration of the free-FAD, released upon protein denaturation, was calculated using the law of Lambert-Beer $A = \varepsilon * C * l$. Since Ht-BVMO is a monomeric protein, as indicated by the size-exclusion chromatographic profile, the concentration of the enzyme is equal to the concentration of free flavin. Once the concentration of the protein is known the law of Lambert-Beer can be used again to determine the extinction coefficient of the flavin-containing enzyme. Usually, a wavelength is chosen in which the flavoenzyme shows the

highest absorbance between 400 and 500 nm.
As shown in Figure 31, the FAD bound to Ht-BVMO presents a maximum absorption pick at 440 nm and the extinction coefficient ε_{440} was calculated equal to 13,6 mM^{-1} cm^{-1}.

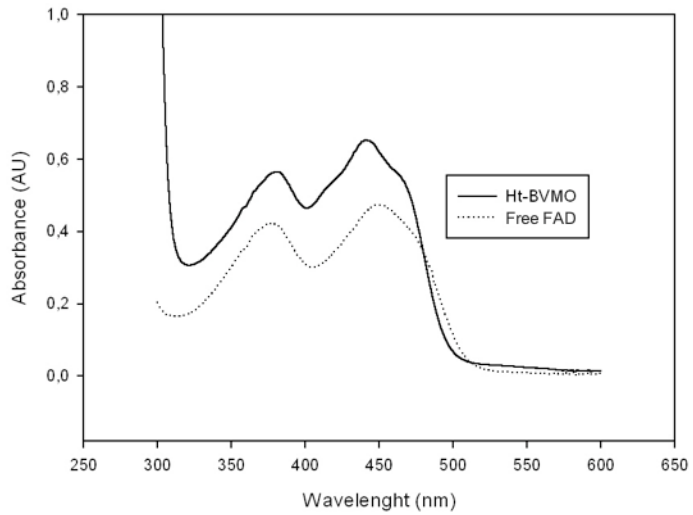

Figure 31 Uv-vis spectra of Ht-BVMO in native (solid line) and denatured (dashed line) states. The thermal denaturation released the FAD of the protein (free FAD).

The reduction of the flavin cofactor is thought to be one of the first step of the biocatalytic mechanism used by BVMOs, and it is characterized by the loss of adsorption in the UV-visible range. To verify the capability of Ht-BVMO in reducing the flavin cofactor, an amount of NADPH equimolar to the protein was added in cuvette. As a consequence of this addition, the loss of absorption at 370 and 340 nm was indeed registered.

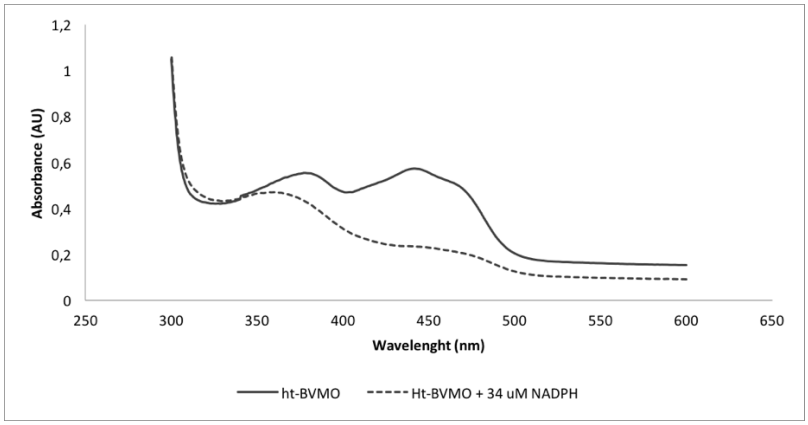

Figure 32. Uv-vis spectra of Ht-BVMO before and after addition of NADPH. Spectra of native protein (solid line) and after addition of NADPH equimolar to the protein sample (dashed line).

3.4.6 Dependence of the enzymatic activity from salt

As illustrated above, purification of Ht-BVMO in the absence of salt led to an inactive form of the protein. As the preliminary purification trials suggested an enzymatic activity strictly dependent on salt, this effect was studied in terms of salt concentration and quality. Activity assays were carried out in buffers containing different concentrations of NaCl or KCl. The enzymes in the final reaction mixtures was diluted 1/100: in such a way, the contribution of the salt present in the initial sample (2M NaCl) was only 1% of the final solution. In the assays, the concentration of salts ranged from 0 to 5 M NaCl or 0 to 4M for KCl. The upper limit of concentration was chosen for each salt near the its saturation level at 20°C, that is 6M for NaCl and 4,5 M for KCl. The initial rate of the reaction catalysed by the enzyme was registered by measuring the consumption of NADPH at 340 nm over the time.

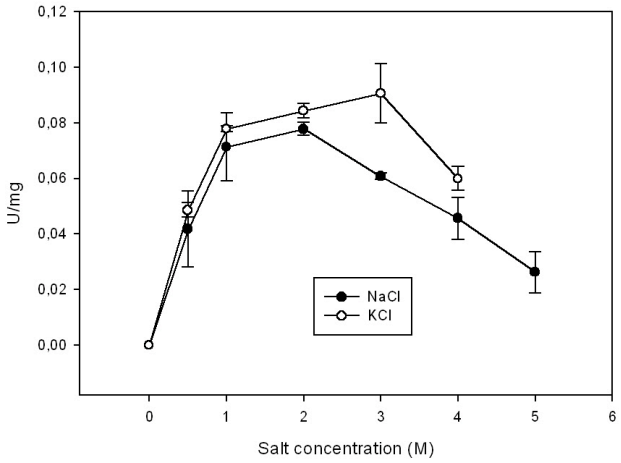

Figure 33 salt dependence activity of Ht-BVMO

A clear salt dependent activity was observed. As suggested by the preliminary assays no activity was detectable in the absence of salt. The optimum salt concentration was reached at 2M NaCl or 3M KCl. The lack of activity in the absence of salt could be due to denaturation of the enzyme. To verify this hypothesis, the active form of the protein was dialyzed in order to completely remove the salt. As expected no residual activity was detected after this step, even if a 2M NaCl buffer was used in the following enzymatic assay.
The possibility to refold the protein and restore the activity of the protein was explored. The inactive protein was dialyzed against 0,5M 1M or 2M NaCl buffer solution, but the activity was no more restored. To be sure that the FAD cofactor would be included in the protein during the refolding process, it was added to the dialysis solution in a final

concentration of 100 μM: no active protein could be recovered in this case too. We concluded that, if the loss of activity in the absence of salt is due to protein denaturation, it seems to be irreversible.

3.4.7 Dependence of the enzymatic activity from pH

To determine the pH optimum at which Ht-BVMO catalyzes the Baeyer-Villiger reaction, a NADPH depletion assay was employed. The absorbance at 340 nm was monitored to determine the initial rate of the reaction at different pH values at the constant NaCl concentration of 2M. For the assays, a buffer composed of TRIS MES and Acetate was used. This kind of buffer covers a wide-range pH spectrum (5.5 - 10), maintaining a constant ionic strength [62].

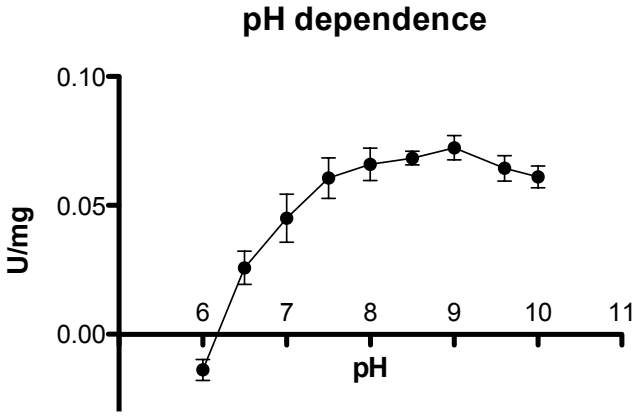

Figure 34 Activity of Ht-BVMO at different pH values.

The enzyme retains most of its activity in a range of pH between 7,5 and 10, reaching the optimum at pH 9. At pH values below 7,5 the activity sensibly decreases, reaching the 35% at pH 6.5 and the 0% at pH 6. On the basis of this test, the activity of the enzyme was considered stable at basic pH even at pH values over 9, but definitely sensitive to (even slightly) acidic environment.
Ht-BVMO is a very acidic protein, its aminoacidic composition being characterized by 22% of acidic residues. It is not unlikely that the protein requires a basic pH to maintain the negative charges of these acidic residues, which may have a role in maintaining the active and stable form of the protein.

3.4.8 Salt dependent folding

To assess whether the salt dependent activity of Ht-BVMO was related to the degree of folding, we recorded the far and near-UV circular dichroism (CD) spectra of the enzyme in presence of different NaCl concentrations. The CD spectrum in the far-UV region, from 250 nm to 190 nm can be used to provide quantitative estimates of the secondary structure content in a protein (63). In this wavelength region, the absorbing chromophore is principally the peptide bond, which is characterized by a weak but broad n-π* transition centerd around 220 nm and an intense π-π* transition at about 190 nm. When the amide chromophores of the polypeptide backbone are aligned in arrays, their optical transitions are shifted or split into multiple transitions due to "exciton" interactions (64). The result is that different structural elements have characteristic CD spectra: in particular, the α-helical content of a protein contributes to the negative elipticity registered at 208 and 222 nm. Since the spectra of proteins are so dependent on their conformation, we exploited this spectrophotometric technique to monitor the conformational changes brought about on Ht-BVMO by variations in the surrounding ionic strength.

The CD data were collected from 200 nm and 250 nm, so avoiding the light absorption and noise contribution of chloride ions in the 190-200 nm region. Although fluoride salts such as KF or NaF would be preferred since fluoride ion does not adsorb light in the far UV region, NaCl was chosen to allow a comparison with the biochemical and kinetic data.

As shown in the graph in Figure 35, the registered far UV-CD spectrum of Ht-BVMO in presence of a concentration of 0,1M NaCl was typical of an unfolded protein, as indicated by the negative elipticity at 200 nm and by the modestly negative elipticity in the 210-225 nm region.

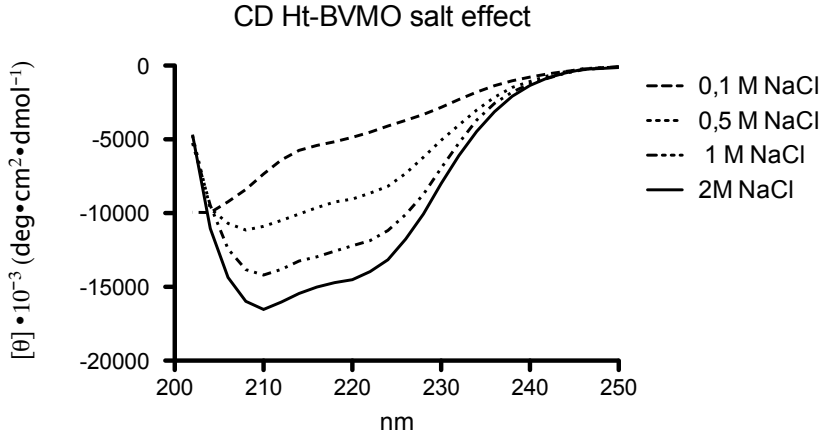

Figure 35. Far-UV CD spectra of Ht-BVMO in 50mM TRIS HCl pH8 in presence of increasing concentration of NaCl.

Table 1. Calculation of α-helical content upon deconvolution of acquired spectra at increasing salt concentration

NaCl (M)	α-helix (%)
0,1	3,95%
0,5	22,79%
1	28,87%
2	35,10%

The increase of salt concentration led to a progressive acquisition of overall alpha helical content. Indeed, the negative elipticity in the 210-225 nm region is more pronounced at increasing salt concentrations. Upon deconvolution of the CD spectra by the algorithm k2d3 (http://cbdm-01.zdv.uni-mainz.de/~andrade/k2d3//), the secondary structure content was quantitatively estimated (Table 1). A decrease in NaCl concentration from 2 to 0,5 M NaCl pointed to a decrease from 35% to 23% in the α-helical content.
Moreover, the unfolding effect of a low salt concentration on Ht-BVMO was found to be time dependent. Ht-BVMO in a 2M NaCl stock solution was diluted in a 0,5 M NaCl buffer and the conformational changes were followed over time.

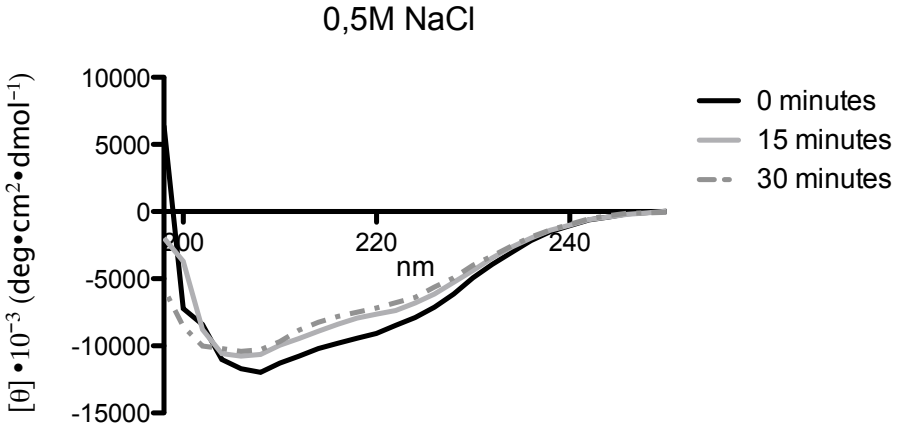

Figure 36. CD spectra registered during time dependent unfolding of Ht-BVMO

As shown in the plot of Figure 36 , in a 0,5 M NaCl buffer solution the alpha helical content of the protein significantly decrease in the first 15 minutes while the change in the following 15 minutes minimal.
The conformational changes of Ht-BVMO exposed to increasing ionic strength were further studied registering the CD spectra in the near UV region.

The near UV CD profile primarily arises from the environments of each aromatic amino acid side chain that absorb in this spectral region. In the case of Ht-BVMO in the native

state (2M NaCl), the side chains of these amino acids are supposed to be placed in a variety of asymmetric environments characteristic of the tertiary structure of the folded protein. Each of the aromatic amino acids are known to have a characteristic wavelength profile: tryptophan has a peak close to 290 nm with fine structure between 290 and 305 nm; tyrosine has a peak between 275 and 282 nm (the fine structure at longer wavelengths may be obscured by that from tryptophan); phenylalanine has a sharp fine structure between 255 and 270 nm [65]. The fine structure in these bands arises from vibronic transitions in which different vibrational levels of the excited state are involved.
Among the factors that can influence the CD spectra of aromatic aminoacids is the rigidity of the protein. The plot in Figure 37 shows a decreasing intensity of the CD spectra profiles consistent with the decrease of salt concentration. The lower ionic strength may influence the rigidity of the protein and contribute to a higher mobility of the aromatic side chain, whose absorption is characterized by a lower intensity in this environment.
The dependence of folding from salt concentration was further confirmed by analysing the thermostability profile of the protein. The melting temperatures of the protein at different salt concentrations were measured by a thermofluor screen and plotted in Figure 38.

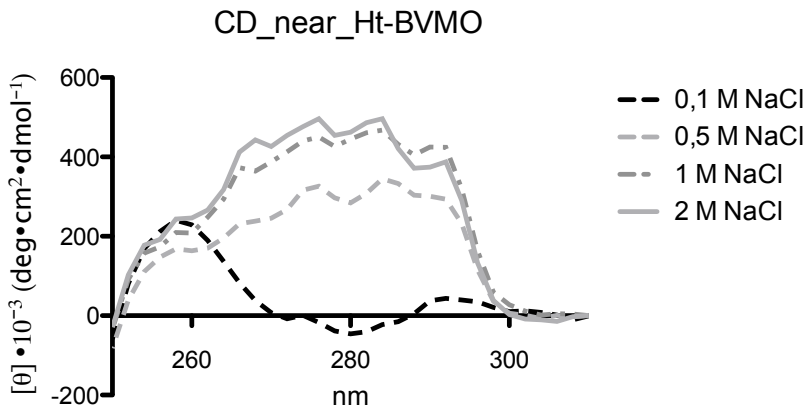

Figure 37. CD spectra of Ht-BVMO registered in the near-UV at different salt concentration

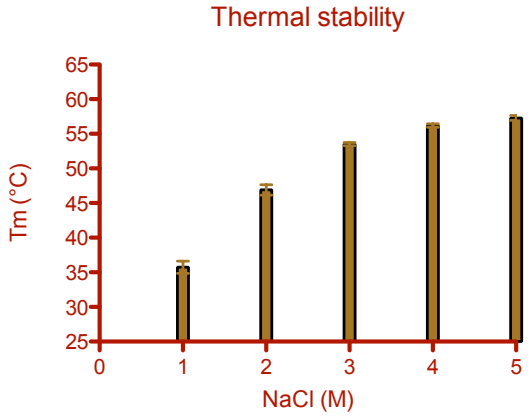

Figure 38. Thermal stability of Ht-BMO measured in solutions with increasing salt concentrations.

The increase in salt concentration correlates with an increase in protein thermostability. The ionic strength probably confers structural rigidity and stabilizes the protein. It is worth noticing that this increasing thermostability does not correlate with an increasing activity of the enzyme. In fact, although the highest melting temperature was found at salt concentration near the saturation level, the protein is not fully active in this environment. This is probably due the structural rigidity reached at this high ionic strength, which constrains the conformational mobility required to achieve catalysis.

3.4.9 Structural modelling of *Ht-BVMO*

In order to obtain structural insights into Ht-BVMO, we generated a tridimensional structural model using the SWISS-MODEL online workspace.
Building a homology model comprises four main steps: identification of structural templates, alignment of target sequence and template structures, model building, and model quality evaluation.
Up to now, among the characterized type I BVMO, the crystal structure have been solved for the four enzymes PAMO (Phenyl acetone monooxygenase), OTEMO (2-oxo-Δ(3)-4,5,5 trimethylcyclopentenylacetyl-coenzymeA), STMO (Steroid monooxygenase) and CHMO (Cyclohexanone monooxygenase).
The global alignment of the amino acidic sequence of Ht-BVMO with each one of the above mentioned proteins was evaluated using the program LALIGN. From the alignment, PAMO resulted the best matching enzyme with 76.9 % sequence similarity and 49.5 % identity. Therefore, the tridimensional model of Ht-BVMO was generated using PAMO PDB structure (PDB id: 1W4X) as template. To estimate the overall reliability of the model, the SWISSMODEL [66] workspace provides a tool to calculate The Global Model Quality Estimation (GMQE) score. GMQE score is expressed as a number between zero and one, reflecting the expected accuracy of a model built by using that precise alignment and that unique template. Higher numbers indicate higher reliability. The GMQE score reported for the model of Ht-BVMO is 0.77. The spatial coordinates of the residues in the obtained model were used to develop a map of the electrostatic potential distribution by using the PDB2PQR server [67]. The CHIMERA software was then used to visualize the electrostatic map as PQR file.

Ht-BVMO is characterized by a very high negative potential that probably results from the presence of clusters of aspartate and glutamate in its primary sequence. From the analysis of the tridimensional model, most of these negatively charged residues results located on the protein surface, exposed to the solvent. This enrichment in negative charges on the protein surface has already been observed in the crystal structure of other proteins from halophile organisms (e.g. the glucose dehydrogenase from *Haoloferax mediterraneii* [68]), and is supposed to favor solvation. The Figure 40 shows how the

negative potential of the protein is lowered and stabilized by increasing concentration of salts.

Some structural features which emerged from the analysis of the amino acidic sequence and the tridimensional model of Ht-BVMO are summarized in Table 2. The structural features of Ht-BVMO in table YY can be compered to that referred to PAMO and to an average globular protein in the Protein Data Bank [69] . This BVMO is characterized by a higher percentage of acidic residues compared to PAMO and to globular proteins of known tridimensional structure (21,66%, 13,84% and 11,76% respectively). Moreover, the ratio between charged (positive and negative) residues and hydrophobic residues is similar to that of PAMO and globular proteins, but the ratio of negative residue over the positive ones is two fold higher.

Always by analyzing the tridimensional model, it can be observed that the acidic residues are numerically predominant on the accessible surface of the protein in comparison to PAMO (42,02% versus 24,39%). Another noteworthy difference between the two proteins is the density of basic residues accessible at their respective surfaces. As a result, the overall electrostatic potentials of Ht BVMO and PAMO are very different. All these features are strongly in accordance with the common features of halophile enzymes and support the hypothesis of the role of the acidic aminoacids in increasing the protein solvation in presence of high ionic strength.

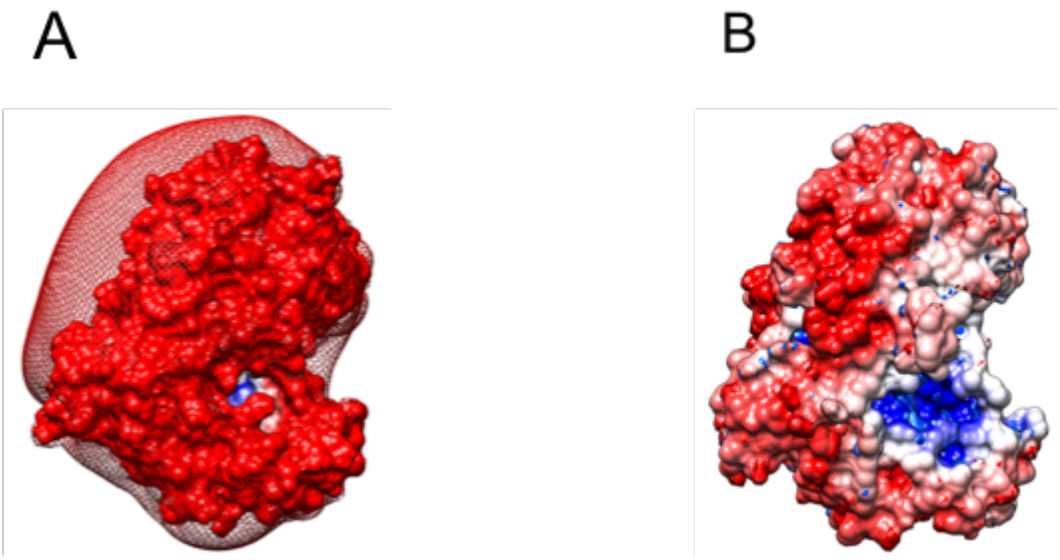

Figure 39. Surface electrostatic potentials of Ht-BVMO (A) and of PAMO (B), with the red color corresponding to negative potential and blue color corresponding to positive potential.

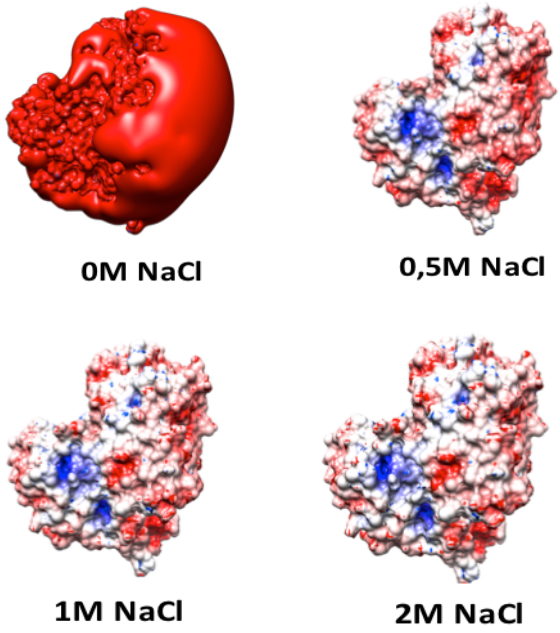

Figure 40. Surface electrostatic potential of Ht-BVMO as calculated by considering the protein in solutions of different salt concentrations.

Table 2. Analysis of amino acid content og accessible surfaces of Ht-BVMO, PAMO and globular proteins.

	Ht-BVMO	PAMO	Globular proteins [69]
Amino acid frequencies			
Asp+Glu (% of total residues)	21,66%	13,84%	11,76%
Arg+Lys (% of total residues)	0,08%	10,30%	10,66%
(Asp+Glu)/(Arg+Lys) ratio	2,73	1,34	1,1
Hydrophobic residues (% of total residues)	41,70%	47,20%	44,73%
Charged/hydrophobic residue ratio	0,52	0,51	0,50
Amino acid surface accessibilities			
Total accessible surface (Å^2)	21614,59	22158,52	
Accessible surface of Asp+Glu (Å^2)	9082,59	5403,37	
Asp+Glu (% of total surface)	42,02%	24,39%	
Accessible surface of Arg+Lys (Å^2)	3040,31	5143,93	
Arg+Lys (% of total surface)	14,07%	23,21%	
(Asp+Glu)/(Arg+Lys) surface ratio	2,99	1,05	
Accessible surface of hydrophobic residues	4444,20	6413,00	
Hydrophobic residues (% of total surface)	20,56%	28,94%	
Charged/hydrophobic surface ratio	2,73	1,64	

3.4.10 Steady-state kinetics

To explore the substrate preferences of Ht-BVMO, a set of ketone compounds, considered standard substrate for BVMOs, were tested in enzymatic assays. The selected substrates were linear aliphatic ketones, cyclic aliphatic and aromatic ketones. All the substrates were tested in the same reaction condition: temperature of 25°C, 50mM TRIS HCl, pH 8, 2M NaCl and 100 μM NADPH. The enzymatic assays were carried out in cuvette detecting and registering the initial rate of NADPH consumption at the spectrophotometer. The values of initial rate were registered for different concentrations of the ketone compounds, which resulted active substrates, and fitted to the Michaelis-Menten curve in order to retrieve the kinetic parameters. Table 3 summarizes the results of the screening and reports the kinetic constants of the accepted substrates.
In general, the enzyme showed a preference for aliphatic linear ketones, whereas cyclic aliphatic ketones, such as cyclopentanone, cyclohexanone or methil-cyclohexanone, were not accepted as substrates (table 4). The enzyme showed turnover numbers (K_{cat}) that fall in the same order of magnitude, with the highest values registered for 2-octanone and 2-heptanone. More relevant differences were found among the K_m values. The catalytic activity registered using the 2-butanone, resulted in the highest K_m, and this indicates that, among the tested substrates, this small molecule presents the lowest affinity for the enzyme. Concentrations of 2-butanone higher then 200 mM were observed to inhibit the activity of the enzyme. This substrate inhibition probably influenced the fitting with the Michaelis-Menten equation and contributed to increase the standard error deviation of the kinetic parameters. Among the aliphatic ketones, the best substrates resulted the 2-heptanone with a K_m of 0,09 mM and a K_{cat} of 0,277. Considering the sequence homology with Phenylacetone monooxygenase (50% sequence identity), the activity towards aromatic compounds was investigated. Interestingly phenyl-acetone was not accepted as substrate, whereas benzyl-acetophenone (4-phenyl-2-butanone) showed the highest affinity for the enzyme (K_m=0,017 mM), the longer carbon chain substituent on the aromatic ring seem to be a discriminant factor for the acceptance of the compound as substrate. Despite the low turnover number (k_{cat}: 0,15 s^{-1}), the highest catalytic efficiency of the enzyme was registered using the benzyl-acetophenone as substrate (Kcat/Km : 8,90).

Table 3. Kinetic state parameters of Ht-BVMO

substrate	Kinetic plot	Km (mM)	Kcat (s^{-1})	Kcat/Km
2-butanone 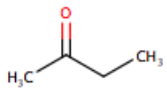	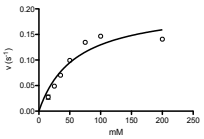	58 ± 14	0,20 ± 0,02	0,0034 ± 0,0009
2-heptanone 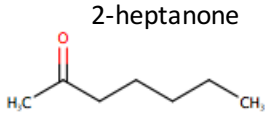	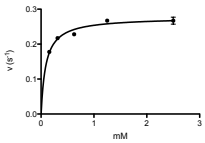	0,09 ± 0,01	0,277 ± 0,005	3,08 ± 0,35
2-octanone 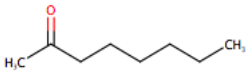	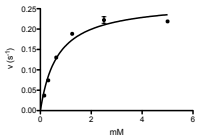	0,7 ± 0,1	0,27 ± 0,02	0,38 ± 0,06
3-nonanone 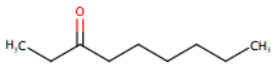	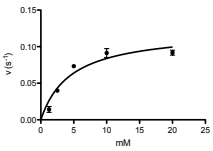	4,5 ± 1,3	0,12 ± 0,01	0,26 ± 0,008
4-phenyl-2-butanone 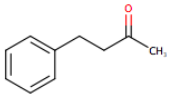	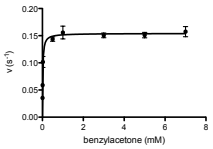	0,017 ± 0,002	0,155 ± 0,003	8,90 ± 0,89

Table 4. Tested compounds that were not accepted as substrates by Ht-BVMO

Ketone compunds not accepted as substrates				
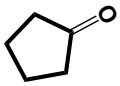	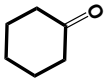	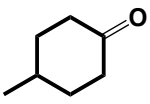	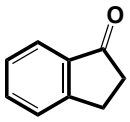	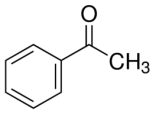
cyclopentanone	cyclohexanone	4-methyl-cyclohexanone	1-indanone	acetophenone

3.4.11 Biotransformations

Enzymes are catalysts with the capacity to synthesize an amount of valuable compounds even at a large scale industrial level. However, many enzymes with potential synthetic applications are underutilized, because they require one or more costly cofactors. In particular, oxidoreductases catalyse a number of industrially interesting reactions, but often they require nicotinamide cofactors (NADH or NADPH) as electron donors of the reaction. These nicotinamide cofactors, especially in their reduced forms, are too expensive compounds to be used in stoichiometric amount, and their, *in situ,* regeneration is often required for a large-scale synthesis. A commonly used method for coenzyme regeneration employs whole cells in combination with the recombinant expression of the required biocatalysts. This strategy has proved particularly successful with recombinant over-expression systems of BVMO [70]. The approach avoids laborious enzyme purification steps and exploits the coenzyme regeneration capacity of the host. Although whole cells have been shown to be effective instruments for Baeyer-Villiger conversions, they also exhibit limitations, for example, substrates and products may be toxic for the cells or be converted to side-products by the cell metabolism, and the conversion efficiency may be limited by a poor oxygen-transfer rates [71].

Another approach to overcome the coenzyme regeneration issue is the use of isolated enzymes, able to reduce the nicotinamide cofactors oxidizing a more sacrificial substrate [72]. Well known examples of such enzymes are alcohol dehydrogenases (ADH), formate dehydrogenases (FDH) and phosphite dehydrogenase (PTDH). Among them, PTDH is one of the most ideal candidate for use as coenzyme regenerating enzyme in combination with BVMOs. Advantages of PTDH include a favorable thermodynamic equilibrium ($K_{eq}=10^{11}$), that makes the oxidation of phospite to phosphate a nearly irreversible process. Moreover, phosphite and phosphate are innocuous compounds that can act as buffer. The selectivity of this enzyme for phosphite prevents any unwanted side-reactions that occurs, for example, when an alcohol dehydrogenase is used. Indeed, alcohol dehydrogenases oxidize alcohols to ketones, which are possible substrates of BVMOs and can generate unwanted side-products in the reaction mixture. Since the discovery of the wild type PTDH from *Pseudomonas stutzeri* [73] rational design was applied to improve efficiency in accepting $NADP^+$ as coenzyme and directed evolution significantly increased its thermostability.

Although a glucose dehydrogenase from the haloarchaea *Haloferax mediterraneii* has been characterized since 1996 [74], its use in bioconversion as cofactor regeneration enzyme in combination with a halophilic catalyst has not been reported in literature. We investigated the potential of Ht-BVMO in converting substrates into ester products using *Pseudomonas stutzeri* PTDH (Ps-PTDH) as cofactor regeneration enzyme. The main issue that we had to face was finding the proper reaction conditions in which a halophilic enzyme, the BVMO from *Haloterrigena turkmenica,* and a mesophilic regeneration enzyme, the PTDH from *Pseudomonas stutzeri,* were both active.

The activity of Ps-PTDH, in presence of different NaCl concentrations, was studied by enzymatic assay, registering the initial rate of $NADP^+$ reduction (Figure 41A).

A B

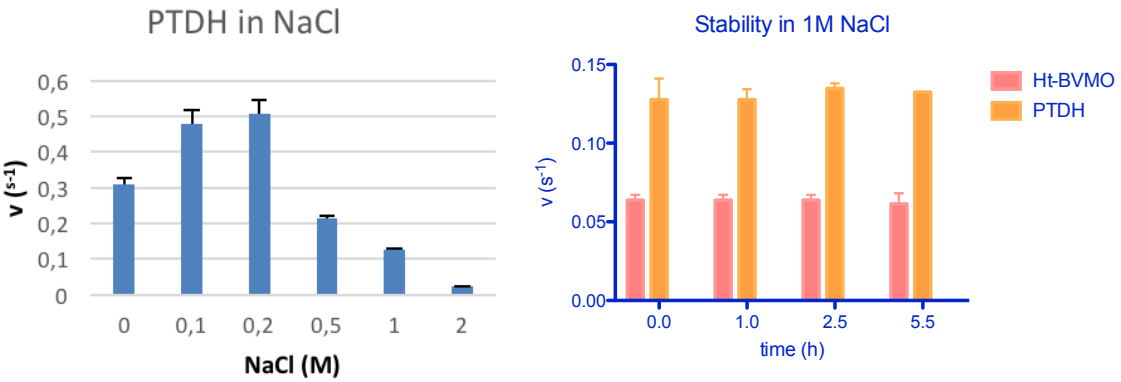

Figure 41. dependence of PTDH avtivity from salt (A) and stability of Ht-BVMO and *Ps*PTDH in 1M NaCl (B)

The activity of PTDH in presence of 200 mM NaCl resulted two fold higher compared to that measured in simple TRIS buffer. Higher salt concentrations caused a progressive loss of activity and in 2M NaCl the enzyme presented only 6% residual activity. In Bioconversions the rate of $NADP^+$ reduction should be faster or at least comparable with the rate of the reaction that convert the substrates into the desired products. Although in 1M NaCl the activity of PTDH was only the 40%, the rate of $NADP^+$ reduction in this condition resulted two fold higher than the rate of substrate (3-nonanone) oxidation catalyzed by Ht-BVMO. The stability of Ps-PTDH and Ht-BVMO in 1M NaCl was evaluated, registering their activity at regular interval of time for 5 hours (Figure 41 B). In this time window both the enzymes maintained their stability without loosing significant catalytic activity. Considering the stability of both the enzymes, we decided to carry out the conversions in 1M NaCl buffer for a prolonged time (20h), aiming to a complete substrate conversion. The reaction mixtures for the conversion were prepared using 25 μmoles of substrate in 5 ml of 1M NaCl buffer and held under continuous shaking for 20h at 24°C. Due to the volatile nature of the compounds, the gasses contained in the head space of the glass vessels were analyzed by Gas chromatography-mass spectromenty (GC-MS).

All the tested substrates were completely converted to the ester products (Table 5). The products of a BVMO-catalyzed oxidation can be classified in “normal” or “abnormal” ester, depending on the regioselectivity of the reactions. The expected “normal” esters are produced by the migration of the more nucleophilic carbon center, which in most cases is the more substituted carbon atom adjacent to the ketone group. Whereas a second

product, the “abnormal” ester is formed by migration of the less nucleophilic carbon center. The conversions catalyzed by Ht-BVMO produced all the expected esters that can be classified as “normal”, since they were produced from the migration of the more nucleophilic carbon center near the ketone functional group. Due to the low boiling point of the butanone compared to the other substrates, the chromatographic peaks assigned to the substrate 2-butanone and the product ethyl acetate were not fully resolved by the chosen analytical method (material and method section) and the yield of the conversion was not determined. However, the mass spectrometric analysis revealed the ethyl acetate as the final product and not the regioisomer methyl propionate. The enzymatic conversion of 2-butanone in methyl propionate is considered of high applicative interest. Indeed, this compound is used on a large scale as an intermediate in the production of acrylic plastics, such as polymers of methyl methacrylate. The principal route to manufacture the methyl methacrylate involves hydrolysis of cyanohydrins in the presence of sulfuric acid. Although widely used, this route coproduce substantial amounts of of ammonium hydrogen sulphate and disposal of this salt is highly energy intensive. The production of this compound by mean BVMO catalysis could significantly reduce its production costs in an environmentally friendly way.

Table 5. Conversion yield and schematic representation of substrates and products.

substrate	Km (mM)	Kcat (s^{-1})	Product	Yield
2-butanone 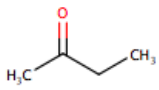	58 ± 14	0,20 ± 0,02	Ethyl acetato 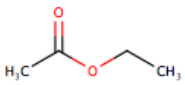	n.d.
2-heptanone 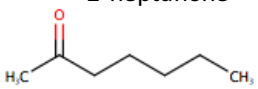	0,09 ± 0,01	0,277 ± 0,005	Acetic acid pentyl ester 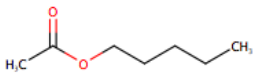	99%
2-octanone 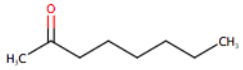	0,7 ± 0,1	0,27 ± 0,02	Acetic acid hexyl ester 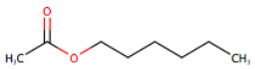	99%
3-nonanone 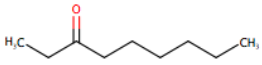	4,5 ± 1,3	0,12 ± 0,01	Propanoic acid hexyl ester 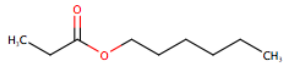	99%
4-phenyl-2-butanone 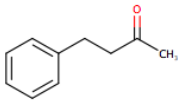	0,017 ± 0,002	0,155 ± 0,003	Acetic acid 2-phenyl ethil ester 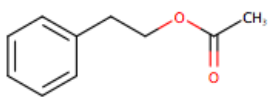	100%

3.4.12 Conversions at low salt concentration

Besides the difficulties that have been found in coupling the reactions catalyzed by this novel BVMO with a NADPH regeneration enzyme, the use of large concentration of salts may imply other applicative limitations for large scale synthesis. The electrolytes in solution can increase the oxidation rate of the metals that compose the pipeline systems and the materials of the chemical reactors, facilitating rust formation and corrosive processes. Therefore, we tried to find out better conditions to carry out the bioconversions, by looking for stabilizing agents of the halophilic enzyme at low salt concentration. Anions and cations with a high density charge have been previously reported to efficiently stabilize the folded form of the halophilic malate dehydrogenase from *Haloarcula marismortui* (75). The effect of magnesium sulphate and magnesium chloride on the activity of Ht-BVMO were investigated (Figure 42A), looking for a stabilizer of the enzyme at low salt concentration. Interestingly, low concentrations of both these salts increased the activity of the enzyme. Using a concentration of 0,1 and 0,2 magnesium sulphate the activity was registered respectively 1,6 fold and 15 fold higher respect the activity at the same concentration of NaCl.

Figure 42. Dependence of the activity of Ht-BVMO (A) and PTDH (B) from NaCl, $MgSO_4$ and $MgCl_2$

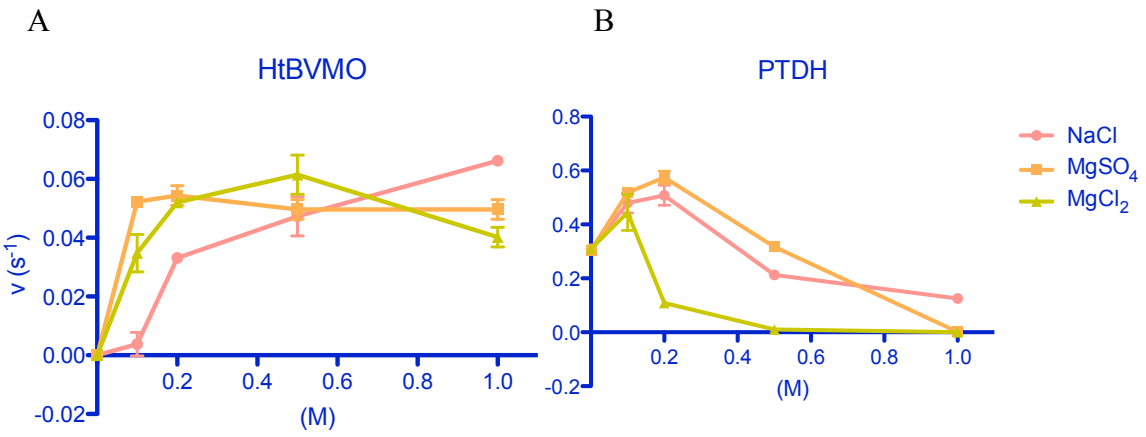

The effect of these salts was also studied on the activity of Ps-PTDH (Figure 42B). At high concentrations, NaCl resulted the most tolerated salt, whereas at low concentrations, magnesium sulphate maintained the highest activity. Magnesium chloride resulted the less tolerated salt by Ps-PTDH, even at low concentrations. Considering the high activity of Ht-BVMO at 0,2 M magnesium sulphate we decided to carry-out a bioconversion at this salt concentration. We were able to completely convert 5 mM 2-heptanone in a 0,2 M $MgSO_4$ buffer (Table 6). The reaction mixture for the conversion was incubated for 20 hours at 24°C but considering the enzyme stability in this kind of buffer the substrate was

fully converted in the first 2 hours. Indeed, the enzyme resulted unstable for a long time in this condition, loosing its activity within only 2h (Figure 43).

Table 6. Conversion of 2-heptanone in acetic acid penthyl ester in 0,2M Magnesium sulphate

substrate	Km	Kcat	Product	Yeld
2-heptanone 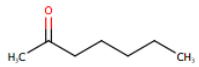	0,09 ± 0,01	0,277 ± 0,005	Acetic acid pentyl ester 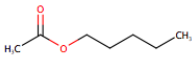	99%

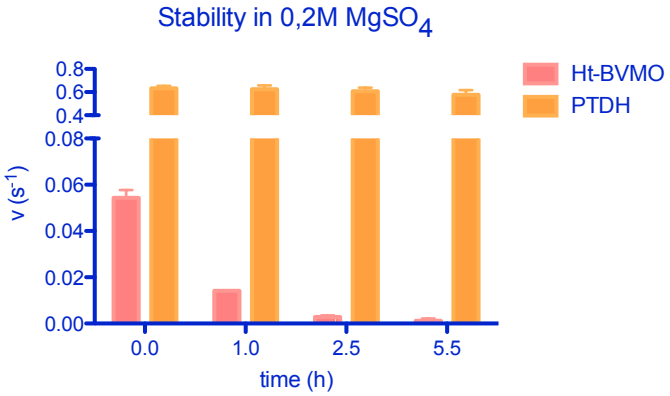

Figure 43. Stability of Ps-PTDH and Ht-BVMO in 0,2M Magnesium sulphate

3.4.13 Stability and activity of Ht-BVMO in organic media

Aqueous media are the conventional media for biocatalysts, but in recent years, research addressed toward the possibility to carry out enzymatic reaction in organic media. Catalysis in organic media offers several advantages among which, the higher solubility of hydrophobic substrates, a minor tendency of both substrates and products to be hydrolyzed, elimination of microbial contaminations in the reaction media [20]. Despite these advantages, enzymes in organic solvents are often denatured because stripped of the external water layer which is essential for their structural stability and catalytic activity, hindering the development and the applicability of this technology [76].
Techniques such as enzyme immobilization, chemical modification, reverse micelles, can stabilize enzymes in organic media, nevertheless the employment of solvent tolerant enzyme, which naturally remain stable in organic media, are the first choice for biocatalysis in non aqueous-media. Halophilic enzymes work in extreme high salt

concentration and considering that salt tend to greatly reduce the water activity, these enzymes may be the choice for biocatalytic processes in low water activity environment such as aqueous/organic media [20].
In order to further investigate the biochemical features of Ht-BVMO, we examined the effect of different water-miscible organic solvent on the activity and thermostability of this enzyme.

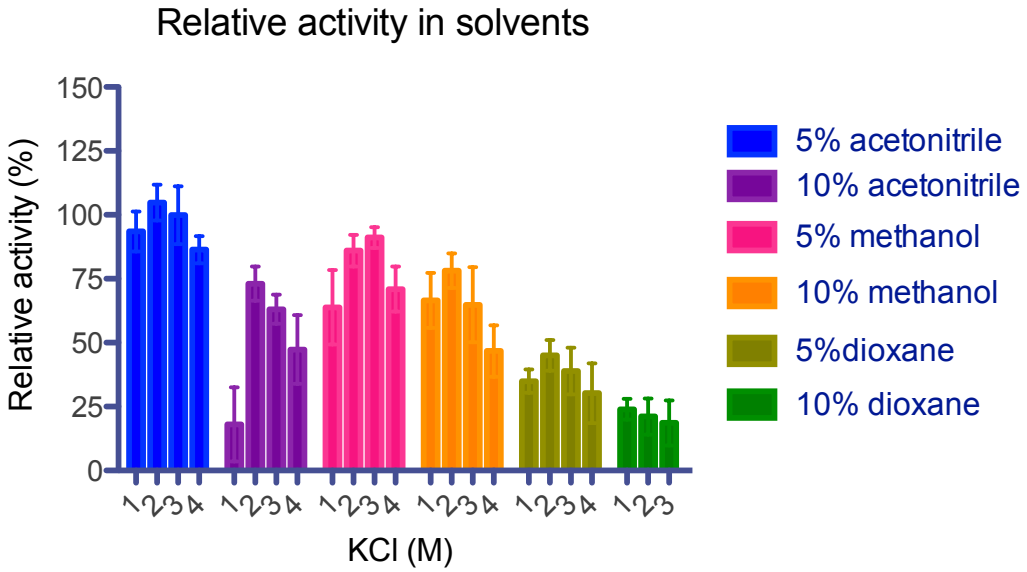

Figure 44. Organic solvents effect on the activity of Ht-BVMO at different KCl concentration.

From the previous investigation on the salt dependence of Ht-BVMO, the enzyme resulted more active in 3M KCl buffer. The graphs below show the organic solvents effect on the enzymatic activity at different KCl concentrations. The activity was reported as relative activity with respect to that observed in absence of solvent at 3M KCl.

The graph in Figure 44 shows a correlation between the organic solvent and salt concentration in maintaining the folded and active form of Ht-BVMO. In presence of 5%(v/V) methanol the enzyme show once again the best activity at 3M KCl. The presence of 5% (v/V) acetonitrile or dioxane shifts the salt preference towards 2M KCl. In all cases, increasing the solvent ratio at 10% changes the salt preference. This effect is particularly evident for methanol and dioxane which shift the best activity to 2 M KCl and 1M KCl respectively.
Acetonitrile and methanol resulted the best co-solvents: at a concentration of 5% v/V, the enzyme showed 100% and 90 % relative activity in acetonitrile and methanol respectively. Incresing the acetonitrile ratio to 10% led to a significant drop of the activity. At this concentration, the enzyme showed a higher tolerance toward methanol. Among the tested solvents, dioxane resulted the most inactivating. Higher solvent concentrations were tested but technical difficulties, such as salt precipitation, came into play.

The thermostability of the enzyme at different salt and organic solvent concentration was studied. For this study we applied the fluorescence-based thermal stability assay. The conceptual basis of this method is that folded and unfolded protein can be distinguished by exposure of a hydrophobic fluorescent probe. The probe is quenched in aqueous solution, but will bind to the exposed hydrophobic interior of an unfolding protein leading to a decrease in quenching, so that a fluorescence emission can be studied as a function of temperature. The technique allows a high-throughput analysis in a multi-well platform, where the samples can be run in parallel and the protein unfolding kinetic can be detected using a real-time thermocycler.
From the screening the melting temperature (T_m) of the protein in different solution buffers were retrieved (table 7). T_m is the temperature point to which the free energy of the unfolded protein is equal to that of the folded one. The data were ordered by both salt concentration and polarity index of the solvent. The polarity index (I) is a measure of the tendency of the solvent to interact with various polar test solutes and is used as guiding parameter for enzyme stability in aqueous-organic mixtures [77].

Table 7. Effect of salt and organic solvent on the melting temperature (T_m) of Ht-BVMO.

	Tm (°C)						
	water (10,2 I)	**5% ACN (9,98 I)**	**5% MeOH (9,945 I)**	**5% Dioxane (9,66 I)**	**10% ACN (9,76 I)**	**10% MeOH (9,69 I)**	**10% Dioxane (9,66 I)**
4M KCl	60,5	55,5	53,5		56,5	49,5	
3M KCl	54,5	50,5	49,5	48,5	47,5	46,5	42,5
2M KCl	46,5	43,5	43,5	42,5	40,5	41,5	38,5
1M KCl	34,5	32,5	33,5	33,5	29,5	32,5	30,5

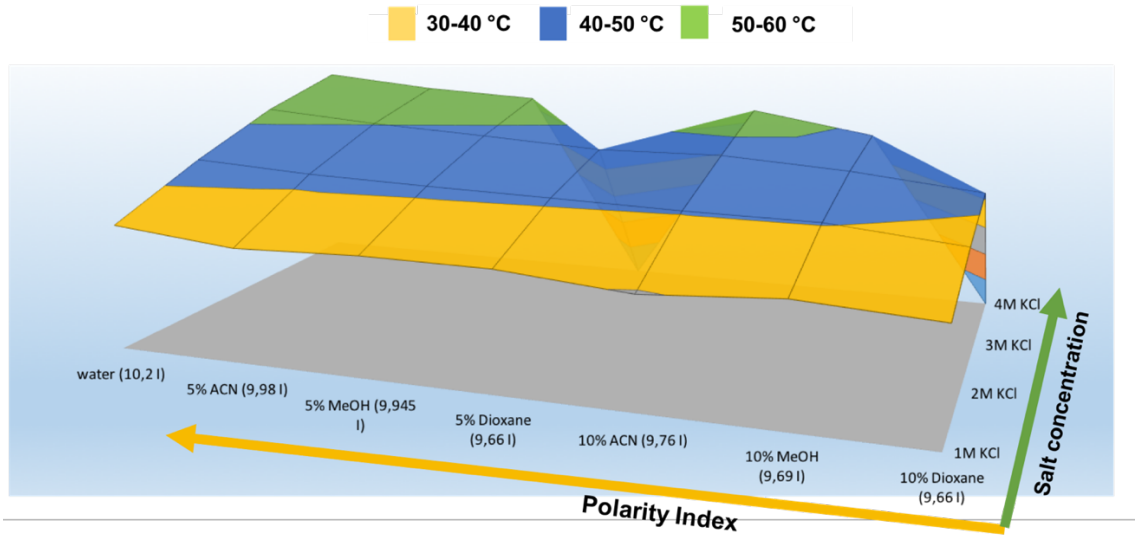

Figure 45. Effect of salt and organic solvent on the thermostability of Ht-BVMO

From the graph it is clear that in all cases, the salt concentration increases the protein thermo-stability, independently from the used co-solvent. Furthermore, the graph shows that also the polarity index of the solvent plays a role in increasing the melting temperature of the protein, increasing the polarity of the solvent rises the melting temperature of the protein. The only exception in this trend is probably the 10% acetonitrile in 4M KCl, in which the protein shows a T_m of 56 C°, higher than 5% methanol and acetonitrile at the same salt concentration. According to the graph, the highest melting temperature was reached using water as solvent and a salt concentration of 4M KCl. For a given solvent, the highest thermostability was always reported for a salt concentration of 4M KCl. Looking at the graph in figure 45, it is possible to observe that buffer conditions for an optimal thermostability do not match those for an optimal activity. Even if it causes an increment of the protein stability, an excess of salts (over 3M) always decreases the enzymatic activity. A stabilizing agent, such as salt, cause a drop in water activity and the subtraction of water molecules on the enzyme surface, contributing to rigidifying effects. This rigidification may restrict the large conformational changes required for catalysis, therefore, even if this halophilic enzyme is adapted to be functional in environments with a low water activity, an excess of salt causes a drop in the activity.

3.5 Discussion

3.5.1 Expression and purification Ht-BVMO

In the field of synthetic organic chemistry, the synthesis of pharmaceuticals, polymers intermediates, agrochemicals are often hampered by expensive process which suffer of low selectivity and undesired byproducts. Enzymes in biocatalitic process are considered one of the most promising instruments to achieve fine chemicals with good yields and enantioselectivity.

Despite their ability to catalyse reactions in mild and environmental sustainable conditions, enzymes from mesophilic organisms are often not well suited for the harsh reaction conditions required in industrial process, because for their lack of thermostability and tolerance to organic solutions. In the last few years the research for enzymes with features applicable in industrial processes addressed towards Extremophiles. These are organisms that have evolved to live in a variety of extreme environments and, as result, they produce unique enzymes that work under conditions that their mesophilic counterpart do not tolerate. In this line of research, we have cloned, expressed and characterized the first Baeyer Villiger monooxygenase from an extreme halophile, the archaea *Haloterrigena turkmenica*, an organism that was isolated from a sulphate saline soil in Turkmenistan and that requires at least 2M NaCl for growing.

One of the first observation we made upon expression of the recombinant BVMO from *Haloterrigena turkmenica* was an aberrant migration of the protein in SDS-PAGE. The identity of the overexpressed protein was confirmed as the recombinant Ht-BVMO by the anti His-tag immunoblot assay and the mass fingerprinting analysis. The aberrant migration can be explained looking at the particular aminoacidic composition of Ht-BVMO. The high rate of charged aminoacids may influence the binding with SDS molecules and consequently its electrophoretic mobility. An enrichment in negatively charged aminoacids characterizes the proteome of halo-archaea and an atypical electrophoretic mobility was found also for other recombinant proteins from these organisms. Reference

Purification of Ht-BVMO was hampered by the tendency of the protein to aggregate in inclusion bodies. The expression at low temperature (12°C), increased significantly the amount of recombinant protein in the soluble fraction of the cell lysate. Despite ARCTIC strain is characterized by a higher growth rate at low temperature, the expression of *Ht*-BVMO in BL21 avoided the co-elution of Cpn60 during the purification process. Expression at low temperature allowed the recover of the protein in a soluble form, but the enzyme resulted inactive and probably only partially folded. The final active form was recovered only by incubating the cell lysate in 2M NaCl buffer. This behaviour can be explained considering the requirement of a high ionic strength for the correct protein folding of the protein. By adding the salt solution and the FAD cofactor to the cell lysate, the protein is supposed to fold *in vitro*, incorporating the flavin cofactor that gives to the

enzyme the typical yellow color. Indeed, halophilic eukaryotes and eubacteria overcame the extracellular osmotic pressure by accumulating small organic molecules that serve as intracellular osmo-protectants; on the other hand, halophilic Archaea accumulate high concentrations of ions, up to a concentration that is isotonic with the environment [57]. Therefore, their soluble enzymes, are themselves adapted to a high salt concentration.
The purification of the protein was optimized using a preliminary IMAC chromatography and a final HIC chromatography. A third step of gel filtration chromatography resulted pointless from the point of view of the quality of the purification, but the technique gave us an indication about the molecular weight of the protein and an experimental confirmation of the monomeric nature of Ht-BVMO in 2M NaCl buffer.

3.5.2 Ht-BVMO salt dependence activity and folding

Ht-BVMO is the first Baeyer-Villiger monooxygenase that shows the phenomenon of enzyme inactivation at low salt concentrations. The enzyme showed a clear salt-dependent resulted more active in KCl buffer than NaCl, in accordance with the salt tolerance mechanism adopted by halo-archaea, which accumulate high concentration of potassium ion in the cytosol excluding sodium ions. CD spectra in presence of different concentration of salts clearly showed that the inactivation is correlated with the denaturation of the protein. The tridimensional model of the protein, that we generated using the PAMO structure as template, gave us the possibility to point out some general features of Ht-BVMO that characterize the halophilicity of this enzyme. One of the most evident differencees between the Ht-BVMO and PAMO proteins is the balance between the acidic and basic residues. Large numbers of acidic residues destabilize the protein structures at low salt concentrations presumably by the repulsive interactions. Nevertherless, a high surface density of negative charges is supposed to stabilize the structure of halophilic proteins in the presence of the high salt concentrations in the cytoplasm of halophilic Archaea. Up to now halophilic adaptation is best explained by the solvation stabilization model: surface acidic residues are believed to bind hydrated ions to form a solvation shell that prevents water or salt enrichment at the protein surface, thus allowing the proteins to remain soluble and properly folded at high salt concentration.
The CD studies also showed the time dependence of the denaturation process in a low salt concentration environment. After removing the salt by overnight dialysis or by purification in normal TRIS buffer, the enzymatic activity of Ht-BVMO has never been recovered indicating that a long incubation time at low salt concentration lead to an irreversible denaturation. Nevertheless, the addition of salt immediately after cell disruption allowed the purification of the active and folded form of the protein. This phenomenon leads to speculate about the existence of a folded or partially folded form of Ht-BVMO inside the *E. coli* cytosol. Although it was once though to be a simple solution of molecules, the cytosol is more like a complex and crowded matrix of macromolecules and metabolites arranged on different level of organizations. In this crowded environment

Ht-BVMO would be stabilized not only by the physiological salt content of the cell (4 mM NaCl) [78] but also by the overall charges of macromolecules and metabolites.

3.5.3 Ht-BVMO as biocatalyst for ketone conversions

Ht-BVMO stability and activity is dependent on the salt concentration in the buffer. The applicability of such an enzyme in chemical synthetic processes may be limited, due to the difficulties that can occur in regenerating the oxidized nicotinamide cofactor, or to the corrosive action of the salt. Using Ps-PTDH as coenzyme regeneration enzyme and a concentration of 1M NaCl, we were able to carry out the conversions of some ketone substrates. The mass spectrometry analysis identified the products as esters, confirming that the catalyzed reactions were Baeyer-Villiger oxidations. The enzymatic assay carried out in magnesium sulphate and magnesium chloride demonstrated that the stability and activity of *Ht*-BVMO do not depend only on the concentration but also on the nature of the salt in the buffer solution. The effect of ions on the folding of halophilic proteins has been extensively studied. The superficial tension of water at high salt concentration seems no to be the only factor that influence the folding of these proteins. Indeed, the formation of specific binding sites for solvated ions on the folded proteins have been suggested. The existence of ion-binding sites on halophilic proteins is more and more documented [79]. The ion binding capability would be related to their specific affinity for the folded protein. Cations and anions with high charge density, have shown to interact most efficiently with the folded form of halophilic proteins, stabilizing them at lower salt concentration than sodium or chloride ions. Stabilization of halophilic proteins like Ht-BVMO at low salt concentrations open new possibility for synthetic applications of these enzymes. The stabilization effects of additives, like nondetergent sulphobetaines have already been demonstred for halophilic malate dehydrogenase [80], furthermore the recent applications of ionic liquid in enzymatic processes offer new fields of investigations for these enzymes.

3.5.4 Potential of Ht-BVMO as biocatalyst in aqueous-organic media

Organic solvents effect on the activity and stability of Ht-BVMO has been studied. The presence of an organic co-solvent in the buffer composition has an effect on the optimal salt requirement. In particular, increasing the solvent ratio of the buffer lowers the salt requirement of the enzyme. The CD spectra of the enzyme highlighted the importance of the salt in maintaining the overall structure of the protein. Considering the effect of organic solvent on the salt requirement it is possible that salt may be partially replaced by suitable solvents, such as methanol, in maintaining the enzymatic activity of the halophilic BVMO. This effect of the solvent on the activity and the salt requirement has been reported for other characterized halophilic enzymes: a *Natrialba magadii* protease [81], a glutamate dehydrogenase from *Halobacterium salinarum* [82] and alchool dehydrogenase from *Haloferax volcanii*. [83] Enzymes from halophilic Archaea are

thought to be important biocatalysts in aqueous/organic, because salt has the effect of reducing water activity. The water activity of saturated NaCl is 0.75, corresponding to a dimethylformamide concentration of 60 vol% (calculated from a published model) [84]. The unique properties of their aminoacidic sequence allow halophilic enzymes to be functional in this kind of media and, for this reason, they may become the enzymes of choice for biocatalysis in organic media.

3.6 Conclusions

In this work we cloned, expressed and characterized, the first Bayer-Villiger monooxygenase discovered in the Archea domain. This BVMO from *Haloterrigena turkmenica* is the first enzyme of this class that shows activity and folding dependent on the salt concentration. The loss of activity and the denaturation at low salt concentration identify this BVMO as a halophilic enzyme. The enzyme shows a substrate preference towards aliphatic and aromatic ketones. Depending on the substrate this BVMO displays different rates of catalysis, but in all cases the measured k_{cat} values were not higher than 0,3 s^{-1}. Since most natural monooxygenase enzymes display k_{cat} values in the range of 1–100 s^{-1} when tested on ketones among those selected for our analysis [85] we conclude that this new BVMOs seems rather inefficient bio-catalysts. Nevertheless, the particular aminoacidic composition of this enzyme permits its employment in high salt concentration buffers and in environments characterized by low water activity. It therefore appears as a promising biocatalyst for those reactions or processes that require aqueous/organic media. Moreover, if the folding and activity of this enzyme strictly depend on the physical and chemical properties of the external environment, a different composition of the reaction medium may change also the biocatalytic properties of the enzyme. Further biocatalytic characterizations of this enzyme would permit to study substrate preference, regio-enantioselectivity and kinetic parameter variations in relation to the properties (e.g. ionic strength, solvent polarity) of the reaction medium.

Chapter II

Studying two novel BVMOs from photosynthetic eukaryotes

4.1 Introduction:
Two new BVMOs from photosynthetic organisms

Most of the characterized type I BVMOs originate from microbial organisms, in particular actinobacteria. As many oxygenases, this class of enzyme is largely found in catabolic pathway, in which they play the role of activating the carbonyl group of an organic molecule for a subsequent hydrolysis and disruption of the carbon-carbon bond. The first evidence of a biological Baeyer-Villiger activity was found in a eukaryotic organism, the ascomycetes *Cylindrocarpon radicola* in the first half of the 20th century [86]. However, only recently the enzyme responsible for this activity has been identified, expressed in recombinant form and recognized as a type I BVMO [30].
A Baeyer-Villiger activity was also found in some plants, involved in the biosynthesis of brassinosteroids, a class of plant steroids responsible for plant growth and development [87]. The enzyme responsible for the oxidation of the B-ring of the plants steroid to give brassinolide was identified in tomato and *Arabidopsis thaliana*. Unlike the enzymes derived from bacterial or fungal source, the lactonization of this plant steroid is not catalyzed by a Type I BVMO but by a member of the family of cytochrome P450 monooxygenases.
Type I BVMOs from eukaryotic photosynthetic organisms were identified and expressed in recombinant form for the first time by Bergantino's group in 2012 [31]. These new BVMOs originate from the moss *Physcomitrella patens* and a primitive red alga *Cyanidioschyzon merolae.* These two organisms can be certainly considered an uncommon source for BVMOs. *Cyanidioschyzon merolae* is a unicellular red alga that live in acid environments like hot springs, even at pH lower then 2 and temperature of 45°C. It is characterized by a simple cell architecture: it not presents a rigid cell wall and it contains o single nucleus, a single mithocondrium and a single chloroplast. The moss *Physcomitrella patens* is a no vascular plant, recognized a model organism, it is employed in many studies for the understanding of the evolutionary transition mechanism from the aquatic environment to the terrestrial one of higher plants.
The biocatalytic characterization of the recombinant BVMOs from these two organisms showed a broad substrate acceptance with a preference toward long linear aliphatic ketone such as 2-dodecanone. The phylogenetic analysis of the two proteins is in accordance with the substrate scope characterization [31]. The protein from *P.patens* is clustered together with Phenylacetone monooxygenase and Steroid monooxygenase, which transform aromatic but also linear ketones. The protein from *C. merolae* is placed in a cluster together Methylethylketone monooxygenase and Acetone monooxygenase, all enzymes that convert linear ketones.
From the kinetic analysis of these two enzymes, the measured k_{cat} values were not higher than 0.4 s^{-1}, displaying a very low catalytic efficiency. This suggests that probably these

enzymes have been subjected to a weak selective pressure during evolution and that they could be involved in secondary methabolism. Their substrate preference toward linear alkanones suggests their possible involvement in modifications of photosynthetic pigments like chlorophylls and pheophytins, which side chain resembles the preferred substrates oxidized by these enzymes.

4.1.1 The moss *Physcomitrella patens*

Phiscomitrella patens is a briophite that grows in late summer to autumn in temperate zones often close to waterlines. It is heavily dependent on water for growing and reproduction, but it can survive to dessication [89]. Its life cycle is dominated by the photoautotrophic haploid generation, the gametophyte, characterized by two different developmental stages: the protonema and the gametophore. A relatively simple and mainly heterotrophic diploid sporophyte is supported by the same gametophytic generation. The life cycle begins with the germination of spores that form the protonema tissue. The protonema is formed by a filamentous network of chloronema and caulonema cells. Chloronema cells are densely packed with large and numerous chloroplasts, while caulonema cells are composed by an oblique cell wall and a small number of chloroplasts. Protonema filaments elongate by tip growth of apical cells and can generate side branches from subapical cells. Bud structures originate from caulonema, that involve the transition from the bidimensional to the tridimensional shoot development. The development of these shots leads to the formation of the second gametophyte stage. The gametophyte is composed by stems that carry the leaves and the reproductive organs. Fertilization generates the diploid sporophyte, characterized by stalk that bears the capsule in which spores are produced.

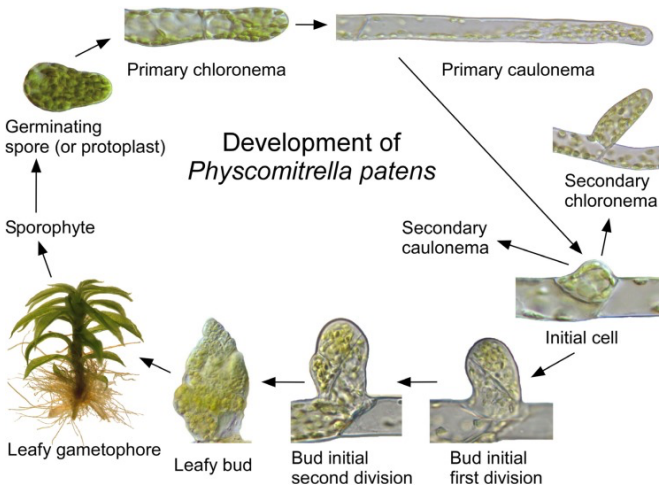

Figure 46. Schematic representation of *Physcomitrella patens* life cycle [89].

Phiscomitrella patens is characterized by a particular capacity to perform homologous recombination, with levels of gene targeting efficiency comparable to that of *Saccharomyces cerevisae* [90]. Due to this capacity, very rare among plants, many molecular genetics and genomic tools were developed for this organism [91]. Moreover, the dominant haploid gamethophytic generation and the relatively simple developmental pattern allow an easy cultivation in laboratory conditions, making this organism a unique model for plant functional genomics.

4.1.2 *Cyanidioshyzon merolae*

Cyanidioschyzon merolae is an unicellular red alga that lives in acidic hot springs rich in sulphate (pH 1.5, 45°C). This alga is characterized by a relative simple structure, composed of one nucleus, one mitochondrion and one plastid, and is considered one of the most primitive algae. [92]. The laboratory manipulation of this organism is facilitated by its simple structure, the absence of a rigid cell wall, and a simple life cycle. Moreover, in 2004 the nuclear genome of *C. merolae* was completely sequenced [93], making this organism a suitable material for studies of biochemistry, structural biology and biotechnology. Despite its usefulness as a model plant system, the basic methods for cultivating *C. meroalae* have not been investigated in detail. The optimization of liquid culture media, and growth conditions are still in progress [94, 95], and a limited use of cultures on solid plate media has been reported for this organism [96]. Indeed, *C. merolae* requires a very acidic medium (MA medium) for growing and the low pH may affect the action of some solidifying agents. A preliminary optimization of the growth conditions for this organism was reported by Minoda in 2004 [94] , who was able to grow and isolate single *C. merolae* colonies on plates of MA medium solidified with 0,4% gellan gum. The same Japanese group also reported the first nuclear transformation and demonstrated that a gene targeting approach can be applicable for genetic and protein functional studies on this organism. A gene targeting approach requires a selectable marker gene and a selection condition. It was revealed that 5-fluororotic acid (5-FOA) at a concentration of 800 ug ml^{-1} effectively prevent the growth of *C. meroalae*. In other organisms such as yeast, 5-FOA is used to select mutants deficient in orotidine 5-monophosphate (OMP) decarboxylase, an enzyme involved in the uracil synthesis pathway. Indeed 5-FOA is converted to a highly toxic compound, 5- fluorouracil, by this enzyme. OMP decarboxylase-deficient mutants show auxotrophy for uracil, and the structural gene for this enzyme (URA 3 in *S.cerevisae*) can be used as a selectable marker for genetic transformation [97]. In *Cyanidioschyzon merolae,* OMP decarboxylase was identified as a fused protein with orotidine-5'-phosphoribosil transferase (URA 5 in *S. cerevisae*), for this reason its corresponding gene was named URA 5.3 in *C. merolae.* Minoda and co-workers isolated the first 5-FOA resistant mutant of *Cyanidioschyzon meroale*. The mutant, called M4, showed an uracil auxotrophy as stable phenotype and sequencing analysis highlighted the insertion of an adenosine nucleotide in the mid-portion of the URA 5.3 open reading frame. This insertion results in a frame shift of the open reading frame, that produces a truncated, non functional, OMP carboxylase. Using the isolated

M4 mutant as recipient and the wild type 5.3 URA as marker gene, the possibility of nuclear transformation was examined. After transformation, the cells were spread on a minimum media to allow the selection of uracil prototrophic clones. Sequencing analysis of the selected colonies that grew on minimum media showed that the frameshift mutation of the 5.3 gene was reverted to the wild type sequence, demonstrating that homologous recombination upon transformation of nuclear genome occurred. Minoda et al. in 2004 described a first protocol for nuclear transformation by cell electroporation [94], but in 2008 Onhuma reported that exhogenous DNA can be introduced into cells also upon Polyethylene Glycol treatment [98].

4.2 Aim of the project

Both *Cyanidioschyzon merolae* and *Physcomitrella patens* undergo homologous recombination with a frequency that allows gene targeting and genetic manipulation [88, 94]. In order to better characterize these two novel enzymes and explore their catalytic potential we aim to discover their natural substrate and their physiological function by a reverse genetic approach. Knowing the natural substrate of these monooxygenases, we could further and more specifically examine their substrate scope, but also make prediction on structural features involved in substrate acceptance. Apart from the basic knowledge that we could get about the role of this new BVMO in its natural context, this research would add information to the already wide panel of BVMOs actually disposable for applications in bio-catalysis.

4.3 Results.

4.3.1 Construct for the disruption of gene encoding the BVMO of *P. patens*

Exploiting the homologous recombination capability of *Physcomitella patens* and the genetic manipulation tools developed for this organism, we disrupted the gene encoding the BVMO, by inserting an antibiotic resistance cassette.
The DNA construct for gene targeting was realized by amplification of a 2608 bp genomic region of *Physcomitrella p.* composed by 1560 bp of the sequence encoding the BVMO and 1048 bp of the non-coding region upstream of the gene. The DNA fragment was amplified using two mutagenic primers, which inserted HpaI restriction sites at both the sequence ends. Thus the sequence was cloned in the pGEM T-easy vector. At the 5' region of the coding gene we identified a sequence of 408 bp flanked by SmaI and BamHI restriction sites. These two restriction sites were used to insert the marker cassette, a gene encoding the resistance for geneticin. Geneticin (G418 sulphate) acts by binding the ribosome and inhibits the protein synthesis in both prokaryotic and eukaryotic cells. The plasmid BNRF with the resistance cassette for geneticin, was digested using SmaI and BglII restriction enzymes. The compatible cohesive ends of BglII and BamHI generated after the enzymatic digestion allowed the ligation of the cassette in the pGEM T-easy vector, disrupting the genomic region of *Phiscomitrella patens* previously cloned. Thus, the final construct for the transformation was composed of the geneticin resistance cassette flanked by 1192 and 1017 bp sequences homologous to the BVMO gene.

4.3.2 Transformation of *Physcomitrella patens* and screening of the colonies

The protonema of a 6 day old *Physcomitrella* culture was employed to obtain the protoplasts for moss transformation. In order to increase the efficiency of the homologous recombination, the plasmid vector designed for the transformation was digested with HpaI, thus the construct for the gene targeting was linearized. In order to get the transformants we followed a PEG mediated transformation protocol. The transformation was performed by adding 15 ug of linearized DNA and the PEG solution to *P. patens* protoplasts. From the selection in $PpNH_4$ medium supplemented with 50 ug/ml G418 more than 100 colonies were obtained. To avoid the selection of "transient tranformants", the resistant colonies were transferred on non selective media for 10 days and then, once again on the selective media. By this additional selection it was possible to select only the colonies that integrated the transgene in their genome. In contrast the "transient tranformants" lines lost their extra-chromosomal elements during the growth in non selective media. Among the colonies that resulted resistant to the second antibiotic

treatment (50% of the original colonies) 6 mutants were chosen for genomic DNA extraction and the disruption of the targeted gene was checked by PCR. For the screening, we amplified the region upstream and downstream the marker gene, using a reverse primer matching the resistance cassette and a forward primer matching a genomic region, outside the homologous sequence (Figure 47).

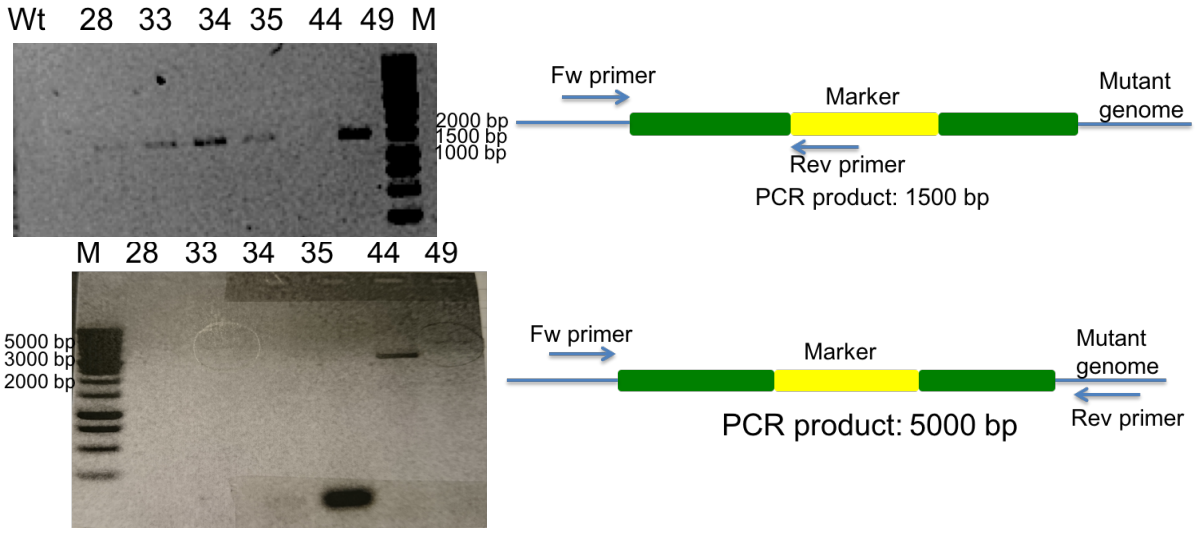

Figure 47. Screening of the geneticin resistance mutants of *Physcomitrella patens*

From the screening, only one colony (colony 44 in Figure 47) resulted negative. A second PCR screening using both primers external to the homologous region, allowed to verify if the transgene was integrated individually or in multiple copy as a concatamer. The PCR screening showed that the gene encoding the BVMO of colonies 33 and 49 was disrupted by the insertion of a single copy of the marker gene.

4.3.3 Characterization of BVMO null mutants of *Phiscomitrella patens*

A preliminary comparison between the BVMO-KO mutants and the wild type moss in standard growth conditions ($PpNO_3$ medium, 24°C, irradiance about 40 uE) did not reveal any clear phenotype in the mutants, neither in the morphology of the structures neither in growth rate. In order to provide the biochemical tools for the investigation on the cellular localization and physiological role of the protein, the recombinant form of Pp-BVMO was used to produce specific polyclonal antibodies in rabbit. The specificity of the collected antiserum was verified by immunoblotting analysis of total extracts of *E.coli* expressing the recombinant BVMO. The produced antibodies, that showed a high specificity against the recombinant protein, were employed for immunoblot assays on the tissues collected from the wild type lineage of *Phiscomitrella patens*, aiming to reveal the native BVMO and eventual variation in its expression.
The protonema of wild type moss was grown in standard condition in minimum medium ($PpNO_3$). After 6 days, the moss tissues, composed by chloronema, caulonema, leafy

gametophore, were collected, homogenized and solubilized in solubilizing buffer for western blotting analysis. The same procedure was applied for the moss cultured in minimum media but at different condition of temperature (4°C – 24°C) and irradiance (1000 uE – 40 uE). These different growth conditions were surveyed as possible stimuli for variation in the expression of the BVMO. To investigate the possible involvement of Pp-BVMO in degradative pathways, samples of senescent tissue (30 days old culture) were also collected for the immunoblot assays. All the collected samples were analyzed by western blotting using the specific antibody against Pp-BVMO, but unluckily, the presence of the native BVMO was not identified in any tested condition.

Despite the mutants did not show any clear phenotype and the expression of the native protein was not verified in the wild type moss, the possible role of Pp-BVMO in the degradation or the synthesis of photosynthetic pigments was investigated. The photosynthetic pigments of wild type and BVMO-KO mutants were extracted from 6 day old cultures by treatment with 80% acetone solution. The extracted pigments were analyzed by reverse phase chromatography and chromatographic profiles of mutants and wild type were compared. A multiple array diode detector allowed the identification of the eluted pigments, providing their absorbance spectrum. Assuming the involvement of the BVMO in the synthesis or degradation of these pigments, we expected to reveal the accumulation of an intermediate of their synthetic or their degradative pathway. From the comparison of the chromatographic profiles, no significant difference emerged (Figure 48).

A

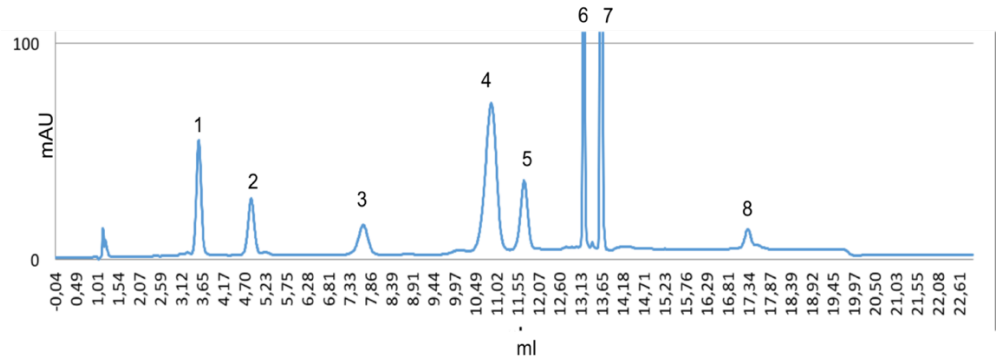

B

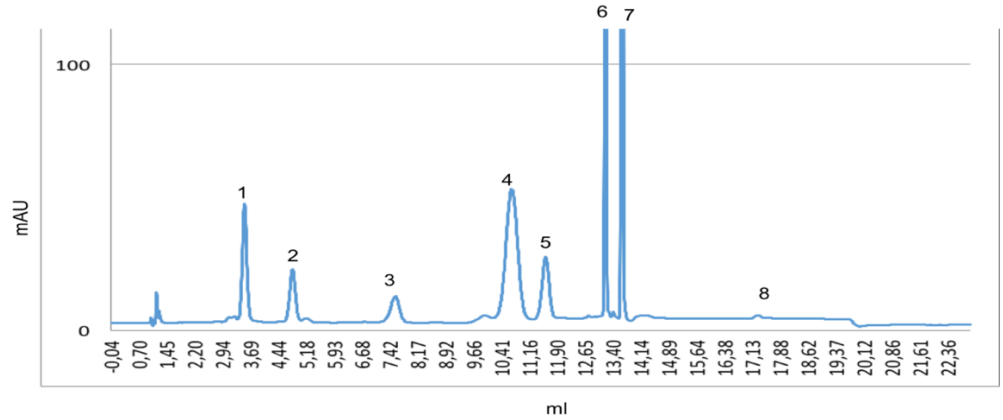

C

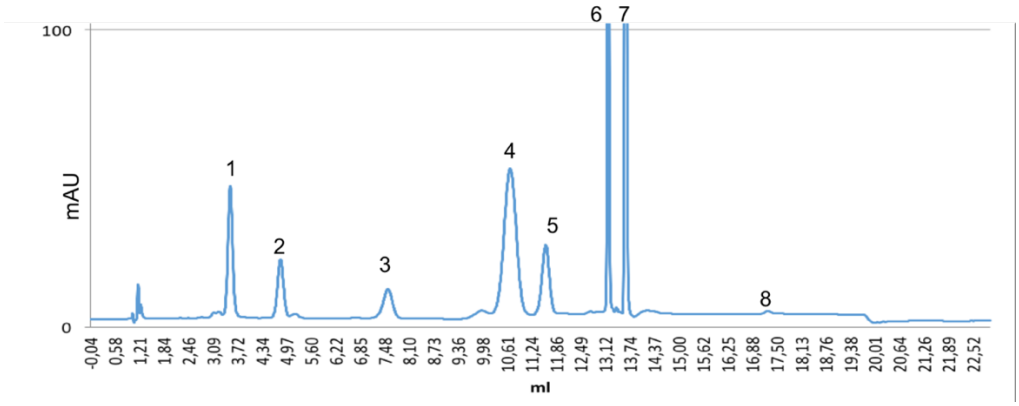

Figure 48. Chromatographic profile of the photosynthetic pigments of *Physcomitrella patens* wild type (A), BVMO KO 49 (B), BVMO KO 33 (C). numbered peaks correspond to: 1. Neoxanthin. 2. Violaxanthin, 3. antheraxanthin, 4. Lutein, 5. Zeaxanthin, 6. Chlorophyll b, 7 chlorophyll a, 8. β-carotene.

4.3.4 Optimizations of growth conditions of *Cyanidioschyzon merolae* in liquid and solid media

In order to optimize the cultivation conditions of *Cyanidioschyzon merolae,* the effect of temperature and composition media on the growth was tested. The conventional growth medium of the alga, called Allen's medium, is a photoautotrophic medium composed by mineral salts and essential trace elements adjusted to a pH of 2.5 with H_2SO_4. The recent literature reports two different versions of this media (MA and MA2) that mainly differ for their salt concentrations and iron contents [94, 95]. The best growth conditions were obtained using the MA2 medium, a temperature of 37°C and an irradiance of 30 uE (Fig 49A). In these conditions we registered a doubling time of 50 hours.

A

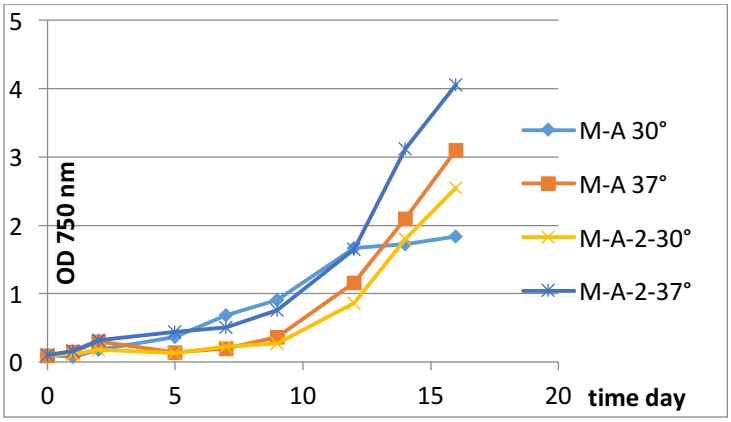

B

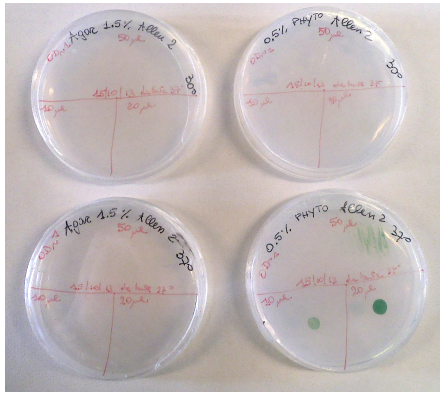

Figure 49. Optimization of *Cyanidioschyzon merolae* growths condition. A growth curves of *C. merolae* in MA or MA2 at different temperatures (30°C-37°C). B *C. merolae* growth in MA2 plates with Agarose 1,5 % or Phytagel 0,5% at 30 or 37°C.

The capability of *Cyanidioschyzon merolae* to growth on solid MA2 medium was tested, verifying the best solidifying agent between AGAR and Phytagel. The extreme low pH of the medium prevented the solidification of the AGAR at a concentration lower than 1,5%, whereas the minimum concentration of Phytagel for solid plate was reported at 0,5%. Single colonies formation of *Cyanidioschyzon merolae* was observed only on Phytagel gel plate at 37°C (Figure 49 B) . The uracil auxotrophic mutant of *C. merolae*, known as M4, was cultivated at the same conditions of the wild type, but 500 ug ml^{-1} of uracil was added to the medium.

4.3.5 *Cyanidioschyzon merolae* BVMO: identification of the native protein and gene targeting approach for the knock-out

In order to provide biochemical tools for the investigation on Cm-BVMO function, we used the recombinant protein to produce polyclonal antibodies in rabbit. The specificity of the antibodies were tested on a total exctract of *E.coli* expressing Cm-BVMO. The produced antiserum was used for immunoblot analysis on the wild type organism. Samples of *Cyanidioschyzon merolae* culture were collected at different phases of the alga life cycle (OD_{750} 0,2 - 4) and the expression of the native BVMO was verified by western blot.

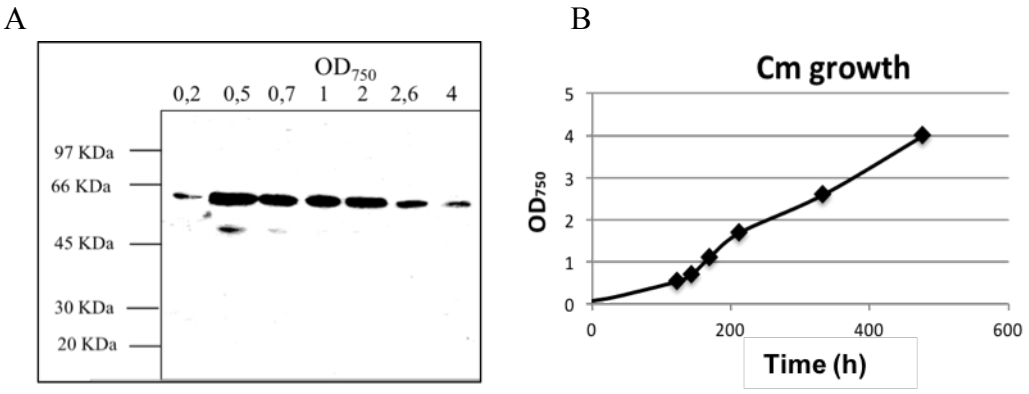

Figure 50. Expression of Cm-BVMO in *Cyanidioschyzon merolae.* **A** Immunostaining anlysis for Cm-BVMO detection in *C. merolae* at different optic densities. **B** growth curve of *C.merolae*. the points indicate the withdrawals for the western blot analysis in A

We planned to disrupt the gene encoding the BVMO in *Cyanidioschyzon merolae* exploiting the homologous recombination that naturally occurs in this organism. Exploiting the M4 mutant as recipient we aimed to target the gene encoding the BVMO with a DNA construct composed by the wild type URA 5.3 as marker gene and the 5' and 3' BMVO sequence as flanking regions. The genomic sequence of Cm-BVMO was

successfully cloned in the pGEM-T Easy vector. The restriction site BamHI and HindIII were identified in the BVMO sequence to insert the URA 5.3 cassette upon enzymatic digestion and ligation.

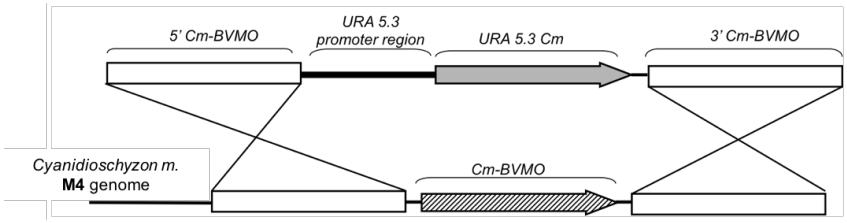

Figure 51. Scheme of the construct for BVMO gene disruption.

The marker cassette consisted of 1055 bp upstream and 207 bp downstream the coding sequence of URA 5.3 gene. This genomic region was chosen to include the promoter and the 5' UTR sequences of the gene to ensure its translation and transcription. The construct for the gene targeting was linearized and purified to optimize and enhance the homologous recombination. 3-4 * 10^8 cells in exponential phase (OD 0,5) were transformed with the DNA constructs, following two different techniques: the electroporation reported by Minoda et al. in 2004 [94] and the PEG-mediated transformation reported by Onhuma et al. in 2008 [98]. After transformation the cells were resuspended in MA2 medium, incubated at 37°C for one day and then spread on minimum media (MA2 0,5% Phytagel), to select colonies with reverted prototrophy for uracil. After one month of incubation we did not observe formation of colonies. Every attempts to optimize the transformation protocols varying DNA amount (0,5 – 10 ug), PEG concentration (20-40%), electroporation parameters (Volts: 200-500, number of electroporation: 1-2, resistance: 100Ω-∞Ω), resulted unsuccessful in obtaining transformants.

4.4 Discussion

4.4.1 *Physcomitrella patens*

Among plants *Physcomitrella patens* is one of the most studied model organism and its endogenous homologous recombination has been exploited for many physiological studies of protein functions. The discovery of a Bayer-Villiger monooxygenase from this photosynthetic eukaryote has given rise new questions about the evolution and the physiological role of this class of enzymes. We tried to investigate on the protein function of Pp-BVMO using a reverse genetic approach and analyzing the phenotypic effect of the disruption of the gene encoding this monooxygenase. The designed strategy to target the BVMO gene and insert the geneticin resistance resulted successful. We were able to obtain geneticin resistance mutants and the PCR screening showed that the marker gene was inserted in single copy in the chromosomal genome of *P.patens,* disrupting the gene encoding the BVMO. Unluckily, we were not able to identify any clear phenotype in the mutants. The immunoblot assay on the tissues of the wild type organism did not reveal the presence of the protein. This indicate a very low expression level of the enzyme, or that the expression is induced by a particular stimulus.

Considering the previous analysis on the substrate scope of the enzyme, we focused on the possible involvement of the enzyme on the synthesis or degradation of photosynthetic pigments. For this reason, we tried to investigate on the expression level of the protein in the wild type organism exposed to conditions that alter the production and the balance of photosynthetic pigments (e.g temperature, light exposure, prolonged growth). Nevertheless, we were not able to find a condition that enhance or trigger the expression of the protein. The comparison of the chromatographic profile of the pigments extracted in 80% acetone from the wild type and the mutants, have not shown any clear difference. This result can only exclude the involvement of the enzyme in the biosynthetic pathway of these pigments at standard growth condition. If the enzyme plays a role in this pathway at other, not tested, conditions is still unclear.

4.4.2 *Cyanidioschyzon merolae*

Cyanidioschyzon merolae is a unicellular red alga that requires high temperature and an extreme low pH for growth. Different growth conditions were tested trying to optimize the laboratory cultivation of this alga. Using the MA2 medium and a temperature of 37°C we were able to lower the doubling time up to 50 h in exponential phase, that indicate a very low growth rate but still sufficient to permit colony formation in one month. The growth conditions for this alga may be further optimized, for example addition of glycerol or CO_2 insufflation in the culture media may increase the growth rate of this alga.

The possibility to growth the alga on solid media was one of the first issues that we had

to face for the feasibility of the project. The low pH of the media prevents the solidification of the agar plates, catalyzing the hydrolysis of the polysaccharide molecules. Even if a higher concentration of agar allowed the formation of solid plates, organic acids may be released by the partial hydrolysis of the polymers and these may inhibit or influence the growth of the alga. Phytagel is a gelling agent produced by bacterial fermentation composed of glucuronic acid, rhamnose and glucose. It showed a more efficient solidification capacity at low pH and a higher compatibility with the alga growth. Probably the use of a lower concentration of gelling agent, allow a higher hydration of the alga cells, expecially at a temperature of 37°C with a fast evaporation rate.

Despite homologous recombination has been demonstrated to occur in *Cyanidioschyzon merolae*, gene targeting approach for functional studies are still in development for this organism. In *Saccharomyces cerevisae* the URA gene, has already been used as marker cassette for transformation of uracil auxotrophic mutants. We tried to exploit the same strategies to disrupt the BVMO gene of *Cyanidioschyzon merolae* by gene targeting. The promoter region and the UTR sequences of *C. merolae* URA gene are not described in detail, but according to the previous works of Minoda and Imamura [94, 95], the selected region of 3039 bps should contain the regulatory sequences for the transcription and translation of the marker gene. In the DNA construct, the long marker cassette was flanked by two sequences of 700 bp for the homologous recombination. The DNA length required to ensure an efficient homologous recombination in this organism has not been studied so far, therefore, we do not exclude the possibility that longer flanking region would increase the efficiency of the technique. The encountered difficulties in obtaining transformants can also be caused by an inefficient transformation protocol. Despite some transformation protocols have been described, the development of biotechnological techniques for the genetic manipulation of this alga are still in progress.

4.5 Conclusions

The two novel BVMOs from *Cyanidioschyzon merolae* and *Physcomitrella patens* are the first type I BVMO that have been identified in photosynthetic eukaryotes. The biocatalytic characterization of these two enzymes, from which long aliphatic ketones emerged as preferred substrates, suggested their possible involvement in modifications of photosynthetic pigments. As both *Physcomitrella patens* and *Cyanidioschyzon merolae* undergo homologous recombination we planned to disrupt the genes encoding the BVMOs of these organisms. We successfully obtained BVMO knock-out mutants of *Physcomitrella patens*, but we were not able to identify any clear associated phenotype. The investigations on the functional role of Pp-BVMO are hampered by difficulties in

revealing the native protein in the wild type organism. At standard growth conditions, we excluded the possible involvement of Pp-BVMO in the modification of the main pigments of the organism. If particular growth conditions influence the expression of Pp-BVMO, it still remains to be determined. The acidophilic alga *Cyanidioschyzon merolae* expresses its BMVO in the phases of its life cycle that we examined. Despite this alga requires an extreme low pH for growing, we were able to cultivate it both in liquid and solid media. Due to the lack of genetic manipulation tools for this organism, we tried to exploit the results of the recent literature to customize a method to disrupt Cm-BVMO gene by gene-targeting approach. Different methods for nuclear transformation were applied, but we were not able to isolate any BVMO knock-out mutants for this organism.

Chapter III

Studying the recombinant expression and the activity of carotenoid cleavage dioxygenases from *Crocus sativus*

5.1 Introduction

5.1.2 Oxidative alkene cleavage

Alkenes are organic molecules that can undergo a wide range of reactions including electrophilic additions, hydrogenation and oxidation. The oxidation of alkenes permits the incorporation of new functionalities into the molecule such as alcohols, acids, aldehydes or ketones and provides opportunities for further synthetic elaboration [99]. The oxidative cleavage of alkenes is a widely employed method in synthetic chemistry, particularly to introduce oxygen functionalities into molecules, remove protecting groups, and degrade large molecules. Moreover, the synthesis of a large number of bioactive compounds involves alkene cleavage as the key step to yield the corresponding carbonyl compounds. Many compounds found in nature possess aldehyde or ketone functional groups. Aldehydes have mostly pungent smell, whereas ketones tend to smell sweet. Vanillin and cinnamaldehyde are examples of naturally occurring aldehydes that confers to vanilla and cinnamon plant their typical fragrance. There are several chemical methods for alkene cleavage. Ozonolysis is the most employed chemical method for cleaving alkenes since it is considered the most efficient and cleanest. Ozone, as an electrophile, adds to an alkene to give ozonide. Ozonides are explosive, but they are easily cleaved to carbonyl products, in the presence of a reducing or oxidizing agent such as zinc or hydrogen peroxide (Figure 52), leading to ketones or aldehydes.

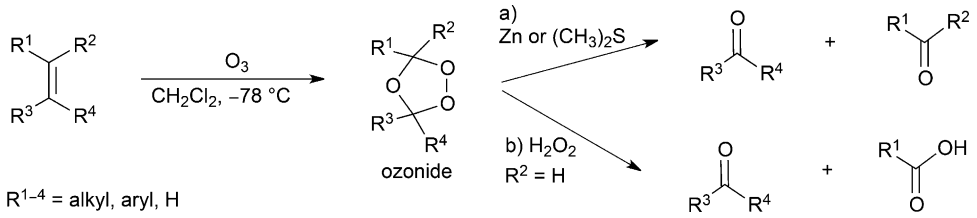

Figure 52. Ozonolysis of alkenes followed by work-up with reducing or oxidizing agents. [129]

However, the ozonolysis requires harsh conditions such as low temperature (ca. −78°C), imposing the use of a special equipment (e.g., ozoniser) and reducing reagents in molar amounts during the workup. Furthermore, application on large scale of this reaction may be limited due to the high risk of explosion [100]. Alternative protocols for the alkene cleavage require the use of poisonous heavy metals such as Cr, Os, or Ru which catalyze the reaction with a mediocre yields and selectivities [101]. In contrast, enzymes can activate the most innocuous oxidant, the molecular oxygen, and catalyze the alkene cleavage at ambient temperature and atmospheric pressure in aqueous buffer. The rising popularity of natural products during the last decades has significantly increased the

research activities to use biocatalysts for the production of, for instance, natural flavour compounds. Besides, some enzymes are capable to cleave the double carbon bond of non natural organic molecules in high chemo- and regioselective fashion, allowing biocatalysis to compete with chemical methods [102]. The enzymes performing alkene cleavage activity can be grouped based on their cofactor dependence. Despite some example of Mn-, Cu- and Ni-dependent alkene cleaving enzymes are reported in literature [103, 104, 105], most of the enzymes that catalyze this reaction showed an iron dependent activity. The iron metal cofactor can be coordinated in heme prosthetic group, as in heme peroxidase or directly by the aminoacids of the active site of the protein, as in non-heme iron dependent oxygenases.

5.1.3 Alkene cleavage by Heme peroxydases

Peroxidases are ubiquitously found in microorganisms, plants, and animals. These enzymes are named according to the organism in which they were discovered, such as horseradish peroxidase, or according to their natural substrates such as cytochrome *c*, chloroperoxidase, and lignin peroxidase. These enzymes possess a ferric protoporphyrin IX (protoheme) as the prosthetic group [106]. Heme-containing enzymes participate in a broad range of biological oxidation reactions, that involve very similar high oxidation state intermediates [107]. Consequently, peroxidases are extremely promiscuous enzymes since they catalyze diverse chemical transformations such as peroxidase, peroxygenase, and oxidase reactions, acting on a vast array of substrates including phenols, aromatic and alkyl amines, alkenes, thioethers, and aldehydes [106]. Some examples of alkene cleavage reactions catalyzed by peroxidases are here presented, focusing on the enzymes that have shown the most promising biotechnological applicability.

5.1.3.1 Chloroperoxidase

Chloroperoxidase (CPO) was isolated from *Caldariomyces fumago* [108], and it is one of the most versatile and promising heme enzymes for synthetic applications. Among the reactions catalyzed by this very promiscuous enzyme, the epoxidation of olefins with a high degree of enantio- and diastereoselectivity is particularly interesting from a biocatalytic point of view [109]. For some substrates such as conjugated dienoic esters, the epoxidation activity was found often accompanied by alkene cleavage and formation of aldehydes. This alkene cleavage activity was observed only under aerobic condition and as a side reaction of the epoxydation. The proposed explanation for the formation of all products, involves the formation of an intermediate radical cation, probably generated by a direct electron transfer from the substrate to the oxoiron centre (compound I Figure 53) formed in the CPO catalytic cycle. Consequently, the radical cation intermediate can react with dioxygen, leading to the cleavage product via a dioxetane intermediate.

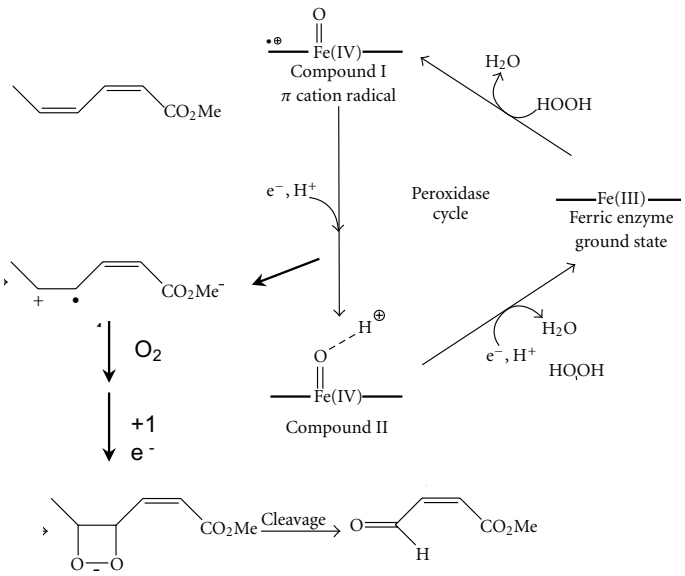

Figure 53. Proposed mechanism for the aerobic alkene cleavage catalyzed by CPO

5.1.3.2 Horseradish Peroxidase

Horseradish peroxidase (HRP) is the most studied and well-characterized peroxidase, whose crystal structure [110] and catalytic pathway have been elucidated. HRP catalyzes the oxidation of phenols, anilines, and a variety of other electron-rich compounds at the expense of H_2O_2. This enzyme catalyse the cleavage of a C=C double bond adjacent to an aromatic moiety at the expense of molecular oxygen and at an acidic pH

5.1.3.3 Myeloperoxidase (MPO) and *Coprinus cinereus* peroxidase (CiP)

These enzymes catalyze the enantioselective epoxidation of styrene and a number of substituted derivates in moderate yield. Both MPO and CiP form significant amounts of substituted benzaldehydes as a consequence of the C=C double bond cleavage of variously substituted styrene precursors. The alkene cleavage is the most prominent reaction catalyzed by CiP, whereas MPO forms a larger amount of epoxide.

5.1.3.4 Alkene cleavage by non-heme oxygenases

The alkene cleavage is mainly a secondary activity for the peroxidases, whereas it is generally the natural and often unique activity for the oxygenases. Carotenoid cleavage oxygenases (CCO are classified as non-heme iron-dependent oxygenases. These enzymes are widespread in bacteria, plants, and animals and catalyze the C=C double bond cleavage of carotenoids to give apocarotenoids The family members require an Fe(II) center which is bound to four highly conserved and catalytically essential histidine residues [111]. CCOs often exhibit substrate promiscuity, which probably contributes to the natural diversity of apocarotenoids and derivates. Despite the substrate promiscuity, these enzyme retain a perfect regioselectivity and are able to cleave a specific C=C double bond of the carotenoid chain. Thus, depending on the enzyme, the alkene cleavage can

occur either at the central C=C double bond of the carotenoid substrates or at another position. CCOs are sometimes referred to as carotenoid cleavage dioxygenases (CCDs) due to the current debate as to whether these enzymes proceed through a monooxygenase or a dioxygenase mechanism. As a result, the terms CCO and CCD are often used interchangeably. The biological role and the catalytic mechanism of the class of enzyme will be discussed more in detail in the next section.

5.1.4 Carotenoid Cleavage Oxygenases, biochemical role and classification.

Carotenoids are long chain C40 poly-ene compounds produced by phototrophic organisms such as algae, plants and certain bacteria [112]. Carotenoids are biologically important due to the conjugation created by the overlap of the p orbitals on the polyene backbone. This conjugation allows carotenoids to serve as accessory pigments in photosynthesis, as antioxidants and as visual pigments. The apocarotenoid products, formed by the cleavage reactions catalyzed by CCDc, are important signaling molecules in plants and mammals.

In animals, the most important apocarotenoid is the C_{20} compound retinal, which plays a crucial role as the chromophore of rhodopsin in the vertebrate visual cycle. In archaea and eubacterial species retinal also serves as the chromophore in bacterorhodopsin proton pumps [113].

In plants and cyanobacteria, apo-carotenoids are found in large amounts in the thylakoid membrane, where they act as accessory and photoprotective pigments [114]. Apo-carotenoids, absorb visible light and often are useful as color pigments. For example the bright orange-red color of saffron is mainly due to glycosides derived from the C_{20} apo-carotenoid crocetin. When used to color plant tissues, apo-carotenoids are found in large amounts in specialized plastids called chromoplasts. Certain apo-carotenoids act as hormones in the regulation of plant growth and architecture. Abscisic acid (ABA) is derived from the C_{15} apo-carotenoid xanthoxin and plays an important role in the regulation of drought tolerance, seed development and sugar sensing [115]

CCD can be classified according to the type of substrate and the position of the cleaved bond, in three main subfamily: NCEDs, BCOs e CCDs [112].

NCEDs (nine-*cis*-epoxycarotenoid dioxygenase) are enzymes that yield xanthoxin as the C_{15} cleavage product, which in turn is the precursor of ABA. NCED have been characterized using violaxanthin and neoxanthin as substrate, but probably they can accept a wide range of 9-*cis*-epoxycarotenoid substrates. As a common feature, none of the NCED family members accept an all-*trans* substrate.

The subfamily of BCOs (beta-carotene cleavage oxygenase) include all enzymes that process all-*trans*-β-β' carotene. Substrates with *cis*-double bonds are generally not accepted by these enzymes.

The third group is constituted by CCD (carotenoid cleavage dioxygenase) and include the subcategories CCD1, CCD4, CCD7, CCD8
The CCD1 are localized in the cytosol, unlike other CCDs, and are able to cut the positions 5-6 (5'-6 '), 7-8 (7'-8') and 9-10 (9'- 10 ') of a wide range of substrates. The most characterized enzyme of this class is the CCD1 from *Arabidopsis thaliana* [116]. The CCD7 and CCD8 are important in the synthesis of strigolactone, a plant hormone that inhibits the formation of side shoots (117). The CCD4 were the latest to be discovered and studied. CCD4 are localized in chromopastics, where they have immediate access to carotenoids. Almost all CCD4 cut in position 9-10 (9'-10 ') and, up to now, they have been found only in plants that produce flowers [118].
Another type of CCDs is represented by zeaxanthin cleavage dioxygenase (ZCD) of *Crocus sativus* that cut in positions closer to the group ionone. The ZCD acts on the double bonds in position 7-8 and (7'8 ') to give two products, which are employed for the synthesis of safranal and crocetin [119]. However, the functional role of ZCD is controversial, due to the irreproducibility of some biochemical data, and recently a novel enzyme subclass, CCD2, has been identified as responsible of the synthesis of safranal [120].

5.1.5 Structure of CCOs

The structural features of a CCO was described for the first time for the apocarotenoid cleavage oxygenase (ACO) from *Synechocystis* PCC 6803 (121). The structure af ACO consist in a seven-bladed β propeller. Each propeller blade consist of four or five antiparallel β strands (figure 54 A), The bottom side of the propeller contains short loops connecting the β strands to each other, whereas the top side is occupied by extended loops with short helices that form a large dome. As a typical β propeller structures, the active center of ACO is located in the cleft formed in the center of the propeller on the top side. The structure of the protein forms a large tunnel that enters from one side in a direction perpendicular to the propeller axis, passes through the active center and leave from an exit parallel to the propeller axis (Figure 54 B). The shape of the tunnel is modulated by the extended loops, that connect the rigid propeller blades. This feature probably allows the members of CCO family to modulate substrate specificity by changing length and sequence of the connecting loops, but conserving the rigid propeller scaffold. Indeed, sequence alignments showed that, among the CCO family members, the most conserved regions correspond to the β strands forming the propeller scaffold. For this reason, all the CCO members may be modelled on the ACO structures. The ACO active site consist of four histidine side chains holding the catalytic iron with their Nε atoms. The ferrous iron is coordinated in an octahedron with the four histidines and a water molecule, the sixth coordination position is empty for the binding with the oxygen. The iron-binding site and thus the four histidines are rigid as they do not change upon removal of the metal ion.

The crystal structure of ACO bounded with its substrate (3-hydroxy-8′-apo-β-carotenol) provides also some clues regarding the recognition of the carotenoids by the CCO enzymes. the β-ionone ring is located on the enzyme surface because it cannot pass through the narrow entrance of the substrate tunnel. The tunnel and its entrance work as a ruler, determining the cleavage position relative to the ionone ring. This enzyme showed selectivity towards apo-carotenoids, which can be explained looking at the entrance of the ACO tunnel. The β-carotene is not accepted as substrate because neither of the two substrate ends can enter the tunnel (Figure 54 C). The entrance is characterized by a large non-polar patch. This hydrophobic region probably is functional to interact with the membrane where the carotenoids and their derivates are localized. After cleavage, the non-polar product is released to the membrane, whereas the more soluble second product dialdehyde probably leaves through the exit of the tunnel and dissociates into the cytosol.

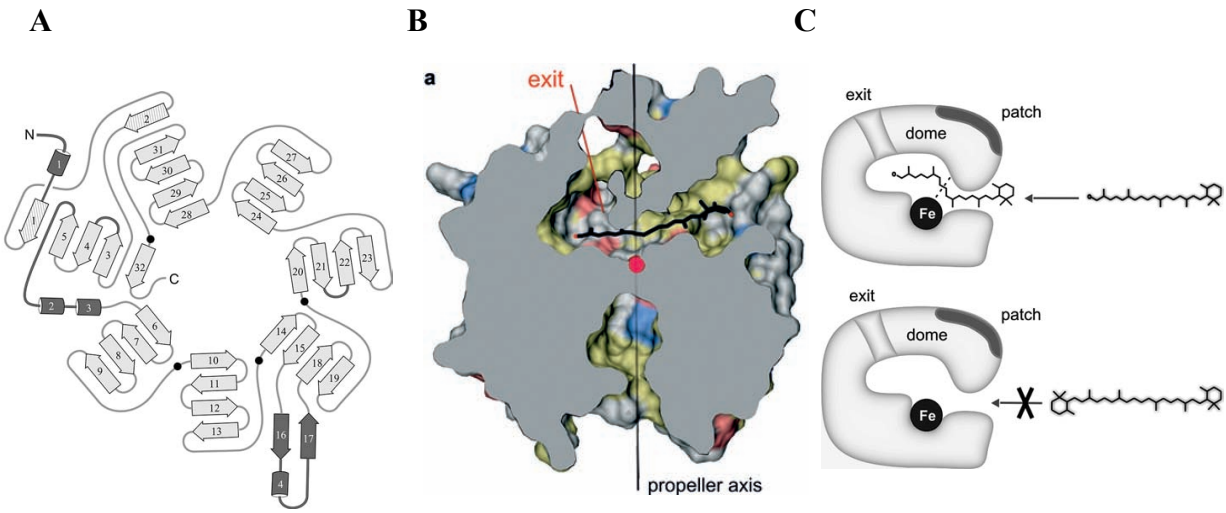

Figure 54. **A**. Sketch of the structure of ACO showing the seven-bladed beta propeller as the basic motif, **B.** surface representation of ACO structure that shows the propeller axis and the tunnel for substrance acceptance and release. **C.** sketch of apo-carotenoid cleavage in ACO. The sketch indicates that apo-carotenoid substrates with only one β-ionone group can enter the enzyme. The distance between the catalytic iron and the entrance determines the cleavage position [112]

5.1.6 Reaction mechanism

The enzymatic reactions for the cleavage of carotonoids are preformed *in vitro* by using a reducing agent, such as ascorbate, DTT, TCEP, that has the function to keep the iron in its ferrous state. The reducing agent does not participate to the reaction, all the electrons involved in the oxydoreduction reaction derived from the carotenoid and the oxygen. For the catalysis of the reaction is essential the the metal ion iron in the ferrous state (Fe^{2+}) and oxygen. The nature of the involved oxygen species is still unclear. The mechanism of the reaction is not well defined but it is clear that the C-C double bond is cleaved to the corresponding aldehydes or ketones using dioxygen as reactant and ferrous iron as a cofactor, but whether the reaction follows a monooxygenase or a dioxygenase pathway has not been established. In the case of a moonoxygenase pathway, the activeted dioxygen form an epoxide with the double bond. Subsequently, the epoxyde is opened by a water molecule, leading to the incorporation of one oxygen atom from dioxygen and another one from a water molecule into the products. In the case of a dioxygenase mechanism, the double bond forms a dioxetane intermediate with the dioxygen, then the unstable dioxetane decays to two aldehydes or ketones (Figure 55).

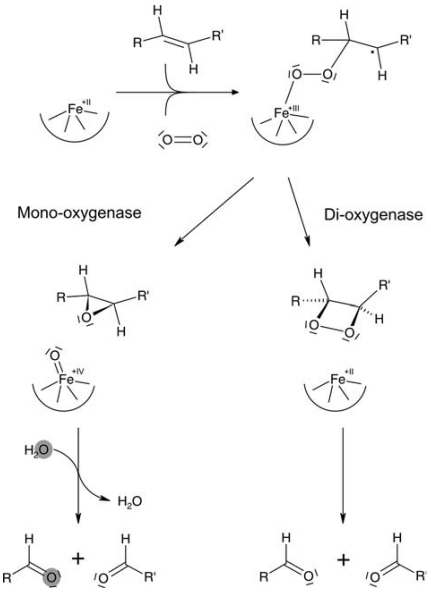

Figure 55. Schematic representation of the proposed reaction mechanisms for CCDs [112]

5.1.7 Carotenoid cleavage dioxygenases from *Crocus sativius*

Crocus sativus, commonly known as saffron, is a perennial herb that is widely cultivated in Iran and other countries such as India and Greece. The styles of the hermaphrodite flowers of this plant are often dried and used in cooking as a seasoning and coloring agent. Saffron is the most expensive spice known, it is almost as costly as gold. The method for the cultivation of saffron contributes greatly to its high price: germination can take 1-6

months, flowers blooms only once a year and should be collected within a very short duration, 3-4 weeks in October-November. Considering that each flower has only three styles, it takes about two hectare for collecting one kg of saffron.

Saffron stigmas accumulate large amounts (up to 8% on dry weight) of the three major carotenoid derivatives: crocetin (and its glycosylated forms, crocins), responsible for the red pigmentation of the stigmas; picrocrocin, responsible for their bitter flavor; and safranal, responsible for the pungent aroma of saffron. The proposed biosynthetic pathway (Figure 56.) starts through the symmetric cleavage of zeaxanthin at the 7,8/7′,8′ positions by a carotenoid cleavage dioxygenase (CCD). The two cleavage products, 3-OH-β-cyclocitral and crocetin dialdehyde, are dehydrogenated and glycosylated to yield picrocrocin and crocins, respectively. To date, conflicting data have been reported about the identity of the enzyme catalyzing the cleavage reaction for saffron production. In 2003 Bouvier et coworkers reported the zeaxanthin cleavage dioxygenase (ZCD) as the enzyme that cleaves zeaxanthin symmetrically at the 7,8/7′,8′ positions, yielding the crocin precursor crocetin dialdehyde (119). However, later work has suggested that ZCD is a truncated form of a CCD4 enzyme localized in the plastoglobules (120) and does not catalyze any carotenoid cleavage reaction. More recently, Sarah Frusciante and coworkers identified in saffron a novel type of plant CCD, called CCD2 (120). The biochemical studies on this novel CCD suggested that this enzyme is the responsible of the cleavage of zeaxanthin, and lead to crocetin biosynthesis in saffron. Despite the work of Frusciante reported a detailed characterization of the novel charothenoid cleavage oxygenase, the physiological role of ZCD and CCD2 is still a topic of discussion.

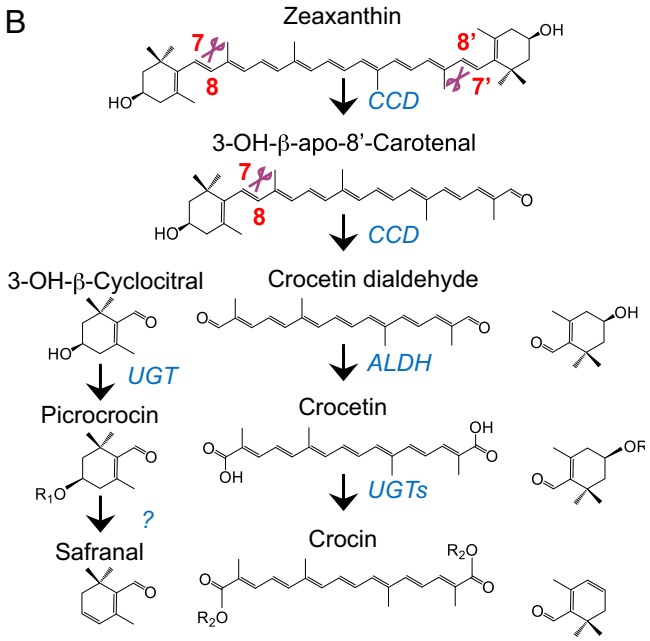

Figure 56. Scheme of safranal and crocin biosynthetic pathway in saffron [120]

5.2 Aim of the project

Carotenoid cleavage dioxygenases are enzymes that catalyze the cleavage of carbon double bond in organic molecules. The possibility to use these enzymes for biocatalytic applications caught the attention of many chemical companies. In contrast to other biocatalysts that catalyze the double bond cleavage (e.g peroxydases), carothenoid dioxygenases are characterized by an exquisite regiosectivity and are not affected by promiscuous activities that can produce side-products. Most of CCDs are able to accept a broad range of carotenoids, but their cleavage activity shows a strict selectivity towards the position of the double bond in the substrate. The double bonds in position 9,10 (9', 10') are cleaved by many CCDs (CCD1, CCD7, BCO), but the only known enzymes that cleave in positions 7, 8 (7', 8'), are the ZCD and CCD2 found in *Crocus sativus*. The characterization of these two CCDs that show this atypical cleavage activity would consent to widen the range of products that are obtainable by enzymatic process. The aim of this project is to characterize the ZCD and the novel CCD2, exploring their potential as enzymes useful for biocatalytic processes. For this purpose, we aim to compare and value the expression of these two enzymes as recombinant proteins and to investigate on their catalytic activity on natural and non-natural substrates *in vitro*.

5.3 Results

5.3.1 DNA sequence optimization for the production in *E.coli*

The project focuses on the characterization of two eukaryotic CCDs from *Crocus sativus*, the CsZCD and CsCCD2. The cDNA encoding these two proteins were identified by Bouvier et al. in 2003 and Frusciante et al. in 2014, and the sequences are available in the NCBI database with the accession number AJ489276.1 (CsZCD) and KJ541749 (CsCCD2). The sequences of both the cDNA were optimized for the expression in *E.coli,* by the online software GeneOptimizer® of the GeneArt® company. The optimization of the sequences aimed to delete or lower the frequency of elements that can hamper the transcription or the translation of the sequences, such as rare codons or secondary structures.

5.3.2 Cloning in pGex 4T1-vector

Both the CsCCD2 and CsZCD were cloned in pGex 4T1 vector following the same strategy. The restriction sites EcoRI and XhoI were introduced in both the synthetic genes to facilitate the cloning in the PGex-4T1 vector. The genes were purified from the original commercial vector by enzymatic digestion and gel purification and then cloned in the expression vector. The ligation products were transformed in E.coli XL-1. The colonies were screened by restriction of the plasmid using the restriction enzymes BamHI/XhoI e EcoRI/XhoI (Figure 57). The restriction pattern allowed the identification and the isolation of the positive clones. The positive clones, were sequenced to check the presence of eventual mutations and the open reading frame of the final construct were verified by virtual translation.

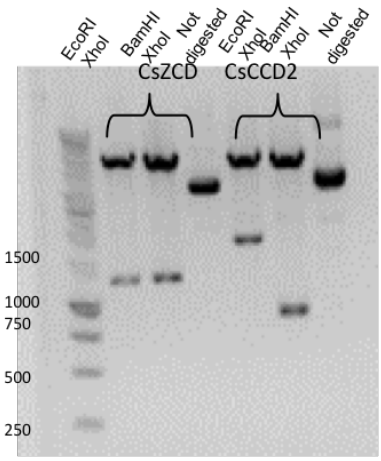

Figure 57. Digestion of pGex vector containing CsZCD and CsCCD2. EcoRI and XhoI were restriction site used for the cloning of the inserts, therefore the double digestion with the corresponding restriction enzymes release a band of 1200 bp for CsZCD and 1700 bp for CsCCD2. The double digestion BamHI XhoI of CsCCD2 resulted in two bands of the same molecular weight (850 bp), due to the presence of a BamHI site in the middle of the CsCCD2 ORF.

5.3.3 Cloning in pETM-22 vector

The ORFs encoding the CsCCD2 were cloned in two different expression vector: the pGex 4T1 and the pETM-22. The pETM-22 is an expression vector designed for thioredoxin fusion proteins and includes an His-tag motif to facilitate the purification.
The ORF encoding the CsCCD2 was cloned in frame with the thioredoxin sequence according to the following strategy: (*i*) The pETM-22 vector was used as template to amplify the thioredoxin sequence; (*ii*) the sequence encoding the CsCCD2 was amplified from the pGEX 4T1 vector; (*iii*) the PCR products of step (*i*) and (*ii*) were used as substrates for a third PCR in order to obtain a fusion product. The complementarity of the reverse and forward primers of the reaction (*i*) and (*ii*) was exploited for the fusion of the two sequences.

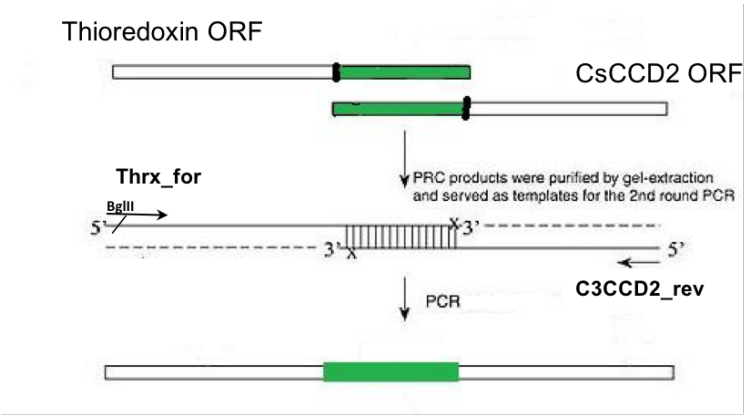

Figure 58. Fusion of Thioredoxin and CsCCD2.

The product of the third PCR (*iii*) was digested by BglII and XhoI restriction enzymes and then cloned in the pETM-22 vector. The colonies were screened by colony PCR and enzymatic digestion. Also in this case, the sequencing confirmed the identity of the ligation products.

5.3.4 Expression

Both the expression vectors are constituted of inducible promoters, the ptac in pGex-4T1 and T7/lac in pETM-22. In absence of inducer, the expression is hampered by lacI repressor (encoded by the plasmids), that bind to the operator region. The inducer isopropil-β-D-tiogalattopiranoside (IPTG) interacts with the lac repressor, modifying its binding with the promoter and activating the protein expression. After induction, we tested two growth temperature: 10°C and 18°C. We chose to express the recombinant proteins at a low temperature to slow down the bacterial metabolism and the protein synthesis in order to improve the correct protein folding and reduce the aggregation of insoluble products.

5.3.4.1 Expression in pGEX-4T1

The promoter ptac of the plasmid pGEX-4T1 is a hybrid promoter composed of the -35 region of the tryptophan promoter and the -10 region of the lacUV5 promoter. The expression of the recombinant protein was tested in two different bacterial strains, BL21 and Invα. Both BL21 and Invα were transformed with the CsCCD2 or the CsZCD cloned in pGEX-4T1 and the expression was valued by SDS-PAGE analysis.

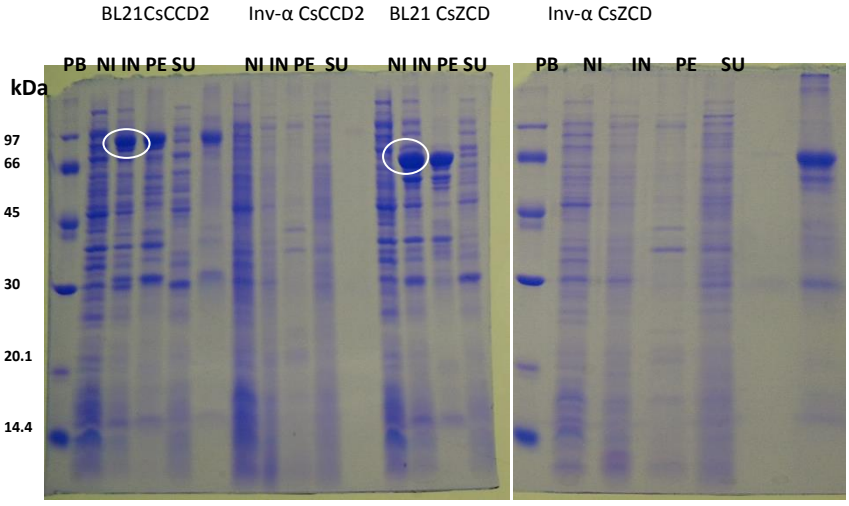

Figure 59. SDS-Page for the expression analysis. PB. Marker, NI: not induced culture, IN: induced culture, PE: pellet, SU: surnatant.

The Figure 59 shows that BL21 cells overexpressed the recombinant proteins upon induction. The calculated molecular weight of the recombinant proteins corresponds to the electrophoretic migration (67,6 kDa for CsZCD, 90,1 kDa for CsCCD2). However, most of the heterologous protein fused with the GST were collected in the pellet fraction, probably due to missfolding and aggregation in inclusion bodies.
The production of the recombinant proteins was not observed in Inv-α strain. Since the aim of this project was to verify the *in vitro* activity of the two charotenoid cleavage dioxygenases, we chose to proceed using BL21 as expression host, in order to ensure the production of a sufficient amount of protein for the enzymatic assay. We did not investigate on the cause of absence of overexpression in Inv-α strain.
The IPTG concentration for optimal expression was evaluated by induction tests on different cultures of BL21.

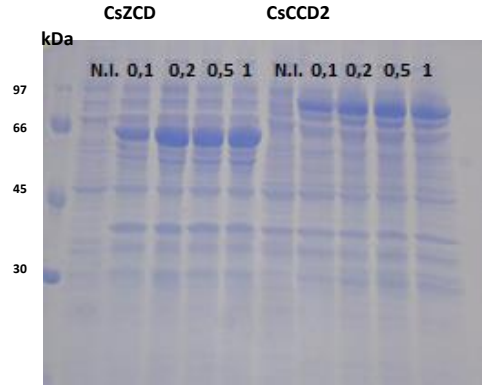

Figure 60. SDS-PAGE for the analysis of the expression at different inducer concentration.. NI: not induced culture. 0,1 0,2 0,5 1 : mM concentration of IPTG used for the induction.

The SDS-PAGE in Figure 60, shows a clear increment in protein production when a concentration of 0,2 mM IPTG is used. However, to ensure a high expression level we chose to proceed using a concentration of 0,5 mM IPTG for the culture induction.

5.3.4.2 Expression in pETM-22

The vector pETM derives from the well known pET vector. These vectors are characterized by a6xHis-*tag*, a protease cleavage site, and a T7/lac promoter. The T7/lac promoter is composed of the operator lac, and a promoter region recognized by the T7 RNA polymerase. Since this expression system requires a bacterial strain that express the T7 RNA polymerase, we chose to express the enzyme in BL21 (DE3).
Also in this case the IPTG concentration for optimal expression level was evaluated. A concentration of 0,2 mM IPTG resulted sufficient to ensure the overexpression of the protein.
A preliminary expression of the tioredoxine-CsCCD2 showed that the fusion protein was

mainly collected in the pellet fraction, and the Comassie coloration did not reveal the presence of recombinant protein in the surnatant fraction. From these analyses we concluded that the thioredoxin did not improve the solubility of the CCD respect to the GST.

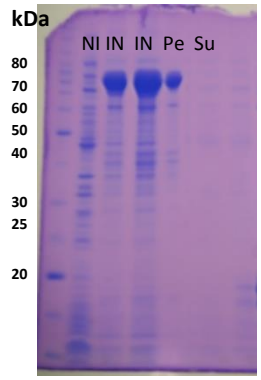

Figure 61. SDS-PAGE analysis of the expression of thrx-CCD2. NI: not induced culture, IN: induced culture, PE: pellet, Su: surnatant.

5.3.4.3 Expression tests in iron-enriched medium

The CCDs are iron dependent enzymes, and their iron center plays an essential role in the catalytic activity [121]. On this basis, we wanted to evaluate if the iron plays a key role in the folding process of these proteins. BL21 cells were transformed with CsCCD2 fused with the GST and the BL21 (DE3) were transformed with the CsCCD fused with the thioredoxin (thrx). The cells were grown in LB medium enriched with 2 mM iron citrate and induced at OD 0,6.

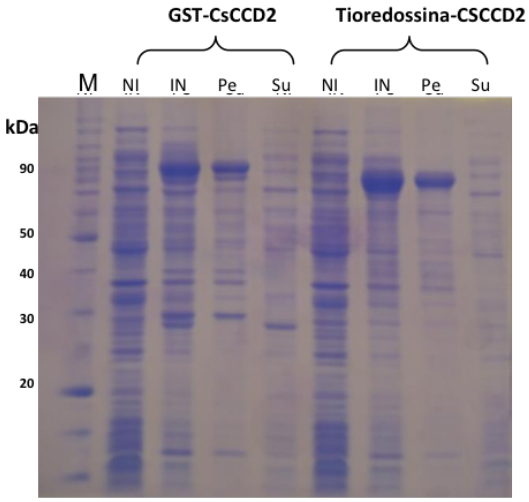

Figure 62. SDS-PAGE analysis of the expression of GST-CsCCD2 and thrx-CsCCD2 in presence of 2mM iron citrate. M: marker, NI: not induced culture, IN: induced culture, Pe: pellet, Su: surnatant

The SDS-PAGE (Figure 62) showed results totally comparable to those obtained in absence of iron citrate, and most of the recombinant protein was collected in the insoluble fraction. Thus, the addition of iron in the culture medium did not influence the folding of the protein.

5.3.5 Purification

5.3.5.1 Purification of of GST-CsZCD and GST-CsCCD2 by GSTrap™

In general, GST is a protein tag that enhances the solubility and facilitate the purification of the fused heterologous protein. Using an agarose matrix functionalized with glutathione molecules is possible to exploit the GST binding to the resin to purify the heterologous protein by affinity chromatography. The binding of the GST to the resin (GSTrap™) is reversible and the fusion protein can be eluted using a solution of reduced glutathione.
BL21 cells expressing the GST-CsZCD and the GST-CsCCD2, were incubated at 18°C overnight. At the end of the incubation, the cells were harvested and mechanically disrupted in French press. The cell lysate was centrifuged and the surnatant fraction was employed for protein purification.

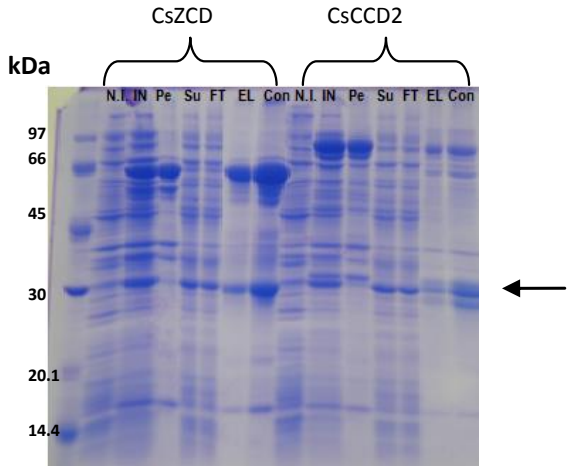

Figure 63. SDS-PAGE analysis of the of samples collected during the purification of GST-CsZCD and GST-CsCCD2. NI: not induced culture, IN: induced culture, Pe: pellet, Su: surnatant, FT: flow through, EL: elution, Con: 5 folder concentrated elution.

The SDS-PAGE in figure 63 shows that all the samples collected after the induction present a significant amount of protein material which molecular weight is consistent with that of the free GST (MW: 29,6 KDa). A further step of gel filtration probably would improve the quality of the purification. Nevertheless, considering the amount of the

recovered protein (0,5 mg/L for the CsCCD2 and 2 mg/L for the CsZCD), we decided to avoid losing protein in a further purification step and save more enzyme for the assays.

5.3.5.2 Purification of TRX—CsCCD2 with HisTrap™

The pETM vector allows the expression of recombinant protein fused with a N-terminal thioredoxin and a C-terminal His-tag. Exploiting the terminal His-tag we purified the fusion protein by affinity chromatography in nickel affinity gel. Despite the expression of the protein was efficiently induced, the SDS-PAGE in Figure 64. shows that the elution fraction is mainly composed by free thioredoxine (12,5 KDa) or degradation protucts of the fusion protein (bands at a molecular weight lower then 78,9 kDa). Since the degradation products are not visible in the induced sample, it is possible that the separation of the thioredoxine from the Cs-CCD2 occurred during the purification process. By IMAC chromatography, we were able to recover only 0,96 mg of protein from one liter of culture.

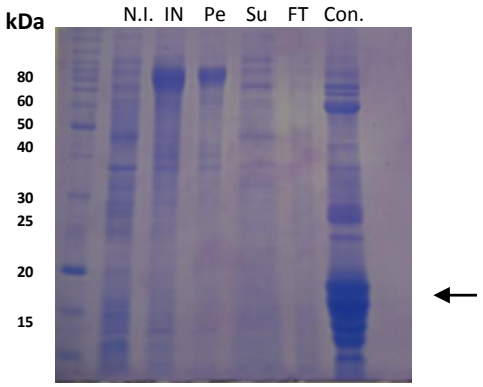

Figure 64. SDS-PAGE analysis of the samples collected during the purification process of thrx-CsCCD2 NI: not induced culture, IN: induced culture, Pe: pellet, Su surnatant, FT flow through, el elution, Con 5 folder concentrated elution.

5.3.6 Activity tests

The activity of the produced recombinant enzymees was evaluated following the indications described in the works of Bouvier [119] and Frusciante [120]. The reaction mixtures were employed to test the activity of both the purified proteins and the cell lysate. The activity was also tested on a reaction mixture, in which the type of the reducing agent, the protein concentration and the amount of detergent added to the substrate, were modified respect to the previously described protocol. The composition of the reaction mixtures used for the enzymatic assays is described in table 8.

Table 8. Composition of the reaction mixtures for the enzymatic assays

Test 1 **Bouvier et al. (119)**	**Test 2** **Frusciante et al (120)**	**Test 3**
Zeaxanthin + octil-β- glucoside 0,2% in Tris HCl 50 mM	Zeaxanthin + Triton X- 100 0,4% in H_2O	Zeaxanthin + Triton 4% in TrisHCl 50 mM
$FeSO_4$ (5 μM)	Incubation Buffer 2X (0,4 mM FeSO4, 2 mg/mL catalasi in 200 mM Hepes/NaOH)	$FeSO_4$ (5 μM)
1 mM DTT	2 mM TCEP	5 mM Ascorbat, 5 μM $FeSO_4$
Enzyme (5 μg) / cell lysate (50 μL)	Enzyme (5 μg) / cell lysate (50 μL)	Enzyme (5 μg) / cell lysatev(50 μL)
V = 200 μL	V = 200 μL	V = 200 μL

5.3.7 Analysis of the reactions by high-performance liquid chromatography (HPLC)

At the end of the incubation (2h at 30°C), the reaction mixture was treated with organic solvent in order to extract the apolar substrates and products from the mixture and separate them from the hydrophilic components, such as salts and proteins. The organic fractions of this *work-up* was analyzed by HPLC in order to reveal the zeaxanthin consumption and the formation of the product (3-OH-β-apo-8'-carotenal). The HPLC analysis were performed in reverse phase using a C18 column. The identity of the peak that correspond to the zeaxanthin in the chromatogram, was confirmed by the chromatographic analysis of a sample of pure zeaxanthin. Moreover, we were able to collect the adsorption spectra of the eluted samples by a multi-diode array detector that facilitates the identification of the substrates or products. Despite a pure standard for the product was not available, the 3-OH-β-apo-8'-carotenal was expected to elute before the zeaxanthin. Since the product of the reaction is an aldehyde and more polar than the substrate, it should present a minor retention time in a reverse phase chromatography.
The Figure 65 reports the chromatographic profiles of the enzymatic reactions. The zeaxanthin peak was observed in all the chromatograms but the peak associated to the product was not revealed. According to the collected chromatograms, the produced enzymes resulted inactive in the reaction conditions that we tested.

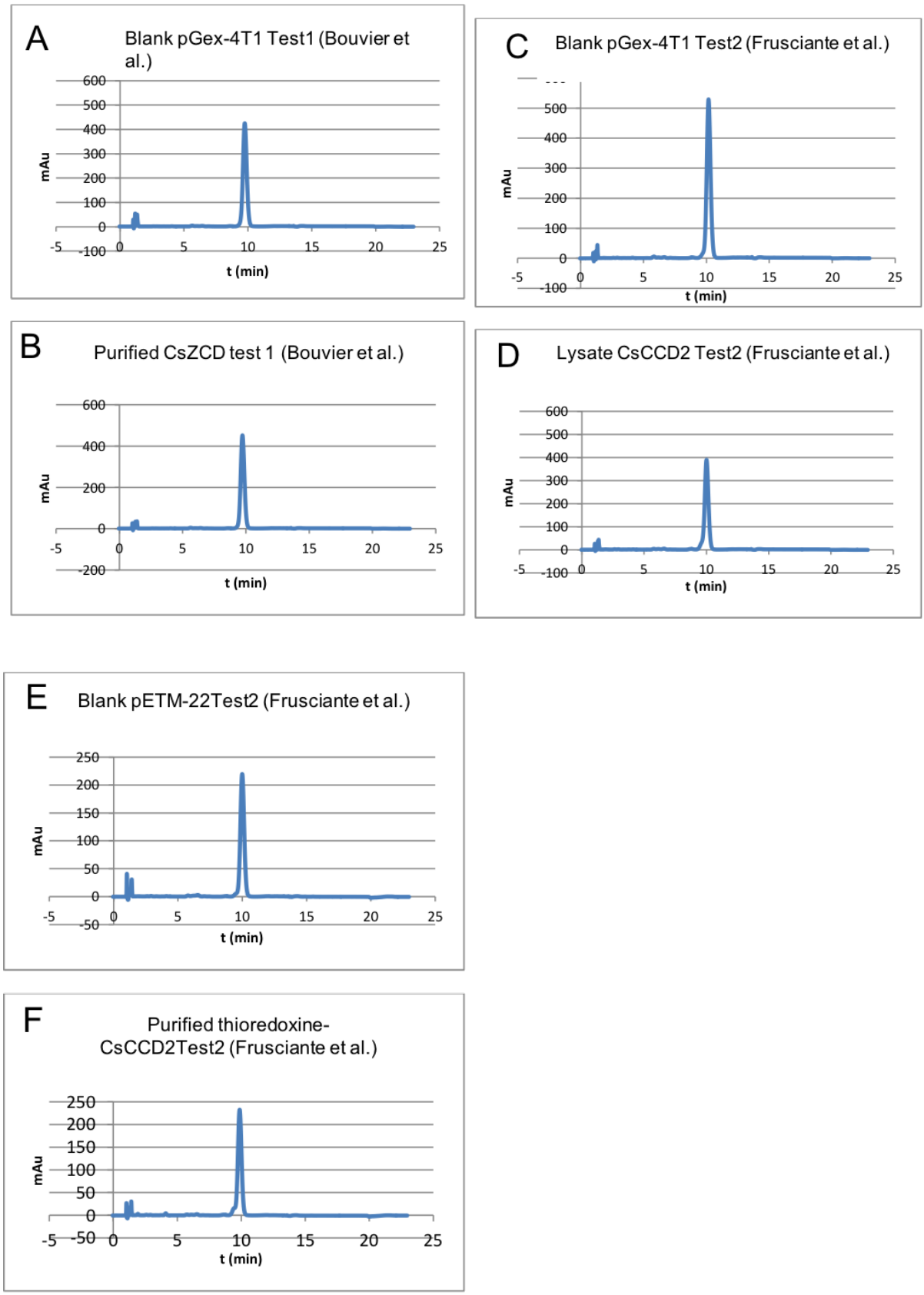

Figure 65. A-F HPLC chromatograms of the organic phase extracted from the reaction mix.

5.3.8 Spectrophotometric analysis

Since zeaxanthin and all carotenoids adsorb in the visible range of light, we tried to follow the progress of the reaction analyzing variations in the intensity or in the shape of the adsorption spectrum of the zeaxanthin in the reaction mixture. We aimed to assess whether the purified enzyme exhibits activity in modifying the substrate and its spectrum. The spectrum of the zeaxanthin in the reaction mix was recorded at the beginning of the reaction and after 16h of incubation. To exclude any contribution in the variation of the spectrum by thermal denaturation of zeaxanthin, we collected the spectra of zeaxanthin incubated without the enzyme. The Figure 66 shows that the absorption spectrum of the zeaxanthin incubated with the enzyme, and the spectrum of the zeaxanthin incubated without the enzyme, are almost overlapped. Variations in the shape or the intensity of the peaks were not observed, therefore, we were not able to detect enzymatic activity also using this different analytical method.

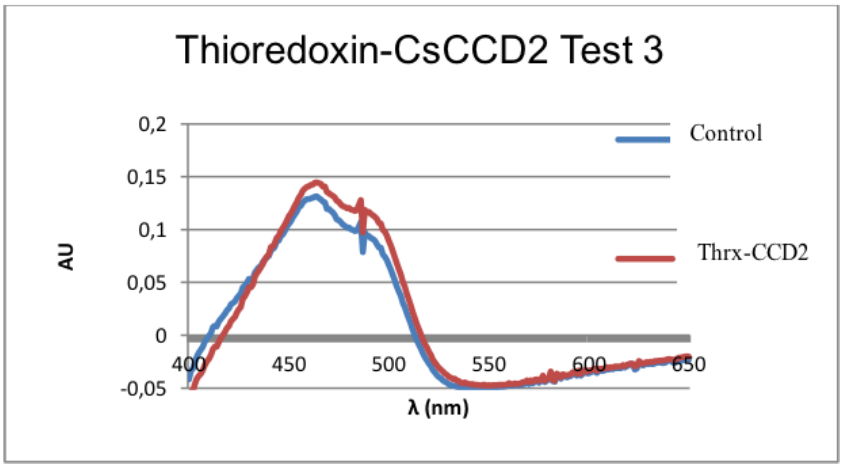

Figure 66. Spectrophotometric analysis of the activity test 3

5.4 Discussion

The CsZCD and CsCCD2 of *Crocus sativus* were expressed in recombinant form in *E.coli,* and their enzymatic activity was tested *in vitro*. The enzymatic assays was carried out following the indications reported in literature, using zeaxanthin as substrate [119, 120]. The results of the HPLC analysis did not reveal any cleavage activity on the zeaxanthin. The cause of the enzyme inactivity has not been identified, but we can speculate on three main reasons: an incorrect folding of the proteins during the expression; a possible denaturation of the enzymes during the purification that leaded to the denaturation and the aggregation of the proteins; reaction conditions unsuitable for the enzymatic activity.

5.4.1 Incorrect protein folding during the purification

As described by the first crystallographic structure of a CCDs, the APO from *Synechosistis*, the members of this enzymatic class are characterized by a hydrophobic patch that facilitate the uptake of the substrates inside the organelle membrane. This exposed hydrophobic patch decreases the solubility of the enzymes and it can facilitate protein aggregation. For this reason, we decided to express both CCD2 and CsZCD fused with proteins known to enhance solubility. The GST is largely used as protein tag to enhance solubility and facilitate the purification by affinity chromatography [122]. The use of GST as fusion protein may present some drawbacks. Indeed, this protein forms homodimers and the oligomerization state may influence the property of the target protein. In place of the GST, we also expressed the CsCCD2 fused with the thioredoxin, a protein smaller than the GST and it does not form dimers.
The induction of the cultures showed that both the fusion proteins were highly expressed but neither the GST nor the thioredoxin permitted to reveal, in the SDS-PAGE, a significant amount of the target protein in the soluble fraction of the cell lysate. The GST fused with the CCD2 seemed to be a more soluble complex compared to the thrx-CCD2. However, the solubility of the fusion complex does not imply the correct folding. In order to assist the folding process, we added to the culture media 2 mM of iron citrate. The ferrous iron is the cofactor of these enzymes and plays a fundamental role in catalytic process. By adding iron citrate to the media, we investigated on the involvement of the metal ion in the folding process of the CCDs. The SDS-PAGE analysis did not reveal any significant increase of the Cs-CCD2 in the soluble fraction of the cell lysate, suggesting that the addition of the metal ion did not contribute to an increase of the correct protein folding. However, it could be interesting to further study this aspect by changing iron source and testing the variations in protein folding by SDS-PAGE analysis and enzymatic assay.
According to the information reported in literature, active forms of recombinant CCDs can be produced in *E.coli* [118, 119, 120], therefore a eukaryotic expression system seems

not to be required for achieving the correct protein folding. Nevertheless, the expression of CsZCD and CsCCD2 in *E. coli* strains that express chaperonins, such as GroES – GroEL or Cpn60 and Cpn10 from *Oleispira Antarctica*, can be promising for the recovery of the active form of the enzymes.

5.4.2 Denaturation of the enzyme during the purification process

Due to the lack of information about the thermostability of CCDs, the three produced recombinant proteins (GST-CCD2, GST-ZCD, Thrx-CCD2) were initially purified at room temperature. The negative results of the activity assays suggested a possible thermal denaturation of the enzymes, therefore we repeated the tests using the proteins purified at 4°C. Indeed, an efficient purification of the GST-fusion proteins requires a very slow flow rate, therefore the proteins of interest were exposed to room temperature for a long time. Although the enzymes were purified at 4°C, the zeaxanthin cleavage activity was not observed.
The SDS-PAGE analysis of the purified proteins showed, in all cases, the presence of a significant amount of proteolytic degradation products. In particular, the purified Thrx-CCD2 resulted largely contaminated y the co-elution of free thioredoxin. The purification of these enzymes requires further optimization, nevertheless, the absence of activity that was registered using the cell lysate excluded the possibility of enzyme inactivation caused by the purification process.

5.4.3 Activity assay and formulation of the reaction mixtures

The reaction mixtures described in literature [119, 120] are all composed by three fundamental elements: an iron source, a reducing agent and a detergent for increasing the solubility of the carotenoids in the aqueous buffer. The reducing agent has the role to maintain the metal iron in the ferrous state (Fe^{2+}) and it was always employed in molar excess respect to iron. The reactions were performed in Eppendorf vessels, that were seven folder more voluminous than the reaction mixture, and incubated under continuous shaking in order to ensure the uptake of the oxygen (the other substrate required for the catalysis). The three different proposed formulations cover a quite broad range of different conditions, including differences in the nature of the reducing agent, the type of detergent and their relative concentrations. Moreover, we exactly reproduced the reaction conditions reported by Bouvier et al. [119] and Frusciante et al [120], expecting the same results obtained by the two groups.
One of the most critical factors that may influence the reaction is the low solubility of the substrates. The hydrophobic nature of the carotenoids hinders the interaction with the enzyme. For this reason, we treated the zeaxanthin with Triton X-100 and octil-β-glucopiranoside, that ,according to the literature, are optimal detergents for carotenoid

solubilization [123]. A solution of detergent in ethanol was employed to mix the carotenoids. The ethanol was then evaporated and carotenoids were supposed to form a complex with the detergent molecules. In this way a micellar system should be formed when the aqueous buffer is added to the substrates. The micellar system should facilitate the interaction with the enzyme but probably it requires further optimizations.
The analysis of the activity assays was performed by HPLC chromatography. The employed analytical method for the analysis is different from that reported in literature, however it was optimized for the separation and the identification of photosynthetic pigments. Since the standards for the products (3-OH-β-apo-8'-carotenal and crocetin dialdheyde) were not available, we advanced hypothesis on their retention time. Both the products are more polar then the substrate, therefore they should be eluted before the zeaxanthin in a reverse phase chromatography. We assume that the adopted analytical method was appropriate for the identification of the products and that, the absence of the product peak in the chromatograms is due to the lack of enzymatic activity.

5.4.4 Incongruence of the information in literature

One of the main difficulties encountered in this work was the incongruence of the reported information about the enzymes that cleave the zeaxanthin, the CsZCD and the CsCCD2. The sequence of the CsZCD was obtained by retrotrascription of the mRNA extracted from saffron styles, and RACE amplification (Rapid Amplification of cDNA Ends) [119]. In 2014 Frusciante et al.[120] suggested that the amplification of the cDNA ends by RACE in the work of Bouvier leaded to the cloning of a truncated transcript. Indeed, the group of Frusciante carried out a 5′-RACE analysis of CCD4 transcripts of *Crocus sativus* obtaining a series of abundant 5′-truncated transcripts. The longest of these transcripts resulted compatible with the length of the ZCD protein. To further demonstrate that the ZCD is a truncated protein they modeled the CCD2, ZCD, and CCD4a structures using the known crystal structure of ACO from *Synechocystis* [121] as template (Figure 67). From the modelling, ZCD resulted as an incomplete enzyme in comparison to the other CCDs predicted structures and ACO. In particular, ZCD lacks blade VII of the β-propeller and part of the dome, whereas CCD2 displays all of the structural features of *bona fide* CCDs.

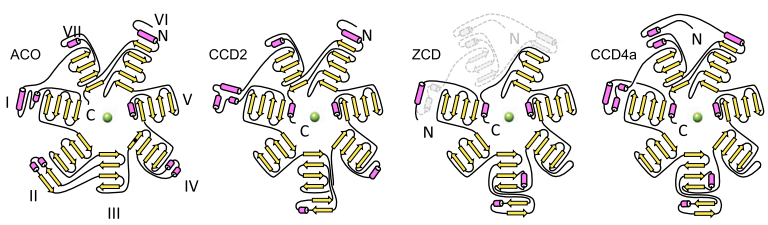

Figure 67. Modelling of CCD2, ZCD and CCD4a of *Chrocus sativus*. The modelling was realized by Frusciante et al. using the RaptorX web server and the ACO structure of *Synechocystis* as template. The figure point out the lack of one blade of the β propeller structure of ZCD [120]

5.5 Conclusions

The initial aim of the project was to evaluate the *in vitro* activity of CsZCD, the enzyme identified by Bouvier et al [119] as responsible of the zeaxanthin cleavage at the position 7-8 (7', 8'). Controversial data are reported in literature about the reproducibility of the enzymatic activity of this protein [120, 124, 125] and, in 2014, a novel carotenoid cleavage dioxygenase, the Cs-CCD2, was identified as the enzyme that cleaves the zeaxanthin at the 7-8 (7'-8') position in *Crocus sativus* [120]. We decided to include also this enzyme of more recent identification into our study. We successfully produced both the carotenoid cleavage dioxygenases in recombinant form, but unluckily we were not able to detect zeaxanthin cleavage activity. Our results lead to conclude that the produced enzymes were both inactive, probably due to an incorrect protein folding. Circular dichroism analysis would permit to further study the folding of these proteins, and their expression in *E.coli* strain co-expressing chaperonins may help to obtain their active forms. Considering the low solubility of these enzymes and the encountered difficulties in obtaining their active forms, the use of these enzymes for applicative purposes still requires the optimization of their production and a more detailed biochemical characterization.

Material and methods

6.1 Chapter I

Molecular biology

All chemicals were purchased from Fluka and Sigma-Aldrich (Milan, Italy). Restriction enzymes were obtained from New England Biolabs (NEB) or Promega. Phusion TM High-fidelity DNApolymerase was from Finnzymes. TSAP Thermosensitive Alkaline Phosphatase was purchased from Promega, whereas T4 DNA Ligase from NEB.
Synthetic gene encoding the Ht-BVMO was purchased by GeneArt® Company. After ligation in pET-28a vector the gene was sequenced using the primers
Ht-1_seq_for: 5'-3' CGTGTTGGTCTGGTTGGTAC
The optimized sequence of Ht-BVMO for the expression in *E.Coli* is indicated below; the 5' NCOI and 3' NotI restriction sites are indicated in bold:

CCATGGGTAGCGATAAACGTGCAGCAGATGCAGCACAGACCGGTGATACCGATGTTGA
TGCAGTTGTTGTTGGTGCAGGTTTTAGCGGTCTGTATATGCTGCATCGTCTGCGTGAT
GAACTGGGTCTGAGCGTTAAAGTTATTGAAAAAGCCGATGATGTTGGTGGCACCTGGT
ATTGGAATAAATATCCGGGTGCACGTTGTGATAGCCGTAGCTGGTTTTATTGCTTTAG
CTTTGATGAAGAAATCCGTGATGAGTGGCAGTATAGCGAAAAATTTCCGGAACAGCCG
GAAATTCTGGAATATCAGCGTTTTGTTGCAGATCGTCTGGATCTGCGTCGTGATATTG
AATTTAATACCGAAGTTACCAGCGCAGCCTTTGATGAAAATGCCGGTGTTTGGAATGT
GGAAACCGATGATGGTAGCACCATTAGCAGCCAGTTTTTTGTTCCGGCAGTTGGTAAT
CTGAGCAAACCGTATCTGCCGGATTTTGATGGTCTGGAAAGTTTTGGTGGCGAATGGT
ATCATACCGCAAAATGGCCTGAAGAAGGTGTTGATCTGAGCGGTAAACGTGTTGGTCT
GGTTGGTACAGGTAGCACCGGTATTCAGATTATGCCTCGTCTGGCAGAACGTAGCGAA
CATCTGACCGTTTTTCAGCGTACCCCGAATTATGGTGTTCCGGCACGTAATGAACCGC
TGACCGATGAAGAATGGGAAGAAATTCGCGAAAACTATGAAGAAATGTGGGAAGAGGC
ACATGCAAGTGATGCAGGTCTGGGTTTTGATACCGAATTTGATAGCATTGATGAAGCC
AGCGAAGAAGAAATTGATCGCGCACTGGAAGAGGGTTGGGAAAATGGTGCACAGGGTC
TGCTGAATGTTTTTACCGATGTTATGGTGAACGAAGAAAGCAATGAACGTGTGGCAGA
ATTTATTCGTAGCAAAATCCGCGAAATTGTGGATGATCCGGAAGTTGCAGAAAAACTG
GTTCCGACCGATCATCCGTATGGTGCAAAACGTCCGCCTCTGACCTATGATGGTTATT
ATGAGAAATATAACCGCGACGATGTGGAACTGGTTGATGTTGGTGAAAGCCCGATTGA
ACGTATTGAAACCGATGGTATTCGTACCGGTGATAGCGTTCATGATCTGGATATTATT
GTTTTTGCCACCGGTTTTGATGCAGTTACCGGCACCTTTGAACAGCTGAACATTCAGG
GTCGCAATGGTATTGATCTGGAAGAAAAATGGGATGCAGGTCCGCGTACCCATCTGGG
TCTGGCAGTTCATGGTTTTCCGAATATGTTTATGGTTACCGGTCCGCAGAGCCCGAGC
GTTCTGACCAATATGACCGTTGCAATTGAACAGCATGTGGAATGGATTAGCGATTGCA

TTGAGTATATGCTGGATAACGACTATAGCTTTATCGAACCGACCGAAGAGGCAGAAAA
TGAATGGAATGAACACAATGATGAGGTTGTTGATCAGACCCTGTTTGATCAGGCAAAT
AGCTGGTATCGCGGTGATAATATTCCGGGTAAAGAAAGCACCTTTCTGATTTATCCGG
GTGGTCTGATTGCCTATAATGAAAAATGTGATGAGGTGGTGGAAAACGATTATGAAGG
CTTTGAACTGAAACGCAGCATTGAAAGT**GCGGCCGC**

Expression

The pET28a constructs containing the relative BVMO gene were transformed into *E. coli* BL21 (DE3) or *E.coli* ArcticExpress. Precultrure were carried out in 5 ml LB medium at 37 °C containing 50 μg/ml of kanamycin. Big culture were carried out using *E.coli* BL21(DE3) in 0,8L LB medium (pH 7.0, 10 g tryptone 5 g yeast extract 10 g NaCl). The cells were grown in shacking incubator at 37°C to an optical density at 600 nm (OD_{600}) of 0.4-0.6, then induced by addition of IPTG to a final concentration of 0.2 mM. The ArcticExpress cultures were incubated at 12°C overnight, whereas BL21 cultures were incubated at 12°C overweekend. The, cells were harvested by centrifugation (4°C, 10 min, 4500xg) and washed with Tris/HCl buffer (Tris 50 mM, pH 8.0). The cells harvested from 0,8 L of culture were solubilized in 20 ml of Tris buffer and disrupted using a pressure of 1,35 Kbar in French Press. FAD cofactor and a concentrated solution of NaCl were added to the crude extract achieving a final concentration of 100 μM FAD and 2M NaCl. The crude extract was incubated overnight at 4°C and centrifuged (4°C, 20 min, 15000xg) to separate soluble e insoluble fractions.
To verify the expression of the BVMO, samples were normalized by OD_{600}, denatured with a SDS buffer, centrifuged, resuspended and used for SDS-PAGE analysis. To verify the identity of the protein also immunoblotting assay was performed using anti His-tag antibody.

In gel digestion and extraction of peptides for ESI MS

The bands corresponding to the putative Ht-BVMO was excised from the polyacrylamide gel. The excised gel band was chopped into cubes and washed with 150 μl of water. 3-4 volumes of Acetonitrile was added to the gel cubes and incubated at room for 15 minunutes until the gel pieces shrunk. Acetonitrile was then removed and the cubes were dried in a vacuum centrifuge. The gel pieces were then swelled in 10 mM TCEP/0,1 M NH_4HCO_3 fand incubated for 30min at 56°C to reduce the protein. All the liquid was then removed and the gel pieces shrinked again with acetonitrile. The acetonitrile was replaced with 55 mM iodoacetamide/0,1M NH_4HCO_3 for 15 minute. All the liquid was removed, gel particles were shrinked again and dried in a vacuum centrifuge.
Gel particles were rehydrated in the digestion buffer containing 50 mM NH_4HCO_3 and 12,5 ng/μl of trypsin at 4°C for 30 minutes and then, they were incubated overight at

37°C. After overnight incubation 50 µl of 5 % formic acid was added to the digestion mix. The solution was mixed and incubated 15 minutes at 37°C. 2 volume of acetonitrile were added to the mix, the gel pieces were spinned down and the supernatant collected. The supernatant, cointaining the digested peptides, was dried in a vacuum centrifuge. Before injection in ESI MS the peptides were resuspended in 50% acetonitrile (CH_3CN), 50% H_2O and 0,1% formic acid (HCOOH).

Enzyme purification

The soluble fraction of the cell lysate was used to purify Ht-BVMO using His_6-Tag metal ion affinity chromatography (IMAC). IMAC chromatography was carried out by gravitational flow, after loading of the cell lysate, the column was washed using three column volumes of Washing Buffer (50 mM Tris HCl 2M NaCl, pH8). The elution was performed using 2 column volumes of Elution Buffer (50 mM Tris HCl, 2M NaCl, 250 mM Imidazole, pH8).
The hydrophobic chromatography (HIC) was performed by FPLC using a flow of 0,5 ml/min

The imidazole elution was loaded in a butyl-sepharose column pre-equilibrated with the Buffer A (50 mM Tris HCl 2M NaCl, pH8). The protein was collected with the solvent front in 8 ml of the same Equilibration buffer. The column was then washed applying a gradient of 100% solution B (50 mM Tris HCl pH8) in 30 min.
The enzyme was concentrated using Vivaspin™ (GE Healthcare) ultra centrifugal filter 30K. The final enzyme concentration was calculated measuring the adsorption of the flavoenzyme at 440 nm. Using the Lambert-Beer law: $A=l\cdot \varepsilon\cdot[flavin]$ it was possible to calculate the enzyme concentration.

Activity assays

BVMO activity is determined spectrophotometrically by monitoring the decrease of NADPH at 340 nm (ε= 6.22 $mM^{-1}cm^{-1}$). Reaction mixtures (100 µl) contained the approprite buffer, 100 µM NADPH, 34 µM of pure enzyme, and 1µl of 1 mM of 3-nonanone in dioxane.. For all the tests a buffer of 50 mM Tris HCl was used but, depending on the acttivity assay the salt concentration, the cosolvent or the type of salt was changed. The reaction was started by adding the enzyme to the mixture. One unit of BVMO is defined as the amount of protein that oxidizes 1 µmol NADPH per minute.
Steady-state kinetic parameters of the different substrates were determined and using substrate concentrations ranging from 0 to 200 mM. Data were fitted using the Michaelis-Menten equation using the program GraphPad Prism.

Circular dichroism

Circular dichroism spectra in the near UV region were collected using a 500 µl cuvette, a lightpath of 1 cm and a protein concentration of 0,5 mg/ml. For the spectra in the far UV we used a 200 µl cuvette with a lightpath of 0,1 cm and a protein concentration of 0,1 mg/ml.

Thermofluor

The unfolding temperatures, *Tm*, were determined using the ThermoFluor method. pure enzyme in a final concentration of 5 µM was added to 44 µl of the chosen buffer in a 96 well plate. The wells were mixed with 5 µl of Sypro-Orange, diluted 1:100 in H_2O mQ. The plate was loaded in in a Real Time PCR machine fitted with a 470 – 543 nm excitation filter and a SYBR Green emission filter (523 – 543 nm). A temperature gradient from 20 to 90 °C was applied (1°C/min), and fluorescence data was recorded. A sigmoidal curve was obtained after plotting the fluorescence against the temperature. The unfolding temperature, *Tm*, was then determined as the maximum of the derivative of the sigmoidal curve.

Conversions and GC/GC-MS analysis

For GC-MS analysis, 5ml of 50 mM Tris–HCl (pH 8), containing 1M NaCl, 5 mM substrate, 100 µM NADPH, 34 µM PTDH, 20 mM phosphite and 34 µM Ht-BVMO was incubated at 24 °C for 20 h. The reactions were carried out in special glass vessels of 20 ml volumes and air-tight stopper. The reactions were then stopped by heating for 20 minutes at 60°C and analyzed by head space GC-MS to determine the degree of conversion. The head space gasses were pre-heated at 150°C and injected in a HP-1MS column. The following program was applied:

Step	Temperature (°C)	Time (min)
0	35	0
1	35	5
2	250	15,75
3	250	25,75

6.2 Chapter II

Primers for Physcomitrella patens BVMO knock-out construct

Primers for amplification of BVMO genomic region and HpaI site insertion were:

Pp_KO_HpaI_for: 5'- GTTAACAGTAGCAGGGAGAGGA -3'

Pp_KO_HpaI_rev: 5'- GTTAACACCATCACAAACTTGGC-3'

Primers for the screening of geneticin resistance mutants

Primers external to the region exploited for the homologous recombination.

Pp_screen_for 5'- AGAAGGCCAGACAACCACAC – 3'
Pp4_Reverse primer 5'- CAACCCTGGACAGCATCGGAAGCCT – 3'

Primer that anneals in the marker region:

Pp_BVMOKO_screen_rev : 5'- ACGGCGAGTTCTGTTAGGTC – 3'

Propagation of *Physcomitrella* in laboratory conditions

Cells from almost any tissue of *Physcomitrella* can regenerate to produce protonemal tissue. The propagation of the moss was carried out collecting the protonema tissue from 6-7 days-old plates; the tissue was blended in water by homogenizing moss material with Polytron (IKA T25 Digital Ultra Turrax). The suspension was then spread in agar plates with medium overlaid with cellophane disks. The cellophane disk facilitates the subsequent collection of biological material. Cultures were grown in a growth chamber at 24°C, with 16 h light/8 h dark photoperiod and a light irradiance of about 40-50 μE. The employed media for the propagation are: $PpNO_3$ (minimum media), and $PpNH_4$ (rich medium). Rich medium was used only to obtain starting culture for further analyses or for moss transformation, minimum media was used for characterization studies.
$PPNO_3$ medium is composed by a phospate buffer of 0,25 g/l KH_2PO_4 pH7 and the following macro and micolements.

Macro elements:
$Ca(NO_3)$ $4H_2O$ 0,8 g/l
$MgSO_4$ $7H_2O$ 0,25 g/l
$FeSO_4$ $7H_2O$ 0,0125 g/l

Micro elements:
$CuSO_4$ 5 H_2O 0,055 mg/l
$ZnSO_4$ $7H_2O$ 0,055 mg/l
H_3BO_3 0,614 mg/l
$MnCl_2$ $4H_2O$ 0,389 mg/l
$CoCl_2$ $6H_2O$ 0,055 mg/l
KI 0,028 mg/l
Na_2MoO_4 $2H_2O$ 0,025 mg/l

Rich medium ($PPNH_4$) is composed of the minimal medium and 500 mg/l NH_4 tartrate and 5 g/l of glucose.
For solid plate, plant agar was added to $PPNH_4$ and $PPNO_3$ medium in a concentration of 7g/l and 8 g/l respectively.

Transformation of the moss *physcomitrella patens*

Protoplasts are isolated from protonema by the digestion (30 min at RT) with 1% (w/v) Driselase (Sigma- Aldrich) dissolved in 8.5% (w/v) mannitol. The digested moss material was filtered through a 100µm sieve, left for additional 15min at room temperature to continue digestion on the filter and carefully washed with 8.5% mannitol. The protoplasts were collected by centrifuging the filtrate at 200g for 5 minutes at room temperature, then supernatant was discarded and the pellet was washed twice in 8.5% mannitol.
Protoplasts were then resuspended in MMM solution (8.5% mannitol, 15mM $MgCl_2$, 0.1% MES, pH 5.6) at a concentration of $1.2*10^6$ cells/ml. Afterwards, aliquots of 15µg of linearized DNA was dispensed in falcon tubes and 300µl of protoplast suspension and 300µl of PEG solution (7% mannitol, $Ca(NO_3)_2$ 0.1 M, PEG 4000 35-40%, 10 mM Tris pH 8) were added mixing gently. The mixture was heat-shocked 5 minutes at 45°C and brought to room temperature for 10 minutes. Samples were progressively diluted with liquid rich medium ($PpNH_4$ supplemented by 66g/l mannitol; adding 5x300 µl and 5x1000 µl) and incubate in dark at room temperature overnight.
The next day, protoplasts were embedded in protoplast top-layer (mannitol 8.5% with 0.84% agar Sigma (A9799); 7 ml of top layer for each tube, thus final agar concentration is 0.42%) and plated on the cellophane covered plate with rich medium ($PpNH_4$) added with 66g/l mannitol and 0.7% agar.
Plates were incubated in a plant growth chamber under standard growth conditions (16/8

h photoperiod, 24°C, irradiance about 40 μE). Selection of transformants started 6 days after transformation by transferring top layer to a new Petri dish with $PpNH_4$ medium supplemented with 50 μg/ml G418, for about 10 days. Resistant colonies are then transferred to non-selective $PpNH_4$ medium for additional 10 days, and then again on selective media to isolate only stable transformants.

Extraction of the pigments and chromatographic analysis

The tissue of wild type and BVMO-KO mutants were collected from 6-days old cultures and placed in 1,5 ml eppendorf tubes. The tubes were centrifuged to remove the water retained by the moss tissues. A solution of 80% acetone was added to the pellet and the tissues were grinded using quartz sand and an apposite pestle. The quartz sand was precipitated by centrifugation and the surnatant, containing the extracted pigments was collected.
The analysis of the extracted pigments was carried out by reverse phase chromatography, using an octadecyl hydrophobic resin (C18) that was preloaded in a steel column. The pigments dissolved in 80% acetone were loaded in the 250 μl loop of the chromatographer. A gradient elution was applied using the following program.

Time (min)	**Solution A** (3,6 % Tris HCl 0.1 M pH 8; 9,6 % methanol; 86,8 % acetonitrile)	**Solution B** (80% methanol; 20% hexane)
0	100%	0%
9	100%	0%
12	0%	100%
18	0%	100%
20,30	100%	0%
33	100%	0%

Primers for *Cyanidioschyzon merolae* BVMO knock-out construct.

Primers for amplification of the wild type URA 5.3 gene

URA_up7_for: 5'-3' GCAGAAGAGCTCGTGGAAGAAAGAG

URA_dw10_rev: 5'-3' CGG TTC TAG TGA GAT AGC TCT TCG GTC

Primers for amplification of URA 5.3 marker cassette and insertion of Hind_III and

Bam_HI restriction site

CmBVMOKO5_HindIII_for**:** 5'- GAC ACA GAG AAG CTT GCG GTG G -3'
CmBVMOKO6_BamHI_rev: 5'- CAC AAA GAC CGG ATC CGA ATT CTG -3**'**

Primers for amplification of BVMO gene and insertion of HpaI restriction site.

CmBVMOKO3_HpaI_for: 5'- GTT AAC CTC GGT ATG TGT GTG AAA TAG C -3'
CmBVMOKO4_HpaI_rev: 5'- GTT AAC TGT GGA AAT GTA TCC AAA TCC C -3'

***Cyanidioschyzon merolae* culture media**

Two different media were tested for *Cyanidioschyzon merolae* 10D growth

M-Allen (Minoda 2004 [94])
Protocol for 100 ml culture

$(NH4)_2SO_4$	262 mg
$MgSO_4$ 7 H_2O	50 mg
KH_2PO_4	54 mg
$CaCl_2$ $2H_2O$	14 mg
A2 trace element stock solution	0,2 ml
H_2O	99,4 ml
A2 Fe stock solution *	0,4 ml

- * A2 Fe stock solution (sterilized by passing through a 0,22 μm Millipore filter) was added after autoclaving the medium

M-Allen 2.0 (Ohnuma 2008 [98])
Protocol for 1 litre medium

$(NH4)_2SO_4$	5,285 g
$MgSO_4$ 7 H_2O	0,985 g
KH_2PO_4	1,088 g
$CaCl_2$ $2H_2O$	0,147 g
A2 trace element stock solution	4 ml
H_2O	994 ml
A2 Fe stock solution *	6,7 ml

- A2 Fe stock solution (sterilized by passing through a 0,22 μm Millipore filter) was added after autoclaving the medium

Both media were titrated at pH 2,5 by adding H_2SO_4

A2 trace element stock solution

H_3BO_3	285 mg
$MnCl_2\ 4H_2O$	180 mg
$ZnCl_2$	10,5 mg
$Na_2MoO_4\ 2H_2O$	39 mg
$CoCl_2\ 6H_2O$	4 mg
$CuCl_2\ 2H_2O$	4,3 mg
Distilled water	100 ml

A2 Fe stock solution

EDTA 2Na	700 mg
$FeCl_3\ 6H_2O$	400 mg
Distilled water	100 ml

For solid plates a 2x MA2 medium was mixed with the same volume of autoclaved distilled water and 0,5% Phytagel.

Cyanidioschyzon merolae uracil auxotrophic mutant (M4) was cultivated in MA2 medium containing uracil (0,5 mg/ml)

C. merolae electroporation

In order to introduce DNA into *C. merolae* M4 by electroporation we followed the protocol described by Minoda et al [94].
1.5 ml cultures were harvested at the mid-exponential phase (A_{750} = 0.3–0.4), and concentrated to 40 µl by centrifugation. The cell suspension containing 3–4 10^8 cells was mixed with 1 µl of pURA5.3-KS (0.5 µg μl^{-1}), and electroporated at a field strength of 2 kV $m^{-1}s^{-1}$. After electroporation, cell suspensions were inoculated with 2 ml MA medium, and incubated overnight in the dark at 40°C with shaking. The cells were spread on MA-0.4% Phytagel plates, and incubated under light conditions with 40 µE at 37°C to allow selection of uracil prototrophic.

C. merolae PEG-mediated transformation

To introduce DNA into *C merolae* M4 by PEG solution, we followed the protocol described by Ohnuma et al [98].
Cells were harvested by centrifugation (2,000 g for 5 min) from a 100 ml culture at

OD_{750} = 0.4. The collected cells were washed once with MA-I [20 mM $(NH_4)_2SO_4$, 2 mM $MgSO_4$, 1 x trace elements] and resuspended in MA-I to concentrate to 150- to 200-fold. After adding 5 μg of DNA in 400 μl of MA-I to 100 μl of cell suspension (containing 1.5–3.3 10^7 cells), 500 μl of PEG solution [60% (w/v) in MA-I] was added to the mixture to make the final PEG concentration 30%. After leaving for 5 min at room temperature, the mixtures were diluted to 50 ml with MA2 medium, and incubated at 37°C overnight. After overnight incubation, cells were collected by centrifugation (2,000 *g* for 5min at 37°C), suspended with 200μl of MA2 medium and spotted on MA2 plates.

6.3 Chapter III

The synthetic genes encoding the CsZCD and CsCCD2 were purchased from GeneArt Company.
The sequences were optimized for the expression in *E.coli* and are reported below (the 5' EcoRI and the 3' XhoI restriction sites are indicated in bold):
CsZCD 5'-3':

GAATTCATGCAGGTTGATCCGACCAAAGGTATTGGTCTGGCAAATACCAGCCTGCAGTT
TAGCAATGGTCGTCTGCATGCACTGTGTGAATATGATCTGCCGTATGTTGTTCGTCTGA
GTCCGGAAGATGGTGATATTAGCACCGTTGGTCGTATTGAAAATAACGTTAGCACCAA
AAGCACCACCGCACATCCGAAAACCGATCCGGTTACCGGTGAAACCTTTAGCTTTAGCT
ATGGTCCGATTCAGCCGTATGTTACCTATAGCCGTTATGATTGTGATGGCAAAAAAAGC
GGTCCGGATGTTCCGATTTTTAGCTTTAAAGAACCGAGCTTTGTGCACGATTTTGCCATT
ACCGAACATTATGCAGTGTTTCCGGATATTCAGATTGTTATGAAACCGGCAGAAATTGT
TCGTGGTCGTCGTATGATTGGTCCGGATCTGGAAAAAGTTCCGCGTCTGGGTCTGCTGC
CTCGTTATGCAACCAGCGATAGCGAAATGCGTTGGTTTGATGTTCCGGGTTTTAACATG
GTTCATGTTGTTAATGCATGGGAAGAGGAAGGTGGCGAAGTTGTTGTTATTGTTGCAC
CGAATGTTAGCCCGATTGAAAATGCAATTGATCGCTTTGATCTGCTGCATGTTAGCGTT
GAAATGGCACGTATTGAACTGAAAAGCGGTAGCGTTAGCCGTACCCTGCTGAGCGCAG
AAAATCTGGATTTTGGTGTTATTCATCGTGGTTATAGCGGTCGTAAAAGCCGTTATGCA
TATCTGGGTGTTGGTGATCCGATGCCGAAAATTCGTGGTGTTGTTAAAGTTGATTTTGA
ACTGGCAGGTCGTGGTGAATGTGTTGTTGCACGTCGTGAATTTGGTGTTGGTTGTTTTG
GTGGTGAACCGTTTTTTGTTCCGGCAAGCAGCAAAAAAAGTGGTGGTGAAGAGGATGA
TGGTTATGTTGTGAGCTATCTGCATGATGAAGGTAAAGGTGAAAGCAGCTTTGTTGTTA
TGGATGCACGTAGTCCGGAACTGGAAATTCTGGCAGAAGTTGTTCTGCCTCGTCGTGTT
CCGTATGGTTTTCATGGTCTGTTTGTTACCGAAGCAGAACTGCTGAGCCAGCAGTAAGG
ACGACACCGTACCACTGAATGATAAAAGATATCCACCTGAACGTATAATCATCACCTCT
CCATATTCGCTGCCA**CTCGAG**

CsCCD2 5’-3’:

GAATTCATGGCCAATAAAGAAGAAGCCGAAAAACGCAAAAAGAAACCGAAACCGCTG
AAAGTGCTGATCACCAAAGTTGATCCGAAACCGCGTAAAGGTATGGCAAGCGTTGCAG
TTGATCTGCTGGAAAAAGCATTTGTTTATCTGCTGAGCGGTAATAGCGCAGCAGATCGT
AGCAGCAGCAGCGGTCGTCGTCGCCGTAAAGAACATTATTATCTGAGTGGTAATTATGC
ACCGGTGGGTCATGAAACCCCTCCGAGCGATCATCTGCCGATTCATGGTAGCCTGCCGG
AATGTCTGAATGGTGTTTTTCTGCGTGTTGGTCCGAATCCGAAATTTGCACCGGTTGCA
GGTTATAATTGGGTTGATGGTGATGGTATGATTCATGGTCTGCGTATTAAAGATGGTAA
AGCAACCTATCTGAGCCGCTATATCAAAACCAGCCGTTTTAAACAAGAGGAATATTTTG
GCCGTGCCAAATTCATGAAAATTGGTGATCTGCGTGGTCTGCTGGGTTTTTTTACCATTC
TGATTCTGGTTCTGCGTACCACCCTGAAAGTTATTGATATTTCATATGGTCGTGGCACCG
GTAATACCGCACTGGTTTATCATAATGGTCTGCTGCTGGCACTGAGCGAAGAGGATAA
ACCGTATGTTGTTAAAGTTCTGGAAGATGGTGATCTGCAGACCCTGGGTATTCTGGATT
ATGATAAAAAACTGAGCCATCCGTTTACCGCACATCCGAAAATTGATCCGCTGACCGAT
GAAATGTTTACCTTTGGTTATAGCATTAGCCCTCCGTATCTGACCTATCGTGTTATTAGC
AAAGATGGTGTTATGCAGGATCCGGTTCAGATTAGCATTACCAGCCCGACCATTATGCA
TGATTTTGCCATTACCGAAAACTATGCCATCTTTATGGATCTGCCGCTGTATTTTCAGCC
GGAAGAAATGGTTAAAGGCAAATTTGTTAGCAGCTTTCATCCGACCAAACGTGCCCGTA
TTGGTGTTCTGCCTCGTTATGCAAAAGATGAACATCCGATTCGTTGGTTTGATCTGCCGA
GCTGTTTTATGACCCATAATGCAAATGCATGGGAAGAAAATGATGAAGTGGTTCTGTTT
ACCTGTCGTCTGGAAAGTCCGGATCTGGATATGCTGAGCGGTCCGGCAGAAGAAGAAA
TTGGTAATAGCAAAAGCGAGCTGTATGAAATGCGCTTTAATCTGAAAACCGGTATCACC
AGCCAGAAACAGCTGAGCGTTCCGAGCGTTGATTTTCCGCGTATTAATCAGAGCTATAC
CGGTCGTAAACAGCAGTATGTTTATTGTACCCTGGGCAATACCAAAATCAAAGGCATCG
TTAAATTTGATCTGCAGATTGAACCGGAAGCAGGTAAAACCATGCTGGAAGTTGGTGG
TAATGTTCAGGGTATTTTTGAACTGGGTCCGCGTCGTTATGGTAGCGAAGCAATTTTTG
TTCCGTGTCAGCCTGGTATCAAATCCGATGAAGATGATGGTTATCTGATCTTCTTTGTGC
ACGATGAAAACAACGGTAAAAGCGAAGTGAATGTGATTGATGCAAAAACCATGAGCG
CAGAACCGGTTGCAGTTGTTGAACTGCCGAGCCGTGTTCCGTATGGTTTTCATGCACTG
TTTCTGAATGAAGAAGAACTGCAGAAACATCAGGCAGAAACCTAA**CTCGAG**

The primers employed for the fusion construct Thrx-CsCCD2 are:

TRX for: ATGCGTCCGGCGTAGAGGATC

TRX rev: TTTATTGGCCATGGGCCCCTGGAACAGAACTTC

C3CCD2 for: TTCCAGGGGCCCATGGCCAATAAAGAAGAAGCCG

C3CCD2 rev: TTTTTAAGCTTTGCCTGATGTTTCTGCAGTTC

Expression of GST-CsZCD and GST-CsCCD2

The pGex-4T1 vectors, containing the genes encoding for CsZCD and CsCCD2 were used to transform E.coli BL21 cells. Precultures were carried out in 10 ml LB medium at 37°C containing 100 μg/ml of ampicillin. The precultures were used as starter for a 500 ml culture. The cells were grown in shacking incubator at 37°C to an optical density at 600 nm (OD_{600}) of 0.4-0.6, then induced by addition of IPTG to a final concentration of 0.2 mM. The cells were grown in shaking incubator at 18°C *overnight* or at 12°C *overweekend.* At the end of the incubation the cells were harvested by centrifugation at 6000 rpm for 10 minutes at 4°C. The pellet was resuspended in PBS (140 mM NaCl, 2.7 mM KCl, 10 mM Na_2HPO_4, 1.8 mM KH_2PO_4, pH 7.3) in case of protein purification or Phosphate buffer (50 mM NaH2PO4, 300 mM NaCl, 1 mM DTT e 0,1% Triton X-100) in case of activity assays with cell lysate. Cell disruption was carried out by French-press, applying a pressure of 1,35 Kbar. The cell crude extract was centrifuged at 28000g for 30 minutes at 4°C in order to separate the cell debryes from the surnatant.

Expression of Thrx-CsCCD2

For the expression of Thrx-CsCCD2, the expression vector pETM-22 were used to transform *E. coli* BL21 (DE3) strain. For the selection we used the kanamycin at a concentration of 50 μg/ml and for the induction a concentration of IPTG of 0,2 mM. After incubation of the induced cultures, the cells were harvested by centrifugation and resuspended in TrisHCl 50 mM and 300 mM NaCl for the disruption by FrenchPress.

Purification of GST-CsZCD and GST-CsCCD2

The surnatant of GST-CsZCD and GST-CsCCD2 were filtered with a 0,2 μm filter and loaded in GSTrap (GE Healthcare®) column. The column was equilibrated using ten column volumes of microfiltered PBS and the surnatant was loaded applying a low flow (0,5 ml/min). The column was then washed using the filtered PBS and the protein was eluted in 5 ml of elution buffer (50 mM TrisHCl, 10mM glutathione pH 7,5). During the elution 6 fractions were collected and the presence of the protein in each fraction were evaluated by Braddford colorant. The fractions containing the protein material were collected together and concentrated by Vivaspin™ ultra centrifugal filter (GE Healthcare). Protein concentration were determined by Bradford assay using different concentration of BSA (bovine serum albumine) for the calibration curve.

Purification of THRX-CsCCD2

The purification was carried out using a Nickel affinity gel (Sigma-Aldrich) by gravitation flow in column. The column was equilibrated with ten column volumes of 50 mM Tris HCl 300 mM NaCl at pH 8. The same buffer was used to wash the column after the surnatant loading. For the elution 3 ml of 50 mM TrisHCl 50 mM, 300 mM NaCl and 250 mM imidazole were employed. The elution fractions that contained the protein material were collected together and concentrated by Vivaspin^{TM} ultra centrifugal filter (GE Healthcare). The final protein concentration was determined by Bradford assay.

Preparation of the substrates for activity tests

For the activity tests a solution of zeaxanthin 160 µM in 100% ethanol was prepared.

Test1: 50 µl of zeaxanthin 160 µM in ethanol were added to 40 µl of ethanol and 1% octil-β-glucopiranoside. The solution was mixed and dried by vacuum centrifuge. The pellet was resuspended in Tris HCl 50 mM pH8.

Test 2: 50 µl of 160 µM zeaxanthin were added to 50 µl of ethanol and Triton X-100 0,4 %. The substrate and detergent were dried by vacuum centrifuge. The formed pellet was resuspended in H_2Omq and reaction buffer 2x, before the enzymatic assay test.

Test 3: For this test we increase the concentration of the detergent trying to optimize the solubility of the substrates and facilitate the interaction of the substrate with the enzyme . 50 µl of 160 µM zeaxanthine were added to 50 µl of ethanol ethanol and triton X-100 4%, and then the solution was dried by vacuum centrifuge. The pellet was resuspended in TrisHCl 50 mM pH 8 before the enzymatic assay.

Reaction work-up

The enzymatic reactions were stopped by addition of 200 µl of acetone.
The substrates and the expected products of the reaction were extracted from the reaction mix using 300 µl of dichloromethane/methanol 1:1 (v/v). After the separation of the phases the hypophase was extracted and dried by vacuum centrifuge.

Reverse phase HPLC chromatography

The analysis of the extracted substrates and products was carried out by reverse phase chromatography, using an octadecyl hydrophobic resin (C18) preloaded in a steel column. The pellet, containing the extracted products and substrates, was resuspended in 300 µl

of 80% acetone and injected in the 250 µl loop of the chromatographer. A gradient elution was applied using the following program.

Time (min)	**Solution A** (3,6 % Tris HCl 0.1 M pH 8; 9,6 % methanol; 86,8 % acetonitrile)	**Solution B** (80% methanol; 20% hexane)
0	100%	0%
9	100%	0%
12	0%	100%
18	0%	100%
20,30	100%	0%
33	100%	0%

Bibliography

1. Pasteur, LCR Hebd. Séance Acad. Sci. Paris 1858, 46, 615
2. Buchner, E. Ber. Dtsch. Chem. Ges. 1897, 36, 117
3. Glick, Bernard R., and Jack J. Pasternak. "Principles and applications of recombinant DNA." *ASM, Washington DC* (1998): 683.
4. Stemmer, Willem PC. "Rapid evolution of a protein in vitro by DNA shuffling."*Nature* 370.6488 (1994): 389-391.
5. Stemmer, Willem PC. "Molecular breeding of genes, pathways and genomes by DNA shuffling." *Journal of Molecular Catalysis B: Enzymatic* 19 (2002): 3-12.
6. Amann, Rudolf I., Wolfgang Ludwig, and Karl-Heinz Schleifer. "Phylogenetic identification and in situ detection of individual microbial cells without cultivation." *Microbiological reviews* 59.1 (1995): 143-169.
7. Cowan, Don A. "Microbial genomes–the untapped resource." *Trends in Biotechnology* 18.1 (2000): 14-16.
8. Jaenicke, Rainer, and Gerald Böhm. "The stability of proteins in extreme environments." *Current opinion in structural biology* 8.6 (1998): 738-748.
9. Van Den Burg, Bertus. "Extremophiles as a source for novel enzymes."*Current opinion in microbiology* 6.3 (2003): 213-218.
10. Paiardini, Alessandro, et al. "Structural plasticity of thermophilic serine hydroxymethyltransferases." *Proteins: Structure, Function, and Bioinformatics* 50.1 (2003): 122-134.
11. Kumar, Sandeep, Chung-Jung Tsai, and Ruth Nussinov. "Factors enhancing protein thermostability." *Protein Engineering* 13.3 (2000): 179-191.
12. Cavicchioli, Ricardo, et al. "Low-temperature extremophiles and their applications." *Current Opinion in Biotechnology* 13.3 (2002): 253-261.
13. Gros, M., and R. Jainicke. "Protein under pressure." *Eur. J. Biochem* 221 (1994): 617-630.
14. Pledger, Ralph J., Byron C. Crump, and John A. Baross. "A barophilic response by two hyperthermophilic, hydrothermal vent Archaea: an upward shift in the optimal temperature and acceleration of growth rate at supra-optimal temperatures by elevated pressure." *FEMS microbiology ecology*14.3 (1994): 233-242.
15. Dill, Ken A. "Dominant forces in protein folding." *Biochemistry* 29.31 (1990): 7133-7155.
16. Timasheff, S.N. "Solvent effects on protein stability". Curr. Opin. Struct. Biol. 2:35 – 39;1992.
17. Madern, Dominique, Claude Pfister, and Giuseppe Zaccai. "Mutation at a single acidic amino acid enhances the halophilic behaviour of malate dehydrogenase from Haloarcula marismortui in physiological salts."*European journal of biochemistry* 230.3 (1995): 1088-1095.
18. Zaccai, Giuseppe, and Henryk Eisenberg. "Halophilic proteins and the influence of solvent on protein stabilization." *Trends in biochemical sciences*15.9 (1990): 333-337.
19. Kuntz Jr, Irwin D. "Hydration of macromolecules. IV. Polypeptide conformation in frozen solutions." *Journal of the American Chemical Society*93.2 (1971): 516-518.
20. Sellek, Gerard A., and Julian B. Chaudhuri. "Biocatalysis in organic media using enzymes from extremophiles." *Enzyme and Microbial Technology* 25.6 (1999): 471-482.
21. Lanyi, Janos K., and Joann Stevenson. "Effect of salts and organic solvents on the activity of Halobacterium cutirubrum catalase." *Journal of bacteriology*98.2 (1969): 611-616.
22. Boicelli, C. A., et al. "The influence of phosphate buffers on the 31 P longitudinal relaxation time in inverted micelles." *Spectrochimica Acta Part A: Molecular Spectroscopy* 38.2 (1982): 299-300.
23. Martinek, Karel, et al. "Micellar enzymology." *European Journal of Biochemistry* 155.3 (1986): 453-468.
24. Luisi, P. L., et al. "Reverse micelles as hosts for proteins and small molecules." *Biochimica et Biophysica Acta (BBA)-Reviews on Biomembranes*947.1 (1988): 209-246.
25. Marhuenda-Egea, Frutos C., et al. "Reverse micelles in organic solvents: a medium for the biotechnological use of extreme halophilic enzymes at low salt concentration." *Archaea* 1.2 (2002): 105-111.

26. Bru, Roque, Alvaro Sánchez-Ferrer, and Francisco García-Carmona. "Kinetic models in reverse micelles." *Biochemical Journal* 310.Pt 3 (1995): 721.
27. Marhuenda-Egea, Frutos C., et al. "Enzymatic activity of an extremely halophilic phosphatase from the Archaea Halobacterium salinarum in reversed micelles." *Journal of Molecular catalysis B: Enzymatic* 10.6 (2000): 555-563
28. Noyori, Ryoji, Tsuneo Sato, and Hiroshi Kobayashi. "The Baeyer-Villiger oxidation of 8-oxabicyclo (3.2. 1) octan-3-ones. Substituent effects on the regioselectivity." *Bulletin of the Chemical Society of Japan* 56.9 (1983): 2661-2679.
29. Fraaije, Marco W., et al. "Identification of a Baeyer–Villiger monooxygenase sequence motif." *FEBS letters* 518.1 (2002): 43-47.
30. Leipold, Friedemann, Rainer Wardenga, and Uwe T. Bornscheuer. "Cloning, expression and characterization of a eukaryotic cycloalkanone monooxygenase from Cylindrocarpon radicicola ATCC 11011." *Applied microbiology and biotechnology* 94.3 (2012): 705-717.
31. Beneventi, Elisa, et al. "Discovery of Baeyer–Villiger monooxygenases from photosynthetic eukaryotes." *Journal of Molecular Catalysis B: Enzymatic* 98 (2013): 145-154.
32. Kotani, Tetsuya, et al. "Novel acetone metabolism in a propane-utilizing bacterium, Gordonia sp. strain TY-5." *Journal of bacteriology* 189.3 (2007): 886-893.
33. Iwaki, Hiroaki, et al. "Pseudomonad cyclopentadecanone monooxygenase displaying an uncommon spectrum of Baeyer-Villiger oxidations of cyclic ketones." *Applied and environmental microbiology* 72.4 (2006): 2707-2720.
34. Kirschner, Anett, Josef Altenbuchner, and Uwe T. Bornscheuer. "Cloning, expression, and characterization of a Baeyer–Villiger monooxygenase from Pseudomonas fluorescens DSM 50106 in E. coli." *Applied microbiology and biotechnology* 73.5 (2007): 1065-1072.
35. Rehdorf, Jessica, Anett Kirschner, and Uwe T. Bornscheuer. "Cloning, expression and characterization of a Baeyer-Villiger monooxygenase from Pseudomonas putida KT2440." *Biotechnology letters* 29.9 (2007): 1393-1398.
36. Völker, Anne, et al. "Functional expression, purification, and characterization of the recombinant Baeyer-Villiger monooxygenase MekA from Pseudomonas veronii MEK700." *Applied microbiology and biotechnology*77.6 (2008): 1251-1260.
37. Leisch, Hannes, Krista Morley, and Peter CK Lau. "Baeyer-Villiger monooxygenases: more than just green chemistry." *Chemical reviews* 111.7 (2011): 4165-4222.
38. Jiang, Jiaoyang, et al. "Genome Mining in Streptomyces avermitilis: A Biochemical Baeyer− Villiger Reaction and Discovery of a New Branch of the Pentalenolactone Family Tree." *Biochemistry* 48.27 (2009): 6431-6440.
39. Wen, Ying, et al. "Function of the cypX and moxY genes in aflatoxin biosynthesis in Aspergillus parasiticus." *Applied and environmental microbiology* 71.6 (2005): 3192-3198.
40. Dover, Lynn G., et al. "EthA, a common activator of thiocarbamide-containing drugs acting on different mycobacterial targets." *Antimicrobial agents and chemotherapy* 51.3 (2007): 1055-1063
41. Kelly, David R., Peter WH Wan, and Jenny Tang. "Flavin Monooxygenases—Uses as Catalysts for Baeyer-Villiger Ring Expansion and Heteroatom Oxidation." *Biotechnology Set, Second Edition* (1998): 536-587.
42. Malito, Enrico, et al. "Crystal structure of a Baeyer–Villiger monooxygenase."*Proceedings of the National Academy of Sciences of the United States of America* 101.36 (2004): 13157-13162.
43. Kamerbeek, Nanne M., Marco W. Fraaije, and Dick B. Janssen. "Identifying determinants of NADPH specificity in Baeyer–Villiger monooxygenases."*European Journal of Biochemistry* 271.11 (2004): 2107-2116.
44. Yachnin, Brahm J., et al. "The substrate-bound crystal structure of a Baeyer–Villiger monooxygenase exhibits a Criegee-like conformation." *Journal of the American Chemical Society* 134.18 (2012): 7788-7795.
45. Yachnin, Brahm J., et al. "The substrate-bound crystal structure of a Baeyer–Villiger monooxygenase exhibits a Criegee-like conformation." *Journal of the American Chemical Society* 134.18 (2012): 7788-7795.
46. Berezina, Nathalie, Véronique Alphand, and Roland Furstoss. "Microbiological transformations. Part 51: The first example of a dynamic kinetic resolution process applied to a microbiological Baeyer–Villiger oxidation." *Tetrahedron: Asymmetry* 13.18 (2002): 1953-1955.
47. Alphand, Veronique, and Roland Wohlgemuth. "Applications of Baeyer-Villiger monooxygenases in organic synthesis." Current Organic Chemistry14.17 (2010): 1928-1965.)

48. Alphand, Véronique, Alain Archelas, and Roland Furstoss. "Microbial transformations 16. One-step synthesis of a pivotal prostaglandin chiral synthon via a highly enantioselective microbiological Baeyer-Villiger type reaction." *Tetrahedron Letters* 30.28 (1989): 3663-3664.
49. Lebreton, Jacques, Véronique Alphand, and Roland Furstoss. "A short chemoenzymatic synthesis of (+)-multifidene and (+)-viridiene." *Tetrahedron letters* 37.7 (1996): 1011-1014.
50. Kamerbeek, Nanne M., et al. "Baeyer–Villiger monooxygenases, an emerging family of flavin-dependent biocatalysts." *Advanced Synthesis & Catalysis* 345.6-7 (2003): 667-678.
51. Iqbal, Hala A., Zhiyang Feng, and Sean F. Brady. "Biocatalysts and small molecule products from metagenomic studies." *Current opinion in chemical biology* 16.1 (2012): 109-116.
52. Ventosa, Antonio, et al. "Proposal to transfer Halococcus turkmenicus, Halobacterium trapanicum JCM 9743 and strain GSL-11 to Haloterrigena turkmenica gen. nov., comb. nov." *International journal of systematic bacteriology* 49.1 (1999): 131-136.
53. Saunders, Elisabeth, et al. "Complete genome sequence of Haloterrigena turkmenica type strain (4kT)." *Standards in Genomic Sciences* 2.1 (2010): 107.
54. Schein, Catherine H., and Mathieu HM Noteborn. "Formation of soluble recombinant proteins in Escherichia coli is favored by lower growth temperature." *Nature Biotechnology* 6.3 (1988): 291-294.
55. Müller-Santos, Marcelo, et al. "First evidence for the salt-dependent folding and activity of an esterase from the halophilic archaea Haloarcula marismortui." *Biochimica et Biophysica Acta (BBA)-Molecular and Cell Biology of Lipids* 1791.8 (2009): 719-729.
56. Ferrer, Manuel, et al. "Chaperonins govern growth of Escherichia coli at low temperatures." *Nature biotechnology* 21.11 (2003): 1266-1267.
57. Oren, Aharon. "Biotechnological applications and potentials of halophilic microorganisms." *Halophilic Microorganisms and their Environments* (2002): 357-388.
58. Bukau, Bernd, and Arthur L. Horwich. "The Hsp70 and Hsp60 chaperone machines." *Cell* 92.3 (1998): 351-366.
59. Heelis, P. F. "The photophysical and photochemical properties of flavins (isoalloxazines)." *Chemical Society Reviews* 11.1 (1982): 15-39.
60. Fraaije, Marco W., and Andrea Mattevi. "Flavoenzymes: diverse catalysts with recurrent features." *Trends in biochemical sciences* 25.3 (2000): 126-132.
61. Fraaije, Marco W., et al. "Covalent flavinylation is essential for efficient redox catalysis in vanillyl-alcohol oxidase." *Journal of Biological Chemistry* 274.50 (1999): 35514-35520.
62. Ellis, Keith J., and John F. Morrison. "Buffers of constant ionic strength for studying pH-dependent processes." *Methods in enzymology* 87 (1982): 405.
63. Johnson, W. Curtis. "Protein secondary structure and circular dichroism: a practical guide." *Proteins: Structure, Function, and Bioinformatics* 7.3 (1990): 205-214.
64. Sreerama, Narasimha, and Robert W. Woody. "Computation and analysis of protein circular dichroism spectra." *Methods in enzymology* 383 (2004): 318-351.
65. Kelly, Sharon M., Thomas J. Jess, and Nicholas C. Price. "How to study proteins by circular dichroism." *Biochimica et Biophysica Acta (BBA)-Proteins and Proteomics* 1751.2 (2005): 119-139.
66. Biasini, Marco, et al. "SWISS-MODEL: modelling protein tertiary and quaternary structure using evolutionary information." *Nucleic acids research*(2014): gku340.
67. Dolinsky, Todd J., et al. "PDB2PQR: an automated pipeline for the setup of Poisson–Boltzmann electrostatics calculations." *Nucleic acids research*32.suppl 2 (2004): W665-W667.
68. Ferrer, Juan, et al. "Crystallization and preliminary X-ray analysis of glucose dehydrogenase from Haloferax mediterranei." *Acta Crystallographica Section D: Biological Crystallography* 57.12 (2001): 1887-1889.
69. Tompa, Peter. "Intrinsically unstructured proteins." *Trends in biochemical sciences* 27.10 (2002): 527-533.
70. Kayser, MargaretáM, et al. "Asymmetric oxidations at sulfur catalyzed by engineered strains that overexpress cyclohexanone monooxygenase." *New Journal of Chemistry* 23.8 (1999): 827-832.
71. Torres Pazmiño, Daniel E., et al. "Self-Sufficient Baeyer–Villiger Monooxygenases: Effective Coenzyme Regeneration for Biooxygenation by Fusion Engineering." *Angewandte Chemie* 120.12 (2008): 2307-2310.
72. van der Donk, Wilfred A., and Huimin Zhao. "Recent developments in pyridine nucleotide regeneration." *Current Opinion in Biotechnology* 14.4 (2003): 421-426.

73. Costas, Amaya M. Garcia, Andrea K. White, and William W. Metcalf. "Purification and characterization of a novel phosphorus-oxidizing enzyme from Pseudomonas stutzeri WM88." *Journal of Biological Chemistry* 276.20 (2001): 17429-17436.
74. Bonete, María-José, et al. "Glucose dehydrogenase from the halophilic Archaeon Haloferax mediterranei: enzyme purification, characterisation and N-terminal sequence." *FEBS letters* 383.3 (1996): 227-229.
75. Zaccai, Giuseppe, et al. "Stabilization of halophilic malate dehydrogenase."*Journal of molecular biology* 208.3 (1989): 491-500.
76. Torres, Sebastián, and Guillermo R. Castro. "Non-aqueous biocatalysis in homogeneous solvent systems." *Food Technol Biotechnol* 42.4 (2004): 271-277.
77. Gupta, Munishwar N., et al. "Polarity Index: The Guiding Solvent Parameter for Enzyme Stability in Aqueous-Organic Cosolvent Mixtures." *Biotechnology progress* 13.3 (1997): 284-288.
78. Castle, Anna M., Robert M. Macnab, and Robert G. Shulman. "Measurement of intracellular sodium concentration and sodium transport in Escherichia coli by 23Na nuclear magnetic resonance." *Journal of Biological Chemistry* 261.7 (1986): 3288-3294.
79. Ruiz, Diego M., and Rosana E. De Castro. "Effect of organic solvents on the activity and stability of an extracellular protease secreted by the haloalkaliphilic archaeon Natrialba magadii." *Journal of industrial microbiology & biotechnology* 34.2 (2007): 111-115.
80. Vuillard, Laurent, et al. "Halophilic protein stabilization by the mild solubilizing agents nondetergent sulfobetaines." *Analytical biochemistry* 230.2 (1995): 290-294.
81. Ruiz, Diego M., and Rosana E. De Castro. "Effect of organic solvents on the activity and stability of an extracellular protease secreted by the haloalkaliphilic archaeon Natrialba magadii." *Journal of industrial microbiology & biotechnology* 34.2 (2007): 111-115.
82. Munawar, Nayla, and Paul C. Engel. "Overexpression in a non-native halophilic host and biotechnological potential of NAD+-dependent glutamate dehydrogenase from Halobacterium salinarum strain NRC-36014."*Extremophiles* 16.3 (2012): 463-476.
83. Alsafadi, Diya, and Francesca Paradisi. "Effect of organic solvents on the activity and stability of halophilic alcohol dehydrogenase (ADH2) from Haloferax volcanii." *Extremophiles* 17.1 (2013): 115-122.
84. Bell, George, Anja EM Janssen, and Peter J. Halling. "Water activity fails to predict critical hydration level for enzyme activity in polar organic solvents: interconversion of water concentrations and activities." *Enzyme and microbial technology* 20.6 (1997): 471-477.
85. Bar-Even, Arren, et al. "The moderately efficient enzyme: evolutionary and physicochemical trends shaping enzyme parameters." *Biochemistry* 50.21 (2011): 4402-4410.
86. Fried, Josef, Richard W. Thoma, and Anna Klingsberg. "oxidation of steroids by micro örganisms. iii. side chain degradation, ring d-cleavage and dehydrogenation in ring A." *Journal of the American Chemical Society* 75.22 (1953): 5764-5765.
87. Kang, Min-Wook, Young-Soo Kim, and Seong-Ki Kim. "Identification and Biosynthetic Pathway of Brassinosteroids in Seedling Shoots of Zea mays L."*Journal of Plant Biotechnology* 30.4 (2003): 411-419.
88. Schaefer, Didier G., and Jean-Pierre Zrÿd. "The moss Physcomitrella patens, now and then." *Plant physiology* 127.4 (2001): 1430-1438.
89. Roberts, Alison W., Eric M. Roberts, and Candace H. Haigler. "Moss cell walls: structure and biosynthesis." *Frontiers in plant science* 3 (2012).
90. Hohe, Annette, et al. "An improved and highly standardised transformation procedure allows efficient production of single and multiple targeted gene-knockouts in a moss, Physcomitrella patens." *Current genetics* 44.6 (2004): 339-347.
91. Cove, David. "The moss Physcomitrella patens." *Annu. Rev. Genet.* 39 (2005): 339-358.
92. Kuroiwa, Tsuneyoshi. "The primitive red algae Cyanidium caldarium and Cyanidioschyzon merolae as model system for investigating the dividing apparatus of mitochondria and plastids." *Bioessays* 20.4 (1998): 344-354.
93. Matsuzaki, Motomichi, et al. "Genome sequence of the ultrasmall unicellular red alga Cyanidioschyzon merolae 10D." *Nature* 428.6983 (2004): 653-657.
94. Minoda, Ayumi, et al. "Improvement of culture conditions and evidence for nuclear transformation by homologous recombination in a red alga, Cyanidioschyzon merolae 10D." *Plant and cell physiology* 45.6 (2004): 667-671.

95. Imamura, Sousuke, et al. "Nitrate assimilatory genes and their transcriptional regulation in a unicellular red alga Cyanidioschyzon merolae: genetic evidence for nitrite reduction by a sulfite reductase-like enzyme." *Plant and cell physiology* 51.5 (2010): 707-717.
96. Toda, K. *Molecular cytological studies of nuclear shapes and chromosomes in an ultra-small primitive red alga, Cyanidioschyzon merolae*. Diss. Master Thesis, University of Tokyo, 1996.
97. Boeke, Jef D., et al. "[10] 5-Fluoroorotic acid as a selective agent in yeast molecular genetics." *Methods in enzymology* 154 (1987): 164-175.
98. Ohnuma, Mio, et al. "Polyethylene glycol (PEG)-mediated transient gene expression in a red alga, Cyanidioschyzon merolae 10D." *Plant and Cell Physiology* 49.1 (2008): 117-120.
99. Hollmann, Frank, et al. "Enzyme-mediated oxidations for the chemist." *Green Chemistry* 13.2 (2011): 226-265.
100. Koike, Kunihiko, Goichi Inoue, and Tatsuo Fukuda. "Explosion Hazard of Gaseous Ozone." *Journal of chemical engineering of Japan* 32.3 (1999): 295-299.
101. Smith, Michael B., and Jerry March. *March's advanced organic chemistry: reactions, mechanisms, and structure*. John Wiley & Sons, 2007.
102. Mutti, Francesco G. "Alkene cleavage catalysed by heme and nonheme enzymes: reaction mechanisms and biocatalytic applications." *Bioinorganic chemistry and applications* 2012 (2012).
103. Hatta, Takashi, et al. "Characterization of a novel thermostable Mn (II)-dependent 2, 3-dihydroxybiphenyl 1, 2-dioxygenase from a polychlorinated biphenyl-and naphthalene-degrading Bacillus sp. JF8." *Journal of Biological Chemistry* 278.24 (2003): 21483-21492.
104. Bugg, Timothy DH. "Dioxygenase enzymes: catalytic mechanisms and chemical models." *Tetrahedron* 59.36 (2003): 7075-7101.
105. Dai, Yong, Pieter C. Wensink, and Robert H. Abeles. "One protein, two enzymes." *Journal of Biological Chemistry* 274.3 (1999): 1193-1195.
106. Adam, Waldemar, et al. "Biotransformations with peroxidases."*Biotransformations*. Springer Berlin Heidelberg, 1999. 73-108.
107. Berglund, Gunnar I., et al. "The catalytic pathway of horseradish peroxidase at high resolution." *nature* 417.6887 (2002): 463-468.
108. Shaw, Paul D., and Lowell P. Hager. "Biological chlorination vi. chloroperoxidase: a component of the β-ketoadipate chlorinase system."*Journal of Biological Chemistry* 236.6 (1961): 1626-1630.
109. De Montellano, PR Ortiz, et al. "Structure-mechanism relationships in hemoproteins. Oxygenations catalyzed by chloroperoxidase and horseradish peroxidase." *Journal of Biological Chemistry* 262.24 (1987): 11641-11646.
110. Gajhede, Michael, et al. "Crystal structure of horseradish peroxidase C at 2.15 Å resolution." *Nature Structural & Molecular Biology* 4.12 (1997): 1032-1038.
111. Marasco, Erin K., Kimleng Vay, and Claudia Schmidt-Dannert. "Identification of carotenoid cleavage dioxygenases from Nostoc sp. PCC 7120 with different cleavage activities." *Journal of Biological Chemistry* 281.42 (2006): 31583-31593.
112. Kloer, D. P., and G. E. Schulz. "Structural and biological aspects of carotenoid cleavage." *Cellular and Molecular Life Sciences CMLS* 63.19-20 (2006): 2291-2303.
113. Spudich, John L., et al. "Retinylidene proteins: structures and functions from archaea to humans." *Annual review of cell and developmental biology* 16.1 (2000): 365-392.
114. Markwell, John, Barry D. Bruce, and Kenneth Keegstra. "Isolation of a carotenoid-containing sub-membrane particle from the chloroplastic envelope outer membrane of pea (Pisum sativum)." *Journal of Biological Chemistry*267.20 (1992): 13933-13937.
115. Schwartz, Steven H., Xiaoqiong Qin, and Jan AD Zeevaart. "Elucidation of the indirect pathway of abscisic acid biosynthesis by mutants, genes, and enzymes." *Plant Physiology* 131.4 (2003): 1591-1601.
116. Schwartz, Steven H., Xiaoqiong Qin, and Jan AD Zeevaart. "Characterization of a novel carotenoid cleavage dioxygenase from plants." *Journal of Biological Chemistry* 276.27 (2001): 25208-25211.
117. Seto, Yoshiya, and Shinjiro Yamaguchi. "Strigolactone biosynthesis and perception." *Current opinion in plant biology* 21 (2014): 1-6.
118. Huang, Fong-Chin, Péter Molnár, and Wilfried Schwab. "Cloning and functional characterization of carotenoid cleavage dioxygenase 4 genes."*Journal of experimental botany* 60.11 (2009): 3011-3022.

119. Bouvier, Florence, et al. "Oxidative Remodeling of Chromoplast Carotenoids Identification of the Carotenoid Dioxygenase CsCCD and CsZCD Genes Involved in Crocus Secondary Metabolite Biogenesis." *The Plant Cell* 15.1 (2003): 47-62.
120. Frusciante, Sarah, et al. "Novel carotenoid cleavage dioxygenase catalyzes the first dedicated step in saffron crocin biosynthesis." *Proceedings of the National Academy of Sciences* 111.33 (2014): 12246-12251.
121. Kloer, Daniel P., et al. "The structure of a retinal-forming carotenoid oxygenase." *Science* 308.5719 (2005): 267-269.
122. Harper, Sandra, and David W. Speicher. "Purification of proteins fused to glutathione S-transferase." *Protein Chromatography*. Humana Press, 2011. 259-280.
123. Schilling, M., et al. "Impact of surfactants on solubilization and activity of the carotenoid cleavage dioxygenase, AtCCD1, in an aqueous micellar reaction system." *Biotechnology letters* 30.4 (2008): 701-706.
124. Rubio, Angela, et al. "Cytosolic and plastoglobule-targeted carotenoid dioxygenases from Crocus sativus are both involved in β-ionone release."*Journal of Biological Chemistry* 283.36 (2008): 24816-24825.
125. Gómez-Gómez, Lourdes, A. Moraga-Rubio, and Oussama Ahrazem. "Understanding carotenoid metabolism in saffron stigmas: unravelling aroma and colour formation." *Func Plant Sci Biotech* 4 (2010): 56-63.
126. Danson, Michael J., and David W. Hough. "The structural basis of protein halophilicity." *Comparative Biochemistry and Physiology Part A: Physiology*117.3 (1997): 307-312.
127. Mihovilovic, Marko D., Bernhard Müller, and Peter Stanetty. "Monooxygenase-Mediated Baeyer− Villiger Oxidations." *European Journal of Organic Chemistry* 2002.22 (2002): 3711-3730.
128. Burton, Stephanie G., Don A. Cowan, and John M. Woodley. "The search for the ideal biocatalyst." *Nature biotechnology* 20.1 (2002): 37-45.
129. Rajagopalan, Aashrita, Miguel Lara, and Wolfgang Kroutil. "Oxidative Alkene Cleavage by Chemical and Enzymatic Methods." *Advanced Synthesis & Catalysis* 355.17 (2013): 3321-3335.